Synthesis, Characterization, Physical Property Studies & Applications Of Perovskite Halide

Thesis submitted for the degree of
Doctor of Philosophy (Science)
In
Nanoscience and Nanotechnology

By

AVISEK MAITY

Centre for Research in Nanoscience and Nanotechnology

University of Calcutta
March 2022

.....To my Father

Acknowledgement

It's having been a wonderful journey of life since last 6.5 years and has finally been comes for an official ending through the documentation called "Thesis". Indeed it is time to pay gratitude to all those persons who plays a role to complete this dissertation and contributed to make it happen both directly & indirectly.

First, I would like to express my deep sense of gratitude to my supervisor **Dr. Barnali Ghosh (Saha)** for her affectionate guidance, support, inspiration to complete this long journey. She is a wonderful, compassionate, loving person who nurtured me a lot and probably put equal efforts to complete this thesis. Her mother like caring, friendly attitude made the problems very easy to discuss most of the times. She gave me absolute freedom to explore science & conduct experiments independently as well as provided fruitful solutions whenever I found any hurdles during this dissertation. Her patience & support were extremely crucial during several crisis times during this dissertation. I feel myself extremely lucky to have a supervisor like her. She is truly an amazing friend, philosopher & guide. A big thank you madam!

Secondly, I would like to express my sincere gratitude to **Prof. Arup Kumar Raychaudhuri**, Ex Director & Professes Emeritus of S.N.Bose Centre for his energetic guidance, wisdom, and support throughout this dissertation work. Without his valuable suggestions & enthusiasm it was never been possible to complete this thesis work. His inquisitiveness, dedication towards research always has been inspirational for me. I learnt from him how to think critically & independently, how to choose & deal scientific problems and most importantly how to explore interesting experimental science with minimum resources. Despite of his tightly packed schedule, he always made him available for scientific discussion whenever I needed with strong curiosity.

I would like to thank **Prof. Abhijit Saha**; Centre Director, UGC-DAE CSR Kolkata for allowing me to avail facility of gamma ray source at his centre. He is so kind and generous that he gave the full freedom to access his lab as well as discussion many times even after his busy administrative schedule. I am also thankful to Dr. Manik Pradhan, at S N Bose centre for his suggestions and encouragement towards completion of this dissertation.

It was indeed a great opportunity to work with a large number of members in our "New Nano Lab" which provided a cordial & friendly atmosphere always. It's my customary duty to acknowledge all seniors & juniors with whom I shared the lab. I am thankful to Soumen Da, Pabitra da, Rabeya di, Kaustuv da, Jashashree di, Rajib da, Rishi Ji, Ankita di, Samik da, Subarna di, Shaili di, Ravi da, Arnab da, Arun da, Mustak Da for their kind helps and fruitful suggestions in different time. In particular I would like to mention Soumen Da for introducing me with the real world of laboratory work and taught many technicalities in his small postdoc tenure in our lab. I cherish the beautiful moments spent with my wonderful fellow juniors namely Chandan, Subhamita, Parushottam, Anirban Vishal, Sudipta, Saikat, Snehamoyee who are friendly and helped several times as per their capabilities. Especially I had several fond memories with Chandan during many conferences attended together and his accompany during Synchrotron Experiment at KEK, Japan. I am thankful to Saikat for his help in MD simulations used in this thesis. I also especially thankful to Sudipta for his support in particular last phase of this dissertation work.

I am extremely lucky to have fiends like Mr. Susovan Das & Mr. Tufan Paul who are like my extended family and really plays a crucial role to complete this dissertation. They have been a source of fun, frolic, and support. Susovan is responsible for shaping my mind, logical

reasoning & personal development which became extremely important during this journey. Tufan is something like “crisis man” whenever I found any kind of difficulties. Being in similar experimental domain, he managed my shortage of reagents, solvents several times, shared interesting ideas which really been helpful during this dissertation. Thank you both for an integral part of this journey.

I had a special association with the members of Technical Research Centre (TRC), a separate wing of this centre for a dedicated project. I thank on my personal behalf to Ayan, Soumitra,Prosenjit, Arindam Da, Suman Da, Abhijit Da for their excellent help several times . It was a pleasure for me to work with them in different projects. A special thanks to Chandni & Sohel for their wonderful assistance and involvement in two my thesis projects.

I would like to acknowledge our institute SNBNCBS for providing peaceful and coherent research environment as well as the hostel facility inside the campus. Within our institute, I wish to recall the association of Arnab, Kartik, Sayan, Krishendu Da, Tilak Da.

I would humbly appreciate the financial support from the Department of Science and Technology. DST, Govt. of India and S. N. Bose National centre for Basic Sciences, Kolkata.

I acknowledge the help of all the members from technical cell Urmi Di, Joyda, Amit da, Sourav for their support and help whenever I needed in our centre. I also would like to thank from the core of my heart to all the people of our institute from administration, engineering, computer, library, electrical, workshop, canteen as well as security personnel’s for their help.

I also would like to thank my good old friends Prosenjit, Surajit Da, Moumita for their support. My sincere gratitude to my teacher Prof. Bahabani Prasad Mandal from BHU for his suggestions in different time, my school teachers Mr. Subir Bera, Mr. Sovan Lal Bhowmik for their encouragement towards this journey.

Finally, needless to say, I reserve my deepest gratitude to my parents and family members for their constant support, encouragement & love.

Avisek Maity

S N Bose National Centre for Basic Sciences

Kolkata

March, 2022

List of Publications & Patents

List of Publication

1. **Avisek Maity,**Chandni Das, A.K.Raychaudhuri, Abhijit Saha,Barnali Ghosh; Highly radiation resistant room temperature organic perovskite halide ($FAPbI_3$) crystal for direct detection of gamma -ray photons down to nano curie activity; ***Journal of Physics D: Applied Physics,*** (2021), 54, 455104

2. **Avisek Maity,** A.K.Raychaudhuri,Barnali Ghosh ; Paper based stable broad band optical detector made from mixed cation Perovskite Halides; ***Journal of Physical Chemistry C*** ,(2021), 125, 19, 10646–10652

3. **Avisek Maity**, Saikat Mitra ,Chandni Das, Sohel Siraj, A.K.Raychaudhuri, Barnali Ghosh; Universal sensing of ammonia gas by family of lead halide perovskites based on paper sensors: Experiment and Molecular Dynamics ; ***Materials Research Bulletin,*** (2020) , 136, 111142

4. **Avisek Maity** ,A.K.Raychaudhuri,Barnali Ghosh ; High sensitivity NH_3 gas sensor with electrical readout made on paper with perovskite halide as sensor material; ***Scientific Reports*** (2019) ,9,1-10

5. **Avisek Maity** and Barnali Ghosh ; Fast Response paper based visual color change gas sensor for efficient ammonia detection at room temperature; ***Scientific Reports*** (2018), 8,1-10

6. **Avisek Maity** and Barnali Ghosh; Perovskite halide based flexible gas sensor for detection of environmental pollutant at room temperature**;** ***AIP Conference Proceedings*** (2019), 2115, 030476

Patents

1. **Avisek Maity**, Arup Kumar Raychaudhuri, Barnali Ghosh; Ammonia gas sensor and a method for manufacturing the same; **Grant No- 316234,** ***India*** *(31/07/2019)*

2. **Avisek Maity**, Arup Kumar Raychaudhuri, Barnali Ghosh; A paper based ammonia gas selective sensor with electrical read out and a method for manufacturing the same; [**File no- 201831001993,** ***India*** *(2018)* ;First Examination Report **(FER)** submitted]

Abbreviations & Notations:

Materials:

MHP: Metal Halide Perovskites

MAI: Methyl Ammonium Iodide

FAI: Formamidium Iodide

DMF: Dimethylformamide

IPA: Isopropyl alcohol/(2 propanal)

Pb_2: Lead Iodide

GaAs: Gallium Arsenide

CdTe: Cadmium Telluride

Cr:Chromium

Cu:Copper

Au: Gold

CNT: Carbon Nanotube

PANI: Polyanyline

MAPI: Methyl ammonium Lead Iodide

FAPI: Formamidium lead iodide

MAPB: Methyl ammonium Lead Bromide

GBL: Gamma butarolactone

Pb:Lead

MA:Methylammonium

FA: Formamidium

HBr: Hydrobromic acid

HI: Hydroiodic acid

LAO:Lanthanam Aluminate

ITO:Indium Tin Oxide

FTO:Fluorine-doped Tin Oxide

RGO:Reduced Graphene Oxide

TCE: Trichloroethylene

Devices:

LED: Light Emitting Diode

PD: Photo detector

DUT: Device under test

Measured Quantities:

I_{ill}: Current under illumination

I_{ph}: Photo Current

I_{dark}: Dark Current

χ: Wavelength

S: Sensitivity (gas sensor)

ν: Frequency

R: Responsivity

G: Gain

D^*: Specific Detectivity

I: Device Current

V: Bias Voltage

μ: Mobility

τ: Life-time

$\mu\tau$: Mobility-lifetime product

t: Time

$\dot{\tau}$: Response time (Visual gas sensor)

Characterization tools & Techniques

XRD:-X-Ray Diffraction

EDX: Energy Dispersive X-Ray Diffraction

FESEM: Field Emission Scanning Electron Microscopy

AFM: Atomic Force Microscopy

TEM: Transmission Electron Microscopy

UV-Vis : Ultraviolet-Visible

PL: Photoluminescence

ITC: Inverse Temperature Crystallization

STL: Solution Temperature Lowering

CVD: Chemical Vapor Deposition

MD: Molecular Dynamics

USPP: Ultra- soft pseudo potential

Miscellaneous:

1D: One Dimensional

2D: 2 Dimensional

3D: Three Dimensional

ε : Octahedral Factor

t: Tolerance Factor

d_{avg}: Recombination length

VBM: Valance band minima

CBM: Conduction band minima

NIR: Near Infrared

ETM: Electron Transport material

PCE: Photo Conversion Efficiency

m_h^*: Effective mass of hole

ppm: Parts per million

ppb: Parts per billion

MOS: Metal Oxide Semiconductors

MSM: Metal semiconductor metal

$N_{2:}$ Nitrogen

$NH_{3:}$ Ammonia

KCi: Kilo curie

mCi: Milli Curie

μCi: Micro curie

$CH_{4:}$ Methene

$Co_{2:}$ Carbon di Oxide

RH: Relative Humidity

nW: Nanowatt

pA: Picoampere

CKD: Chronic Kidney Disease

GΩ: Giga Ohm

eV: Electron volt

nm: Nanometer

A: Ampere

Gy: Gray

Contents:

Chapter 1

Introduction

This chapter of this thesis provides brief information about fundamental properties of perovskite halide systems with the help of existing literatures. This chapter also describes the motivation behind the thesis work. This thesis work focuses on various application potentials along with underlying science of the perovskite halide system growing series of perovskite compounds on substrate like paper as well as good quality bulk highly oriented crystals to study the gas sensing, optoelectronic & radiation detection properties leading to three distinct kind of solid state detectors namely gas detector, photo detector and radiation detectors by structural, morphological and ionic tuning. Attempt has also been carried out towards technology transfer through developing prototypes utilizing novel and new application potentials of these emerging classes of materials investigated in this thesis. The basic objectives and detailed chapter wise plans also been discussed in this chapter.

1.1 Introduction to metal halide perovskites:

Metal Halide Perovskites are one of the most emerging classes of materials in last decade. There is considerable serge in exploring Halide perovskite in recent past. The attributes like high carrier mobility, long carrier diffusion lengths, and tunability of the band gap with suitable dopants make perovskite halides attractive materials for investigating the basic physics as well as other device applications [1-3]. In the current trend of research in this area, detailed study of synthesis &different physical properties of hybrid halides is thus quiet exciting. Although Metal Halide Perovskites (MHP) encompasses/generalizes a large classes of compounds, but lead based halide perovskites are mostly & widely studied among them due to their better stability relative to their other counterparts [4-5].

When I started my PhD in 2015, metal halide perovskites was widely explored mainly in Photovolatic applications. Successful use of metal halide perovskite as a absorber layer in solar cells enabled to achieve a Photo Conversion efficiency (PCE) up to 23% making halide perovskite based photo voltaic device comparable with the most conventional material like Si for solar cell[6-7]. Interestingly, due to such excellent electronic properties, other optoelectronic applications also emerged as well. Then this halide perovskite system has been realized in number of other optoelectronic devices like photo detector as sensitive photo detection, light emitting diode (LED) for tunable color emission etc [8-9].

Though perovskite halides are widely being studied but controlled growth of size, structures, surface morphology tuning by various parameters still remains less explored area. Moreover, finding the new application potentials in addition to solar cell/optoelectronic tuning of crystal structure & charge carrier by application of different external stimuli leading to several application potentials would be a value added welcome addition to such emerging class of materials.

This thesis work concentrates on some selected section of important application potential and physical properties of perovskite halides by structural, morphological and ionic tuning. This thesis focuses on controlled growth of thin/thick film nano & microstructure films of hybrid organic –inorganic lead halide perovskites using wet chemistry route. Importantly, piece of "paper" has been introduced as substrate to grow the materials which provides a simple & effective approach to produce compact, good quality films as well as making halide perovskites compatible towards "paper electronics". To the best of our knowledge, growth of halide perovskite films using paper substrate has not been explored earlier. Moreover, growth

of good quality single crystals of halide perovskite using low temperature solution processing is another development achieved in this thesis.

The as grown films and single crystals have been further utilized for in depth study of modification different physical properties i.e structural & optoelectronic under different external stimuli like gas, optical illumination & hard radiation.

In this thesis, we explored the gas sensing properties of organic halide using innovative paper electronics. We established the family of lead based perovskite halides as active material for new generation solid state gas sensor that can reach sub ppm sensitivity using simple low power paper electronics operable at room temperature.

Further to get an integrated understanding of color change as well as fascinating gas sensing behaviour by halide perovskite details study has been carried out using different structural and spectroscopic tools along with theoretical simulation. Till date such detailed study on gas sensing behaviour of family of lead based halide perovskite has not been explored yet.

Apart from gas sensing we focused on the optoelectronic properties of halide perovskite by fabricating paper based stable broadband (300-900nm) photo detector; a new approach of halide perovskite towards smart paper optoelectronics, which is also the first study on perovskite optoelectronics using paper substrate.

There are few reports on detection of hard radiation like gamma ray using halide perovskites. However, all the studies are based on energy resolution techniques [10-12]. We have explored direct detection of γ -ray using simple technique based on electrical out-put operational at room temperature and normal ambience using a solution grown halide perovskite crystals as well paper based devices.

Attempt has also been carried out towards technology transfer through developing prototypes utilizing novel and new application potentials of these emerging classes of materials investigated in this thesis.

1.2. Basic Properties of Halide Perovskites:

1.2.1Crystal Structure & Dimensionality:

Perovskites are in general a large family of compounds that follow the same chemical formula ABX_3. 'A' and 'B' denote cations, where A is typically much larger than B, and 'X' an anion. Halide perovskites employ an inorganic halide (I^-, Cl^-, Br^-) to replace the oxygen anion of oxide perovskites as the name implies [13].

The hybrid or organic-inorganic perovskite halides discussed in this thesis are a sub-group basically of this broad family of compounds. The family of hybrid organic—inorganic perovskite materials introduces a well-defined molecular assembly that basically bridges these organic and inorganic worlds.

They are part of thehalide perovskite (ABX_3 with X = Cl^-, Br^-, I^-etc) and generally consists of organic or inorganic monovalent A^+cations, A typically methylammonium $CH_3NH_3^+$ (MA), or formamidinium $HC(NH_2)_2^+$ (FA) and divalent B^{2+}metal cations, B = Pb^{2+}, Sn^{2+}, Mn^{2+}, etc. The typical hybrid organo-metallic halide perovskites discussed in this thesis are lead based family and are namely Methylammonium lead triiodide, $CH_3NH_3PbI_3$ ($MAPbI_3$/MAPI), Methylammonium lead tribromide, $CH_3NH_3PbBr_3$ ($MAPbBr_3$/MAPB) & Formamidium Lead Iodide ($CH(NH_2)2PbI_3$ ($FAPbI_3$/FAPI). [14]

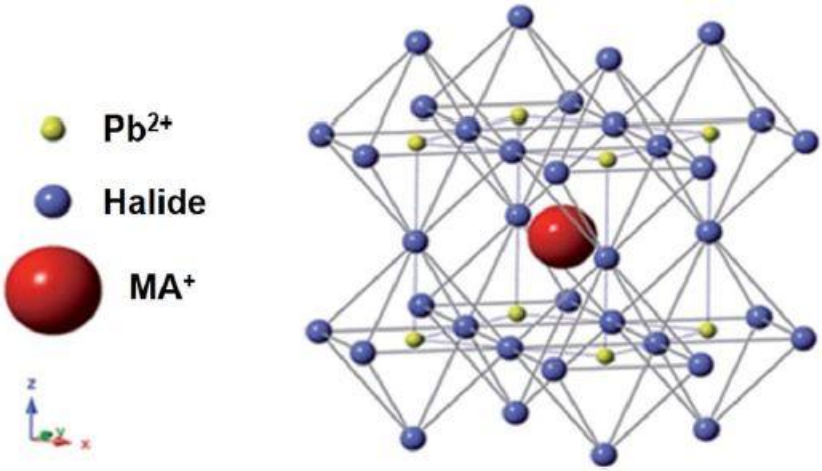

Figure 1.1*(a) Schematic of general crystal structure of halide perovskite; shown for $MAPbI_3$/MAPI [15]*

The versatility of perovskites makes them highly attractive as they can form multidimensional structures keeping the same chemical formula through using different combinations of various components. A large variety of elements/constituents can be

incorporated each with different valency, so long as charge neutrality is satisfied, enabling perovskites one of the most promising materials. The exceptional structural tunability of these compounds also enables them to possess not just three-dimensional (3D), but alsotwo-(2D),one- (1D) and zero-dimensional (0D) structures at the molecular level . Especially 2D halide perovskites, which have recently emerged as a more stable and more tunable material compared to their 3D counterpart may be considered as layers ripped of a specific crystallographic direction of the 3D perovskite [16]. Single or multiple corner-sharing layers separated by organic cations are regarded as the Ruddlesden-Popper-type perovskites. The general chemical formula is $An\text{-}1A'_2B_nX_{3n+1}$, where *A*' is an organic cation Organic-inorganic halide perovskite of different layers (usually large ligands with long alkyl chains) and *n* stands for the number of metal halide monolayer sheets in between the insulating *A*' organic layers [17-19]. Typically $n = \infty$ corresponds to a 3D structure, while $n = 1$ is the condition of a 2D perovskite monolayer. One example of the Ruddlesden-Popper-type of 2D perovskites can be seen in the work of Stoumpos et al. in the case of $CH_3(CH_2)_3NH_3)_2(CH_3NH_3)_{n-1}Pb_nI_{3n+1}$ (n =1,2,3,4)[20].

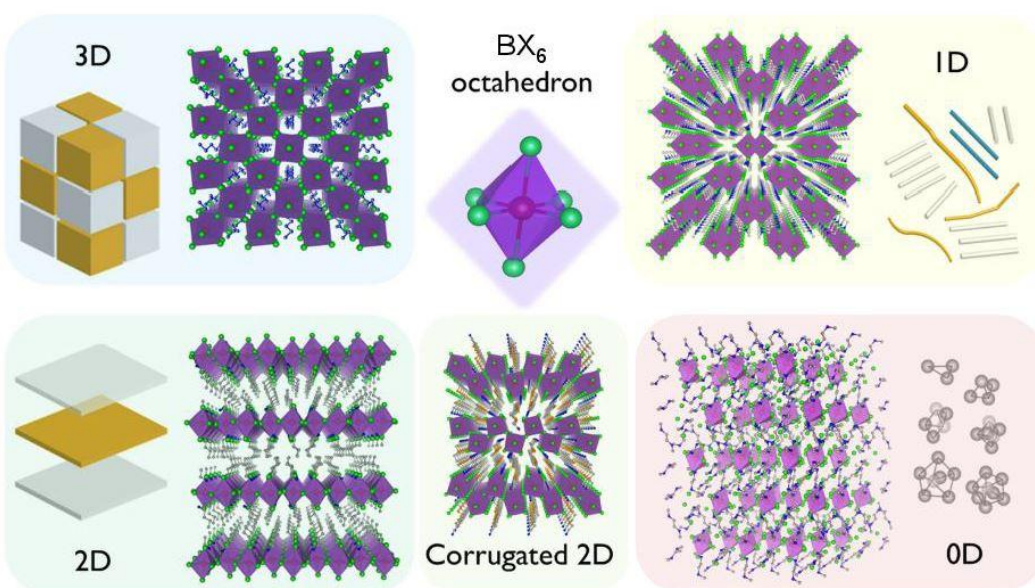

Figure 1.2*Different dimensionality of halide perovskites ranging from bulk 3D to quantum dot (0D) structure [17]*

1.2.1.2 Symmetry & Phase:

The electronic properties of halide perovskites are mainly governed by the B-X bond of the inorganic framework. While the A site cation does not directly contribute toward electronic properties, although its size can cause distortion of the B -X bonds thus adversely affecting symmetry [21-23].

In traditional ABX_3 perovskites, the B-site element is octahedrally coordinated in a BX_6 configuration. The A component is situated within the cuboctahedral cavity formed by nearest-neighbour X atoms in an AX_{12} polyhedron. Incorporation of an organic component gives rise to the series of materials known as organic–inorganic hybrid perovskites that have become archetypes in MHP optoelectronic applications.

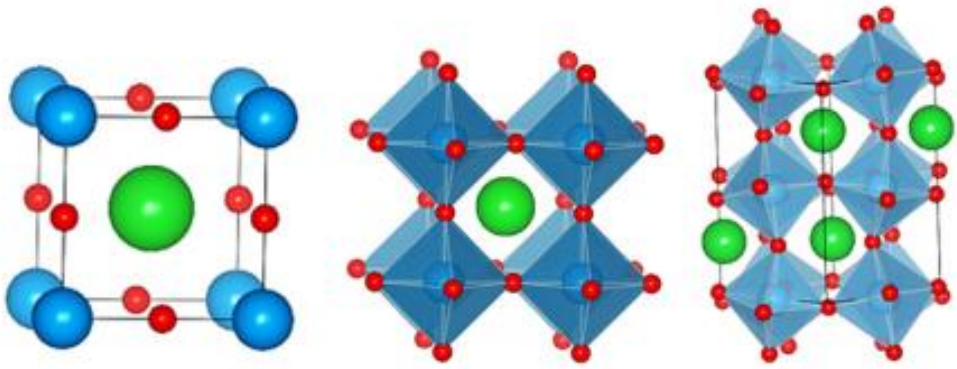

Fig 1.3: *The ideal perovskite unit cell a)A cations (blue) occupy the lattice corners, B cations (green) occupy the interstitial site, and X anions (red) occupy lattice faces. b) An alternative view depicting B cations assembled around X anions to form BX_6 octahedra, as B X bonds are responsible for determining electrical properties.c)Tilting of BX_6 octahedra occurring from non-ideal size effects and other factors, inducing strain on the B-X bonds.[13]*

The tolerance factor (t), a parameter first introduced from Goldschmidt in 1926, is often used to predict the stability of the perovskite lattice on the basis of the ionic radii (r) of A (r_A), B (r_B), and X (r_X), and is given as $t = \frac{(r_A + r_X)}{\sqrt{2}(r_B + r_X)}$ ……..(1.1) [24]

For a perfectly cubic perovskite lattice, t is close to 1. Empirically, the majority of MHPs synthesized to date form in the range $0.81 \leq t \leq 1.0$. Hexagonal structures are typically formed when $t>1$, and non perovskite structures are formed when $t \leq 0.8$.

Besides t, the octahedral factor (ε), i.e., the ratio of the ionic radius of B site to the A site, provides a measure of the octahedral stability of the perovskite and is usually found in the

range of 0.44 ≤ (ε), ≤ 0.9. The combination of those two factors defines the important parameter space for perovskite formability and stability [1, 2].

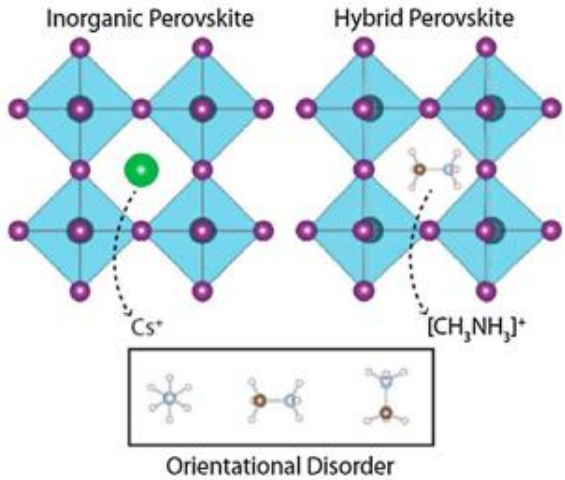

Fig 1.4: *Orientational disorder associated with non spherically symmetric organic methyl ammonium cation ($CH_3NH_3^+$) versus spherically symmetric inorganic cesium ($Cs^{+)}$ cation [29]*

This space is shown graphically as a 2D map of A and X ionic radii in Figure 1.5, with contour lines corresponding to the general outer limits of MHP formability for the Pb and Sn family of compounds

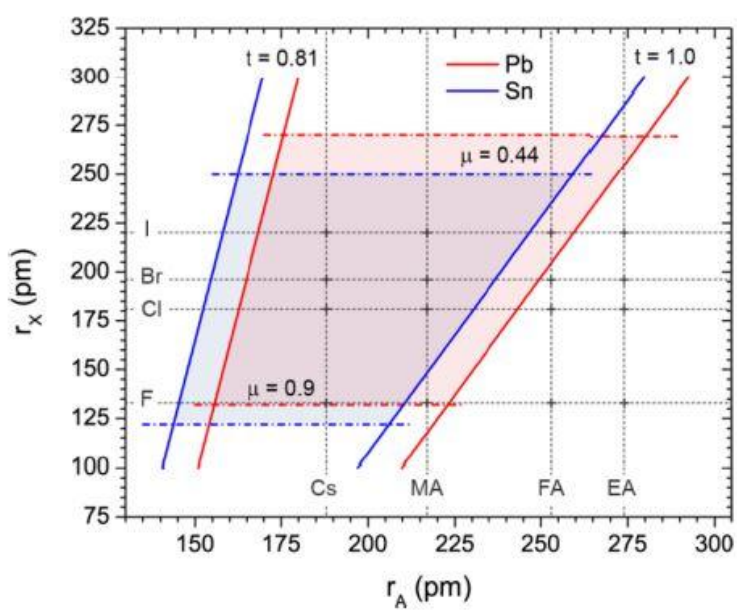

Figure 1.5: *Tolerance factor as a function of A site cation and X anion radii for different halide perovskites [1]*

Analysis of perovskite crystal has revealed three distinct phases mainly via X-Ray diffraction [25].

a) Cubic
b) Tetragonal
c) Orthorhombic

Generally, perovskites adopt cubic structures and undergo phase transitions from cubic to tetragonal to orthorhombic upon temperature reduction [26]. Symmetry of perovskites increases with temperature, for instance room temperature $MAPbI_3$posses a tetragonal structure, and $MAPbBr_3$ form cubic structures [26].

Furthermore, transmission electron microscopy (TEM) has revealed a 'pseudo-cubic' structure resulting from octahedral tilting and cation rotation [27]. It has been shown that $MAPbI_3$ undergoes a phase transformation to a lower symmetry from tetragonal to pseudo cubic at temperatures in the range of 300 K and 400 K [28].

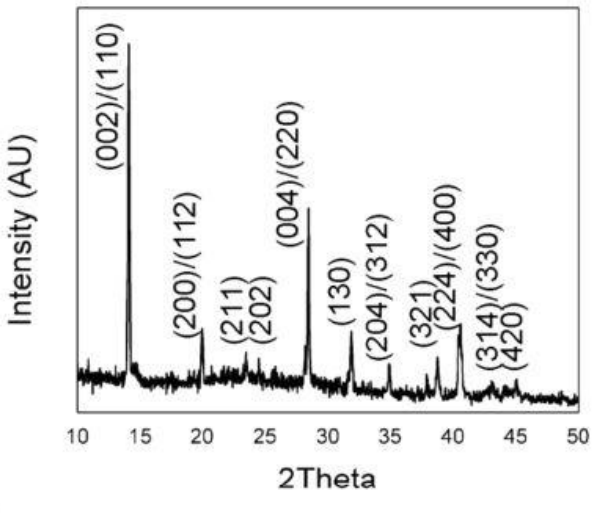

Figure 1.6: *Crystal structure of methyl ammonium lead halide perovskite at room temperature [29]*

	Phase	Structure	Temperature	Space Group
$MAPbI_3$ ($CH_3NH_3PbI_3$)	α	Cubic	<400K	P4mm
	β	Tetragonal	<293K	I4cm
	γ	Orthorhombic	<172K	$Pna2_1$

Table 1.1*: Structural phase transition of methylammnium leads iodide and transition temperatures with corresponding space group [13]*

There is a stringent structure—property correlation for perovskites regarding to both crystal composition and ion arrangement that is governed by its structural, optical and electronic properties.

1.2.2 Electronic Structure /Band Structure:

Studies on the electronic structures of 2D and 3D perovskite structures have shown that the electronic levels for hybrid perovskites consist of an antibonding hybrid state between the B-s and X-p orbitals that correspond to the valence band maximum (VBM) and a non-bonding hybrid state between the B-p and X-p orbitals that determines the conduction band minimum (CBM)[30,21-23]. In 2004, Park and Chang conducted first-principles pseudo potential studies on electronic properties of $MAPbX_3$ and $CsPbX_3$[21]. It was demonstrated that the electronic levels of MA lie deep within the valence and conduction bands (VB, CB), indicating that the contribution of MA toward electronic properties is miniscule and that the resulting band edges stem primarily from the BX_6 octahedra. Thus, it is apparent that band structures are only slightly affected by change from organic (MA) to inorganic (Cs) A cations as a result of size effects. The electronic states are however affected by substitution of the halide component, such that a VB transition from 3p → 4p → 5p occurs for substitution of Cl → Br → I. This accordingly lowers the ionization potential (binding energy) [23].

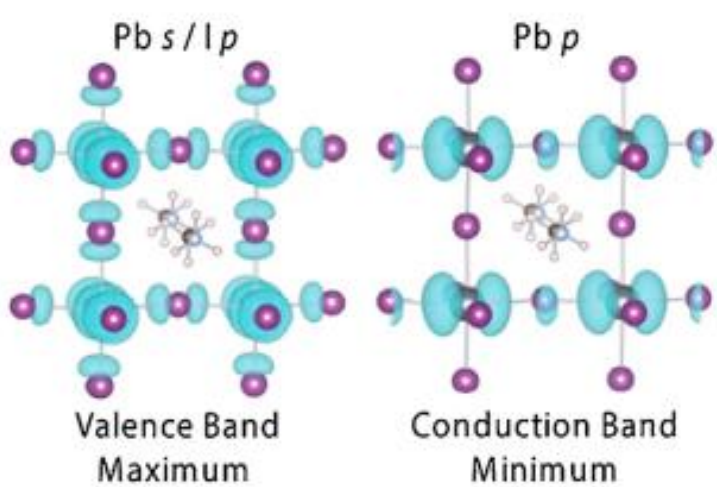

Fig 1.7: *Representation of the orbital arrangements for $MAPbI_3$ (a) VBM, showing Pb-s and I-p orbital overlap, and (b) CBM, showing Pb-p orbitals [30]*

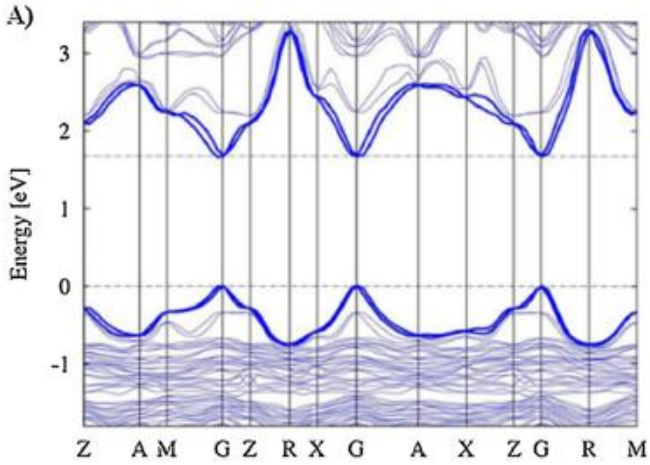

Fig 1.8: *Calculated band structures for $MAPbI_3$ by SOC-GW method [32]*

1.2.3 Optical Properties

The spectacular performances of hybrid perovskites stem from the substantial characteristic properties they possess. Hybrid perovskites demonstrate a strong optical absorption, an adjustable band gap, long diffusion lengths, ambipolar charge transport, high carrier mobility, and a high tolerance of defects. The ability to tune electronic and optical properties of hybrid perovskites with such ease presents a major attraction [31-35].

1.2.3.1 Absorption

Hybrid perovskites exhibit strong optical absorbance, allowing for a much reduced thickness necessary to efficiently facilitate collection of charge carrier's .Absorption across the entire visible spectrum is achievable and absorption up to the tail end of the red region of the spectrum, approximately 800 nm. It has been demonstrated that Sn-based halide perovskites can extend optical absorbance up to 1000 nm into the near infrared region (NIR).A layer of $MAPbI_3$ shows a linear absorption coefficient in the range of 10^4-10^5 cm^{-1} for visible light illumination[36]. These values are higher than those from conventional semiconductors (GaAs, CdTe) utilized in thin film solar cells or photo detectors.

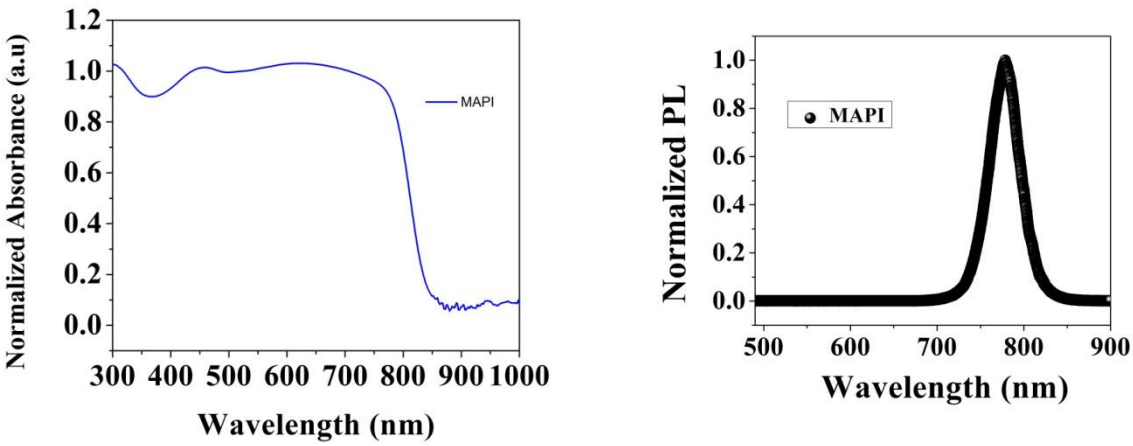

Fig 1.9 Typical *(a) absorption and (b) PL spectra of halide perovskite MAPI*

1.2.3.2 Carrier Diffusion Length

Another essential property of a sensitive semiconductor is its electron-hole diffusion lengths. Many groups have shown that in the case of perovskite halides these diffusion lengths are long and balanced. Carrier diffusion lengths (L_D) can be up to 100 nm for both electrons and holes in $MAPbI_3$ and exceeding 1 m in the mixed halide $MAPbI_{3-x}Cl_x$have been reported via transient photoluminescence (PL) measurements [25]. However, it has been demonstrated that holes are much more efficiently extracted than electrons in $MAPbI_3$ thus explaining the necessity of a mesoporous ETM for $MAPbI_3$-based devices, whereas in $MAPbI_{3-x}Cl_x$, both electrons and holes have diffusion lengths exceeding 1 m and do not require a mesoporous ETM[37].

1.2.3.3 Carrier Mobility

The electron-hole diffusion lengths of a material are highly dependent on the mobility (effective mass) and lifetime of the charge carriers. $MAPbI_3$ based halide perovskites have very small effective masses of both photo generated electrons and holes, $m_e^* = 0.23m_0$ and $m_h^* = 0.29m_0$, respectively, making them suitable candidates for solar cells in a p-i-n configuration [16, 38]. Whereas, materials like GaAs or CdTe have a much larger effective mass for holes than electrons, therefore devices fabricated with these materials rely on a formation of a p-n junction. The small effective masses are directly correlated with the mobilities, resulting in very high values up to 2000 $cm^2\ V^{-1}\ s^{-1}$ and 300 $cm^2\ V^{-1}\ s^{-1}$ for electrons and holes respectively [39].

A near instant charge generation has been observed in $MAPbI_3$, dissociating into essentially balanced free charge carriers within 2 picoseconds (ps) of high mobility (25 cm^2/Vs) that remain so for up to tens of microseconds [40] .

1.2.3.4 Low excitation binding energy

Exciton binding energies have been reported in between 37 and 50 meV for $MAPbI_3$ in its low temperature phase (orthorhombic, 5 K), which is significantly weaker, 6 meV at room temperature (tetragonal, 300 K). These exciton binding energies lower the absorption threshold, but also increase the strength of above band gap absorption that generates unbound electron-hole pairs. This offers a comparable or even stronger optical absorption above the band gap than many direct-band gap III-V semiconductors (GaAs). Yet, the binding energy is still sufficiently low. Therefore, following photo excitation, both free charge carriers and excitons may be present [41-42].

1.2.3.5 Tunable Optoelectronic Properties

One of the biggest advantages of organic-inorganic halide perovskites is the possibility of tuning their electronic properties (e.g. bandgap, carrier mobility) by modifying their chemical composition through the complete or partial replacement of one of the three constituent elements.

Firstly, the iodine in $MAPbI_3$ can be replaced with chlorine and bromine. Experiments have shown that with smaller halide anions (Cl < Br < I) the band gap increases. In the case of single crystals of $MAPbI_3$, $MAPbBr_3$ and $MAPbCl_3$ these values are 1.51, 2.18 and 2.82 eV, respectively [43-44]. By precisely controlling the halide composition, one can change the band gap and optical absorption. This could potentially be utilized by light emitting devices to cover the entire visible spectrum.

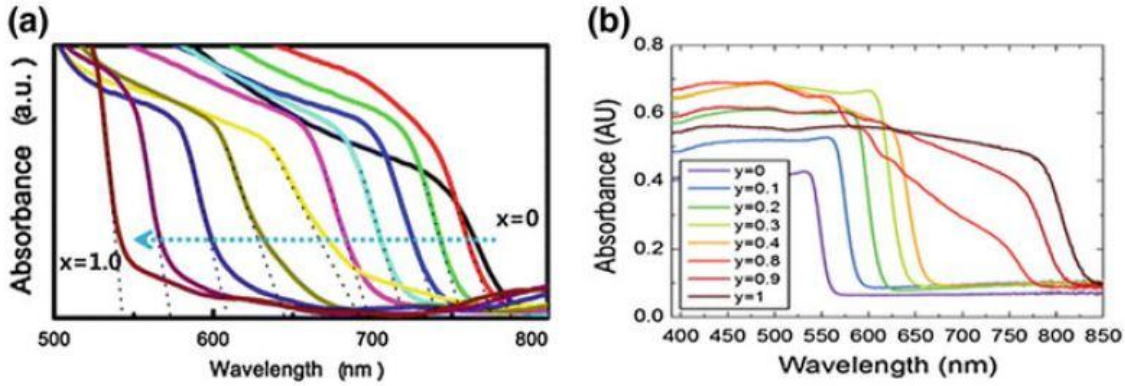

Figure 1.10 *Typical Absorption spectra of (a) $MAPbBr_xI_{3-x,}$ (b) $FAPbI_yBr_{3-y}$ perovskite films with varying x and y from 0 to1* [45]

1.3 Broad Motivation of this Thesis:

Since the class of emerging materials like perovskite halides exhibit several interesting electronic & optical properties, it is really fascinating to explore its potential applications in

different domains. Owing to its excellent optoelectronic properties, these perovskites are mostly and widely used in photovoltaic and optoelectronic like photo detector, LED, solar cells applications as we stated introduction section [1-3]. In light of that, it would be extremely rewarding to find any other applications of these kinds of materials. We are very much intrigued to find if there is any other application potential of perovskite halides in the areas like sensing under different external stimuli, and also wish to understand the underlying science behind them.

One of the pertinent issue that has been attempted to address in this thesis to make smooth, pinhole free, uniform films for sustained device operation using halide perovskites. Though perovskite halides are really interesting, there is a serious issue of uniform, pinhole free films of them for stable device operation. Most of the devices for halide perovskite research have been realized by polycrystalline films grown on common substrates like glass, ITO, FTO etc. In available earlier reports, the device structure based on such substrates suffers lack of high film quality, uniformity; pinhole actually acts as road block for high performance & sustained device operational stability [46]. Though, several strategies like suitable engineering of composition, solvent engineering etc have been carried out to achieve good, compact films to address such issue, but there are lot of scope & research needed to improve this further.

We wish to see whether tuning of substrate could play any role to address these issues. A major focus has been emphasized in this thesis to address this issue. We have achieved good quality, uniform; pinhole free films by simple & effective way by introducing paper as substrate which also enabled us to explore paper electronics based devices using halide perovskite. Moreover, paper is eco-friendly, disposable, flexible, low cost and light weight that makes them attractive substrates for smart flexible electronics. Since perovskites are solution processed, growth of perovskite on paper would be easy to fabricate as well as could open up a horizon to translate perovskite halides to successful candidate into paper based smart, flexible, disposable electronics. Thus one of our aims is to growth and fabrication of the perovskite halides into cellulose rich paper substrate to combat non-uniformity of films, better surface coverage and study the physical properties and applications of the halide perovskites using paper electronics.

Study on semiconductor gas sensor is quiet contemporary research tend, but mostly limited to metal-oxide semiconductors [47-48]. In that context, it would be really worthwhile to explore the gas sensing properties of this kind of emerging material which would not only be

the new application potentials of these kind of materials, but also could serve as new active material for solid state gas sensors. As in previous point we mentioned out the advantages of paper substrate in translating the devices made from perovskite, we are aspired to study the gas sensing behaviour by them using paper electronics where, these materials can be used innovatively by visual colour change based as well as sensing via electrical readout. It would also be valuable to understand the mechanism of gas sensing and underlying science behind them whether the sensing mechanism is similar nature like metal oxide semi conductors. A detailed study of gas sensing behaviour by lead halide perovskites has been investigated along with an understanding the underlying science behind such fascinating behaviour and corroborated with simulation results.

Though perovskites are well researched in optoelectronics photo detector (PD), there is issue with stable broadband response with complete comprehensive study of different properties of the optical detectors. One of our motivation was to study optoelectronic properties of halide perovskites by fabricating perovskite PD with stable response by tuning various parameters like composition, substrate etc. On top of that, flexible detector combined with broadband responsivity and relatively high photo sustainability is essential to meet the growing demands of high performance smart wearable, optoelectronic devices. Since, growth of perovskite on paper could serve the stable device operation for its uniform growth; we are motivated to attempt whether such kind of flexible, paper based PD's can be addressed by perovskite halides for stable broadband response for new generation broadband photo detector.

Since perovskite halide posses excellent optical properties like long carrier diffusion length (due to large carrier recombination time) , large bulk resistivity, and low cost solution growth of bulk crystal which features would also be extremely important ingredients for designing a radiation detector like hard radiation (like X-ray &γ-ray)[11-13]. This motivates us to explore whether the radiation detection can be possible by perovskite halides apart from their optoelectronics applications also.

Moreover, in recent past, a major emphasis has been imparted on translational research to transfer the technology from the new, novel invention of scientific observation in laboratory**.** It is quite interesting approach to make halide perovskites in the field of translational research which has been explored to some extent in this thesis.

So in a nutshell, our basic motivation is to study how a same class of material can be used for multifunctional applications under several external stimuli like specific gas

molecule, photo & radiation by tuning their crystallographic structure & charge carrier. In order to study that we have engineered the halide perovskite family, so that it can be used in the form of different detectors namely gas detector, photo & radiation detector using innovative paper electronics as well as good quality bulk crystals.

So, halide perovskite as a new generation solid state detector for multifunctional applications as gas sensor & optical detector as well as radiation detector devices is the essence of thesis.

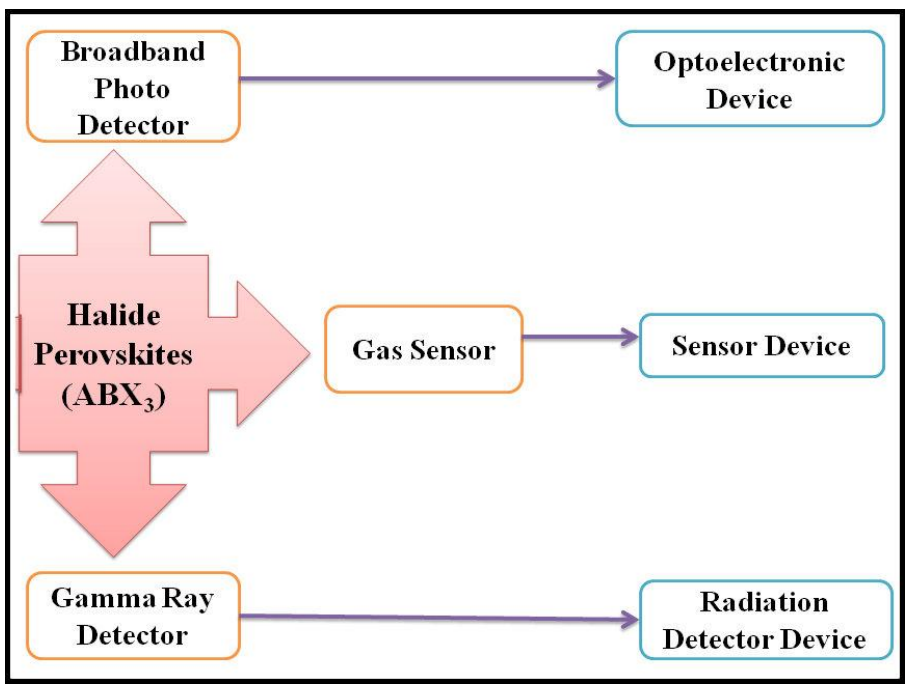

Figure1.11: *Schematic of multifunctional use as different detector devices of halide perovskites investigated in this thesis*

Hope readers will get a feel of multifunctionality of halide perovskite as a new emerging class of materials through this thesis.

1.4. Objective of this Thesis:

So, based of the above motivations, the main objective of this thesis are-

- To explore the science of halide perovskites by tuning of crystal structure & charge carrier under different external stimulus like gas, optical illumination & radiation.
- To fabricate paper based devices using halide perovskites as a viable simple, alternative approach for uniform pinhole free films for stable devices
- To study gas sensing, optoelectronic & radiation detection properties of hybrid halide perovskites using novel paper electronics
- To extend the novel application potentials as translational research trough developing prototypes and filing patents.

1.5 Layout of the Thesis:

In this thesis, we aimed to investigate some of the important science and as well as application potential of perovskite halides by tuning various parameters and an attempt has been taken towards translational research utilizing novel application potentials of them.

This thesis is based on the major following works:

I. Growth of perovskite halide highly oriented bulk crystal, nano and microstructures and their characterizations
II. Paper electronics based device fabrication
III. Investigation of gas sensing property by family of lead halide perovskites using paper electronics
IV. Study of optoelectronic properties of oriented and mixed cation perovskites using paper electronics: paper electronic based photo detectors
V. Approach to radiation detection by halide perovskites

In this present chapter, a brief overview of metal halide perovskite crystal structure, physical properties and the associated study on it has been presented. This chapter also includes the necessary literature of the work in the field of binary oxide major motivation and objective of the dissertation work.

In the 2nd Chapter describes the different synthesis routes using wet route chemistry for the materials under investigation of family of halide perovskites for growth of good quality highly oriented bulk crystals & thin films by tuning various parameters like precursor's concentration, substrate etc to get definite results. It has also been explained the innovative use of 'paper' as substrate to grow the family of hybrid perovskite lead halides of different surface morphology and crystal structure. This chapter also describes device fabrication using novel paper electronics, customization of measurement set up development for different measurements. The Characterization of the grown materials using different tools has also been shown in this chapter.

The 3rd Chapter gives the description of a new application potential of halide perovskite as an active material for gas sensors grown on paper using novel visual color colorimetric method for tracing ammonia gas sensing down to ~10ppm with very high selectivity/sensitivity. Development using this novel color change method to detect ammonia gas has also been

discussed in details in this chapter. The visual sensor acts as a quick and easy method to detect hazardous gas like ammonia at work places and extremely useful when people working in any environment prone to ammonia for their safety.How this application potential leads us to develop 'prototype' for practical usage and 'Granting Patent' has also been shown in this chapter.

4th Chapter depicts the very high sensitive gas detection capability of perovskite halide using electrical readout via paper electronics at sub ppm level (down to ppb level) towards ammonia gas with high selectivity/sensitivity and stability besides visual sensing capability. A details study about above gas sensor characteristics has been discussed. A proof of concept of prototypes and its social impact based on such high sensitive gas detection has also been briefly discussed.

In 5th chapter we have given a detailed description of universal ammonia gas sensing behaviour (both visual and electrical) by cation and anion engineered family of lead halide perovskites. Based on experimental results, a generalized sensing mechanism has been proposed. The proposed mechanism has been substantiated by molecular dynamics simulations.

6th Chapter describes an broad view of the optoelectronic properties of halide perovskite by fabricating paper based mixed cation ($MA_{1-x}FA_xPbI_3$) stable broadband (300-900nm) photo detector by tuning compositions, morphology etc enabling a new approach of halide perovskite towards smart paper optoelectronics. It has been observed that the cation engineering not only enhances the photo response but also makes stable & broadband detector as compared to the single cation detector. The as fabricated detector is thus flexible, broadband and workable at low optical illumination intensity as well as low bias making compatible with battery powered electronics. The detailed optoelectronic properties and photo detector characteristics has been discussed in this chapter.

In 7th chapter we have explored an interesting behaviour of hybrid halide perovskites as highly radiation resistant Gamma ray detector by fabricating both high quality highly oriented crystal of $FAPbI_3$& paper electronics based $MAPbBr_3$ film. Generally Gamma detection in nuclear imaging, security checking cancer therapy etc is done by conventional energy resolution technique which requires special arrangements of γ- spectrometry and nuclear

instrumentation which are not easy tool for rapid detection. Whereas, here we have given details experimental results, how a deviated approach for gamma ray detection can be taken not by energy resolution rather via electrical read out method at room temperature using perovskite halide as a quick marker of γ radiation. This detection technique could be extremely useful in radiation prone areas, in a cost effective way, where fine energy resolution is not a primary concern. A detailed comprehensive study has been carried out on these hybrid halide perovskite based radiation detectors in this chapter.

In the last chapter (Chapter 8), we have provided summary and concluding remarks of this thesis along with major achievements of the dissertation work and future challenges.

References:

1.1 Joseph S. Manser, Jeffrey A. Christians, and Prashant V. Kamat; *Chem. Rev.* 116, 12956−13008, 2016

1.2 Amrita Dey.et.al; *ACS Nano,* 15, 10775−10981, 2021

1.3 Javad Shamsi, Alexander S. Urban, Muhammad Imran, Luca De Trizio, and Liberato Manna .*Chem. Rev.* 119, 3296−3348, 2019

1.4 Rohit Prasanna.et.al; Nature Energy , 4 ,939–947, *2019*

1.5 Luis Lanzetta, Nicholas Aristidou and Saif A. Haque**;** *J. Phys. Chem. Lett.* 11, 2, 574–585, 2020

1.6 Correa-Baena, J. P.; Saliba, M.; Buonassisi, T.; Gratzel, M.; Abate, A.; Tress, W.; Hagfeldt, *Science* ,358, 739−744, 2017

1.7 Park, N.-G. *Nano Today* 18, 65−72, 2015

1.8 Yixin Zhao and Kai Zhu; *Chem. Soc. Rev.* DOI: 10.1039/c4cs00458b

1.9 Samuel D. Stranks and Henry J. Snaith; *Nature nanotechnology* ,10 ,2015

1.10 Nazarenko. Olga. et.al; *NPG Asia Materials* 9, e373, 2017; doi:10.1038/am.2017.45

1.11 HaotongWei.et.al;, *Nature Materials*, 16, 826–833 , 2017DOI: 10.1038/NMAT4927

1.12 He, Yihui.et.al; *Nature Communication*,9,1609 , 2018,DOI: 10.1038/s41467-018-04073-3

1.13 Qi Chen , Nicholas De Marco , Yang (Michael) Yang , Tze-Bin Song , Chun-Chao Chen , Hongxiang Zhao ,Ziruo Hong , Huanping Zhou , Yang Yang **,** *Nano Today* , 10, 355—396, 2015

1.14 T. Chien, and N. Mathews, *Energy & environmental science* 7, 2518–2534, 2014.

1.15 Z. Ku, Y. Rong, M. Xu, T. Liu and H. Han, *Sci. Rep.*, 3,3132, 2013

1.16 Pavao Andricevic, PhD Thesis submitted to École polytechnique fédérale de Lausanne,2019

1.17 H. Lin, C. Zhou, Y. Tian, T. Siegrist, and B. Ma; *ACS Energy Letters*, 3, 54–62, 2017.

1.18 C. Ortiz-Cervantes, P. Carmona-Monroy, and D. Solis-Ibarra, *ChemSusChem* 12, 1560–1575, 2019

1.19 B. Cheng, T. Y. Li, P. C. Wei, J. Yin, K. T. Ho, J. R. D. Retamal, O. F. Mohammed, and J. H. He; *Nature Communications 9*, 5196, 2018.

1.20 C. C. Stoumpos, D. H. Cao, D. J. Clark, J. Young, J. M. Rondinelli, J. I. Jang, J. T. Hupp, and M. G. Kanatzidis, *Chemistry of Materials* 28, 2853-2867, 2016.

1.21 Y.H. Chang, C.H. Park, *J. Korean Phys. Soc.* 44, 889—893, 2004

1.22 T. Umebayashi, K. Asai, T. Kondo, A. Nakao, *Phys. Rev. B* 67, 155405, 2003

1.23 P. Umari, E. Mosconi, F. De Angelis, *Sci. Rep.* 4, 4467, 2014

1.24 Goldschmidt, V. M. Die Gesetze Der Krystallochemie. Naturwissenschaften, 14, 477−485, 1926

1.25 S.D. Stranks, G.E. Eperon, G. Grancini, C. Menelaou, M.J.P. Alcocer, T. Leijtens, L.M. Herz, A. Petrozza, H.J. Snaith; *Science* ,342 , 341—344, 2013

1.26 D. Weber, *Inst. Anorg. Chem.* Univ. Stutt. 33b, 1443—1445, 1978.

1.27 T. Baikie, Y. Fang, J.M. Kadro, M. Schreyer, F. Wei, S.G. Mhaisalkar, M. Graetzel, T.J. White, *J. Mater. Chem.*, 1 , 5628—5641, 2013

1.28 C.C. Stoumpos, C.D. Malliakas, M.G. Kanatzidis, *Inorg. Chem.* 52 , 9019—9038, 2013

1.29 Andrew Barnabas Wong.et.al; *Nano Lett.* 15, 5519−5524, 2015

1.30 F. Brivio, A.B. Walker, A. Walsh, *APL Mater.* 1 ,042111, 2013

1.31 J. Burschka, N. Pellet, S.-J. Moon, R. Humphry-Baker, P. Gao, M.K. Nazeeruddin, M. Gratzel, *Nature* 499 , 316—319, 2013

1.32 M. Liu, M.B. Johnston, H.J. Snaith; *Nature* 501, 395—398, 2013

1.33 A. Kojima, K. Teshima, Y. Shirai, T. Miyasaka, *J. Am. Chem. Soc.* 131 , 6050—6051, 2009

1.34 L. Etgar, P. Gao, Z. Xue, Q. Peng, A.K. Chandiran, B. Liu, M.K. Nazeeruddin, M. Grätzel,;*J. Am. Chem. Soc.* 134 , 17396—17399, 2012.

1.35 M.M. Lee, J. Teuscher, T. Miyasaka, T.N. Murakami, H.J. Snaith, *Science,*338, 643—647, 2012

1.36 Y. Wang, Y. Zhang, P. Zhang, and W. Zhang, *Physical Chemistry Chemical Physics* 17, 7, 11516–11520, 2015.

1.37 G. Xing, N. Mathews, S. Sun, S.S. Lim, Y.M. Lam, M. Grätzel, S. Mhaisalkar, T.C. Sum; *Science* 342, 344—347.

1.38 W. J. Yin, T. Shi, and Y. Yan, *Advanced Materials* 26, 4653–4658, 2014.

1.39 I. Grinberg, D.V. West, M. Torres, G. Gou, D.M. Stein, L. Wu, G. Chen, E.M. Gallo, A.R. Akbashev, P.K. Davies, J.E. Spanier, A.M. Rappe, *Nature* 503 , 509—512, 2013

1.40 K. Tanaka, T. Takahashi, T. Ban, T. Kondo, K. Uchida, and N. Miura, *Solid state communications* 127, 619–623, 2003.

1.41 Y. Yamada, T. Nakamura, M. Endo, A. Wakamiya, and Y. Kanemitsu, *IEEE Journal of Photovoltaics* 5, 401–405, 2015.

1.42 C. Wehrenfennig, G. E. Eperon, M. B. Johnston, H. J. Snaith, and L. M. Herz, *Advanced Materials* 26, 1584–1589, 2014

1.43 M. I. Saidaminov, A. L. Abdelhady, B. Murali, E. Alarousu, V. M. Burlakov, W. Peng, I. Dursun, L. Wang, Y. He, G. Muculan, and A. Goriely, Nature *Communication* 6, 7586, 2015.

1.44 G. Maculan, A. D. Sheikh, A. L. Abdelhady, M. I. Saidaminov, M. A. Haque, B. Murali, E. Alarousu, O. F. Mohammed, T.Wu, and O. M. Bakr; *The journal of physical chemistry letters* 6, 19, 3781-3786, 2015.

1.45 GE Eperon, SD Stranks, C Menelaou, MB Johnston, LM Herz, HJ Snaith ; *Energy Environ Sci* 7:982, (2014)

1.46 Teddy Salim, Shuangyong Sun, Yuichiro Abe,Anurag Krishna, Andrew C. Grimsdalea and Yeng Ming Lam, *J. Mater. Chem. A*, 3, 8943, 2015.

1.47 Samà , J. et al.;. *Sensors and Actuators B*, 232, 402–409 , 2017

1.48 Meixner, H., Gerblinger, J., Lampe, U., Fleischer.M. *Sensors and Actuators B*, 23,119-125,1995

Chapter 2

Synthesis, Characterization & Description of Device Fabrication and Experimental Techniques

In this chapter of thesis we have described facile synthesis routes using wet route chemistry for the materials under investigation of family of halide perovskites namely films and bulk highly oriented crystals of them. One step & two step solution growth techniques have been adopted for the growth of micro/nanostructured films and Inverse temperature crystallization growth (ITC) method was used to grow good quality of highly oriented crystals. It has also been explained the innovative use of 'paper' as substrate to grow the family of hybrid perovskite lead halides of different surface morphology and crystal structure. The as grown films and crystals were characterized by several characterization tools like X-Ray Diffraction (XRD), Field Emission Scanning Electron Microscopy (FESEM), and Atomic Force Microscopy (AFM) for structural & morphological characterization. Photoluminescence (PL) & UV-Visible (UV-Vis) spectroscopy have been used for their optical characterization. Apart from growth we have described the device fabrication using innovative "paper electronics" as well as development and customization experimental set up in this chapter.

2.1 Introduction:

As we have seen in previous chapter Perovskite Halides are really booming candidates for various application potentials in several fields like photovoltaics, LED, sensitive photo detection etc past few years[1]. It has been widely popular as an important solar cell material since its inception in last decade [2-3]. Synthesis of such promising materials in well controlled manner is extremely important as good quality material shows well structure property relationship which essentially enhances the device performances. The feature and quality of the material is highly influenced by the growth process. Tuning of growth parameters helps to "engineer" the desired physical properties of the material.

Perovskite halides mostly used in the form of thin film to form devices although in recent past bulk crystals are also being used for application aspects. There are several strategies followed to grow the perovskite halide thin films such as vapour phase deposition, template assisted growth, solution growth techniques etc [4-5]. Among them solution growth/wet chemistry approach has been widely adopted because room temperature operated, cost effective ,easy to synthesize without help of much sophisticated instruments. Moreover, there are modified techniques invented in solution growth approach like two step spin coating and solvent annealing approach, volume expansion control etc to improve better surface morphology [6]. In application point of view, perovskite thin film based devices highly demands uniform, pinhole free, smooth and uniform coverage of films for its outstanding device performances. All aforesaid techniques are being applied to improve the film coverage and compactness. Still there are open challenges to improve film morphology, composition control, controlled crystallization and coverage. Hence, the growth of perovskite thin film with controlled size, shape, composition with uniform compactness is very important issue to be resolved.

In this thesis we have investigated the effect of different growth parameters like growth time, precursor concentration, substrates to effectively tune the morphology and compactness of perovskite halides. We have worked on family of lead halide perovskite material by altering cation and anion as well as and mixture of suitable substitutions/doped cations which follow a common synthesis route. We followed mostly one step solution process to synthesis our materials. The details of solution growth techniques have been provided in the following section. We have shown surface morphologies can be tailored in lead based perovskite halides extending from micro to nanostructured by tuning growth parameters. It has also been

shown that the halide perovskite can be grown in substrates like “paper” to make alternative approach for simple & scalable method for growth of films with better coverage and pinhole free growth as compared to the common substrates like glass, ITO, FTO coated glass etc [4-5]. Moreover, in some cases the paper grown lead halide perovskites can specifically provide nanostructures which improve application potential due to higher surface to volume ratio of the nanostructure.

We have also worked on bulk single/highly oriented crystals to investigate physical properties and applications, as single crystals provide better transport of carrier for reduced defects, absence of grain boundary. We adopted inverse temperature crystallization (ITC) method to grow the bulk highly oriented crystals because it is relatively fast and helps to grow large crystals [7]. The details of advantages than other methods available and growth mechanism of crystal has been discussed in the respective following section.

The characterization techniques, method of device fabrication and different physical measurement techniques are discussed in this chapter. Several characterization tools were used to check the crystal structure, stoichiometry, surface morphology, surface roughness etc. Phase formation, phase purity and crystallinity of the grown material were confirmed by X-ray diffraction analysis. Energy dispersive analysis of X-ray (EDX) is employed to determine the elemental composition of the material. The surface morphology and surface roughness are investigated using scanning electron microscopy (SEM)and atomic force microscopy (AFM). Similarly, photoluminescence (PL) spectroscopy is used to characterize the emission spectra as well as defect study and UV-Visible spectroscopy is used to determine the optical band gap.

The “paper electronics” based device was made by making two probe metal contacts using metal masking. Metallization on paper substrate is an important achievement addressed in this thesis. These devices are used to optoelectronic, gas and radiation induced electrical and optical measurements using paper electronics. In electrical measurements we performed room temperature current -voltage $(I-V)$ and current-time $(I-t)$measurements and gas induced optical spectroscopic (UV –Visible & Photo Luminescence) measurements. We have used our own LAB View based program for data acquisition using Keithley Source-Meter through GPIB interface employing two probe configuration.

2.2. Synthesis of Micro and Nanostructured Thin Films of Family of Perovskite Halides (ABX_3)

We have adopted wet chemistry route to grow the micro and nano structures of family of perovskite halides(ABX_3) by tuning different growth parameters. This method is solution processed, room temperature operated, easy to synthesize without help of much sophisticated instruments. We have investigated controlled growth of size, structures, surface morphology tuning by different parameters like substrates, growth time and studied basic growth kinetics and stability of the systems.

There are two most commonly used strategies for solution processed film of perovskite halides namely, --i) one step solution process ii) two step solution process

We applied both techniques to prepare our samples. Let us briefly describe these two processes.

One Step Solution Process: The one step solution process mainly invokes two issues, i.e removal of excess solvent through evaporation and crystallization of solid perovskite film. In a standard one step crystallization method, the aforesaid processes happen simultaneously. However, the problem in one step process is film shrinkage.

Two Step Solution Process: In two step process generally a seed layer is deposited first. Due to layer structure of lead halides it is easy to fabricate a compact, uniform film of seed layer. Then this film is immersed in suitable solution of A site cationic halide (i.emethylamine iodide (MAI) etc) which favours intercalation. [4-6]

These two processes are schematically illustrated in the following figure 2.1.

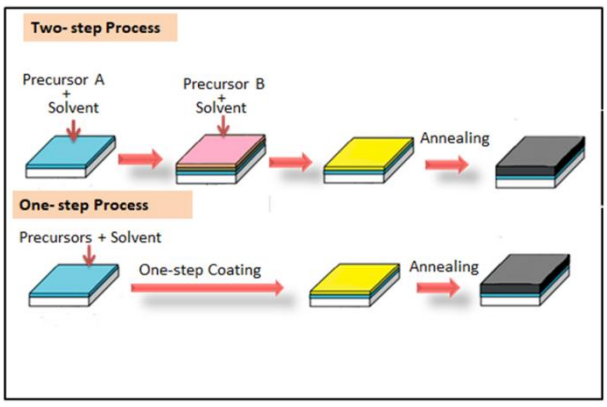

Figure 2.1: *Schematic of one step vs. two step process for growth of solution processed halide perovskite films [4]*

However for any synthesis process, precursors are primary ingredients. Since we have worked on different materials under family of perovskite halide system, in following table the precursors related to different material synthesis are listed following.

	Materials	Precursors		Used in study
		A	B	
1	$CH_3NH_3PbI_3$/($MAPbI_3$) Methyl ammonium lead iodide	PbI_2	CH_3NH_3I	Gas Sensing Property/ Optoelectronic
2	$CH_3NH_3PbBr_3$/($MAPbBr_3$) Methyl ammonium lead bromide	$PbBr_2$	CH_3NH_3Br	Gas Sensing Property
3	$CH(NH_2)_2PbI_3$/($FAPbI_3$) Formamidium lead iodide	PbI_2	$CH(NH_2)_2I$	Gas Sensing Property/ Radiation detection/Optoelectronic
4	$MA_xFA_{1-x}PbI_3$ Mix Cation lead iodide	PbI_2	CH_3NH_3I +$CH(NH_2)_2I$	Optoelectronic

Table 2.1: *The compounds of halide perovskite family with their related precursor and respective applications studied in this thesis*

First we thoroughly describe the detail synthesis routes of methylammonim lead iodide ($CH_3NH_3PbI_3$) halide by both techniques (one step and two step) and see their consequences of growth processes. Then we simply translate the process to the other system as well since techniques are similar.

2.2.1. Synthesis of Nanostructured Thin Films of Methyl Ammonium Lead Iodide by wet route chemistry:

Methylammoium lead iodide micro and nanostructure synthesis involves two parts:

a) Synthesis of Methyl ammonium Iodide

b) Chemical growth of micro and nano structure in different substrates:

2.2.1.1 .1Synthesis of Methyl ammonium Iodide:

Methyl Ammonium was taken in a conical beaker keeping inside a thermocol box filled with ice cubes. Hydro Iodic acid was then slowly added to the above solution during stirring at 900 rpm. The reaction was continuing for 4 hours. Then we got the dark brown color solution.

$$CH_3NH_2 + HI \longrightarrow CH_3NH_3I$$

The above dark brown solution was heated for 1 hour at 100^{o} C until the amount of liquid evaporated to half. Then it was kept for cooling in normal condition and obtained colorless crystal & light brown color solution. After that, cold diethyl ether was added for cleaning. The process was repeated until getting the colorless crystals.

Recrystallization: The colorless crystals were dissolved by adding Ethanol & cold ether was added until the full colorless solution transformed to white precipitation powder. Then the white powder was taken out from filter paper for vacuum annealing. Then the whole precipitation powder was heated at 60^{o}c for 24 hours to obtain the final product. A typical flow diagram has been shown in the following figure 2.2.

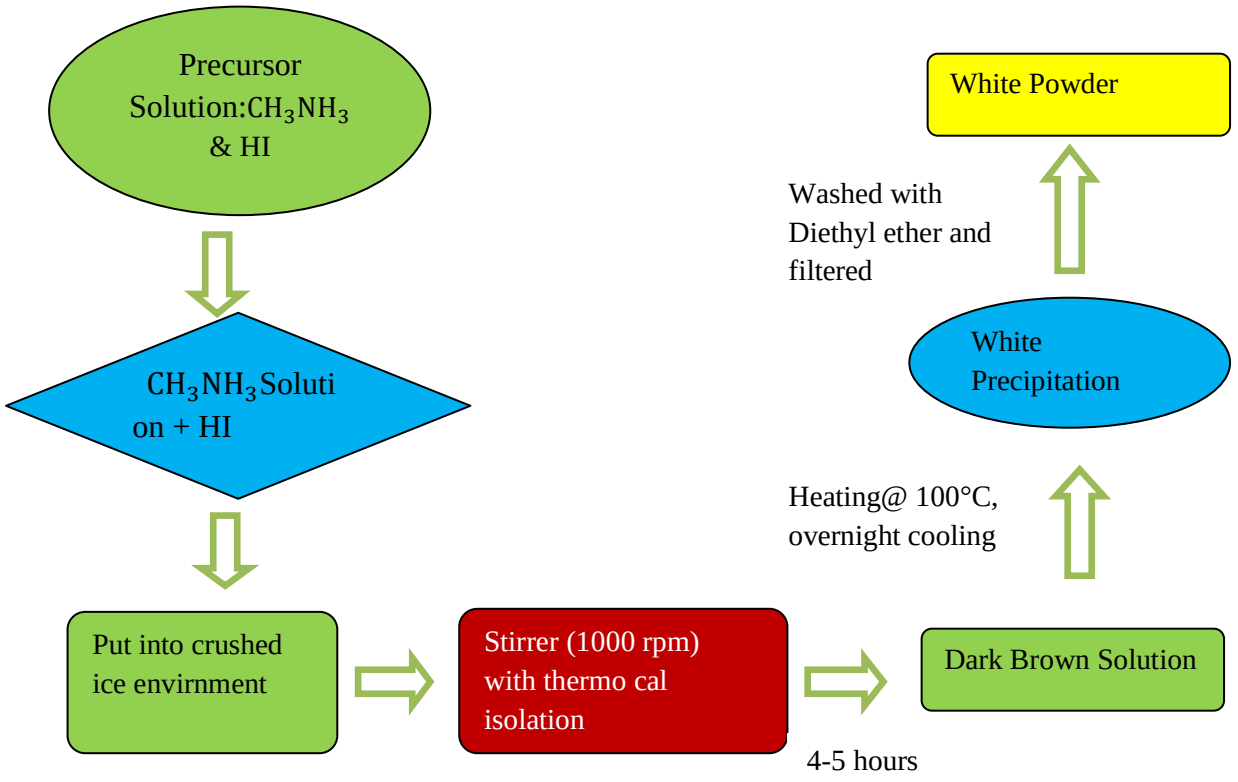

Figure 2.2: *Flow chart of preparation of methyl ammonium iodide (MAI) powder*

2.2.1.2 Chemical growth of micro and nano structure on different substrates:

- **Two step Process:**

First we prepared saturated solution of lead iodide by mixing lead 1 molar Iodide (PbI_2) in N, N, DMF (dimethylformamide). Later this solution was spin coated on different substrates like SiO_2/Si, ITO coated glass, FTO, some other flexible substrates like, kapton, paper etc. at

2000 rpm for 30 sec to investigate different morphology. After that the spin coated substrates are heated at around 70°C for 30 minutes. The CH_3NH_3I was mixed with IPA (2 propanol) at different concentrations. Finally substrates were immersed in the CH_3NH_3I/IPA solution and allowed for different reaction time to get subsequent morphologies. A typical flow chart has been shown below in figure 2.3.

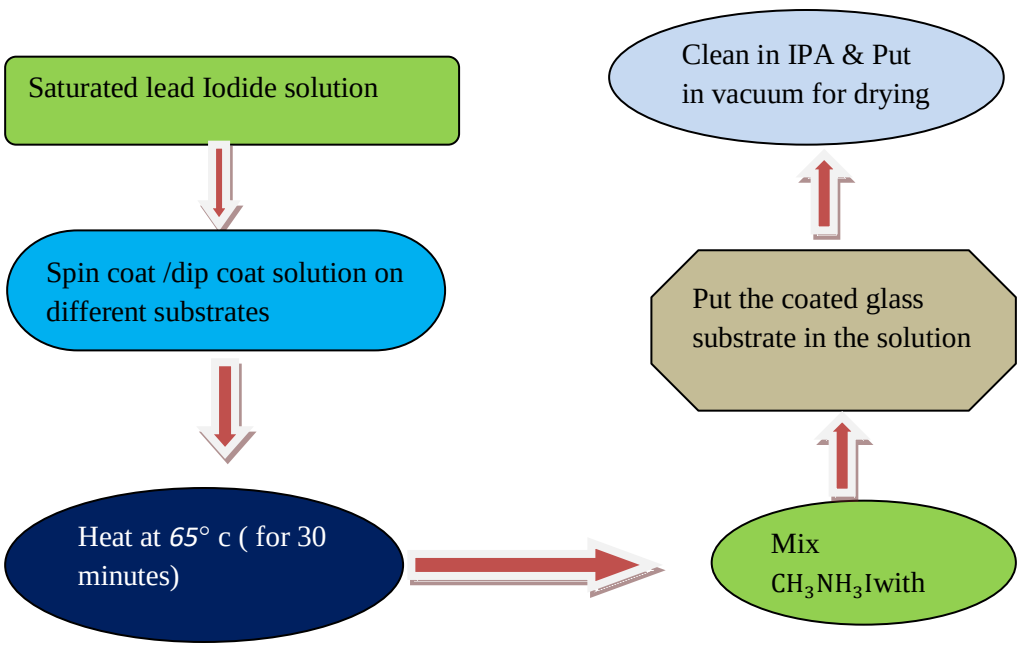

Figure 2.3: *Schematic of two step process used in this thesis for growth of halide perovskite films*

- **One Step Process:**

For one step solution growth process, first by equimolar lead Iodide (PbI_2) with methyl ammonium Iodide (CH_3NH_3I) are mixed at 1:1 molar ratio in dimethylformamide (DMF). Then different substrates are spin or dip coated for ~30 sec to in the solution. Then, the coated substrates are kept at 100° C in an oven for ~ 20 minutes drying. Finally this forms the desired morphology on different substrates. In figure 2.4 the flow chart of one step process in described.

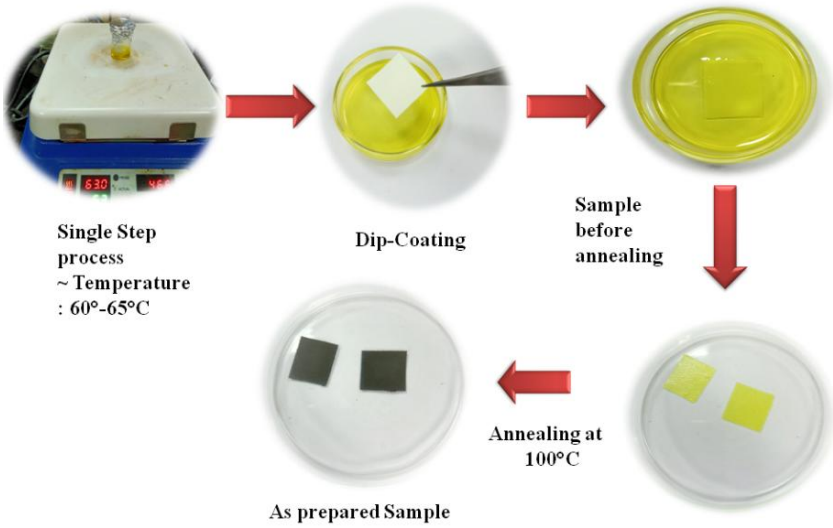

Figure 2.4: *Flow chart of one step process used in this thesis for growth of the films*

2.2.2. Study of influence of growth parameters on synthesis:

Controlled growth tuning shape, size and morphology is very crucial for experimental purpose and getting superior properties. Particularly, current days semiconductor 1D nanowires and nanorods are very promising for observing different exciting properties along with application potentials in many fields like optoelectronics, sensors etc. In case of perovskite halide materials, film compactness is highly desirable as it greatly influence the device performances. In particular, the halide film needs to be uniform, pinhole free for better performances. As mentioned in introduction section, there are several reports where film compactness hinders the device performance especially in case of perovskite solar cell [4]. There are different strategies followed for getting uniform, compact perovskite films like solvent co evaporation, chemical vapor deposition (CVD).However, still there is open challenge to improve film compactness to enhance its performances. Hence, we have focused to investigate for a uniform, pin hole free with special attention to form nano/micro structures; nanowire/ nanorods like surface morphologies, as these morphologies are preferred for superior application impact.

2.2.2.1Effect of Substrates on Surface Morphology:

There are reports on to control better surface coverage like solvent engineering, growth time etc [4-5]. We investigated whether varying substrates can achieve the good compact film. Since, flexible, low cost, portable substrates are in great demand in current semiconductor device application like flexible TFT, flexible Photo detector& LED etc, We checked this

issue varying range of substrates from common FTO coated glass, ITO coated glass to flexible kapton paper keeping in mind to explore perovskite as flexible devices for different applications. Different substrate induced surface morphologies are shown below in figure 2.5.

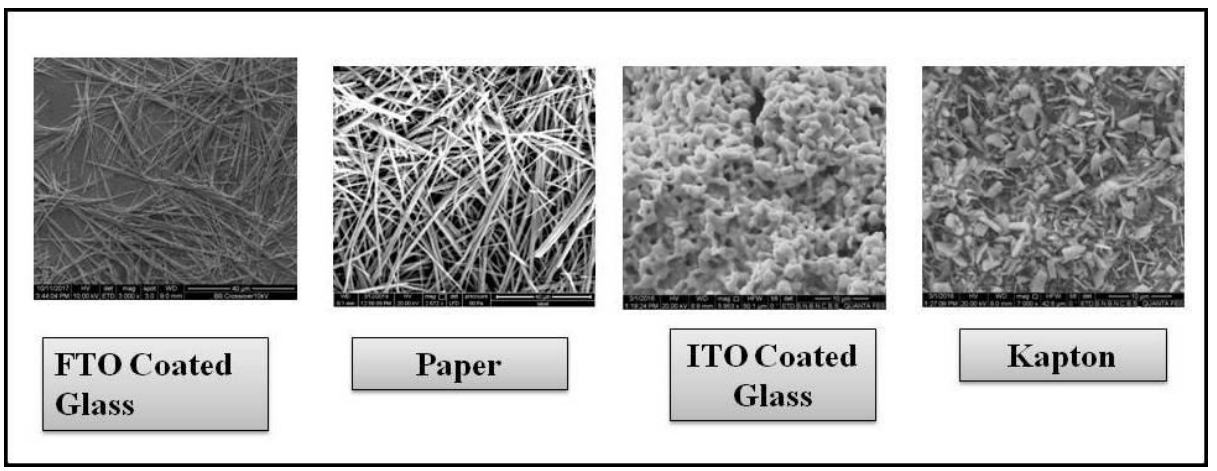

Figure 2.5: *Different surface morphologies of $MAPBI_3$/ MAPI films grown on different substrates*

Innovative use of paper as substrate to develop paper electronic based device for detectors:

Interestingly we have observed that compare to other substrate, paper substrate under same condition could give rise the nanorods morphology with much uniform and compact coverage, pinhole free morphology which is more prominent in figure 2.6. Not only that, we have observed that paper grown samples are stable relative to the others grown on conducting substrates. Thus paper could be an important attempt for providing compact and scalable approach for better coverage of the film for stable device performance. Thus we choose paper as substrate for our study. In our whole thesis, we mainly restrict our self to study different properties of perovskite halides using paper substrate. Another advantage of paper substrate is, being flexible and low cost and can also be used as cost effective wearable devices.

Since paper substrates can be easily dip coated in the solution, we adopted one step solution process to grow the films in substrate like paper. Finally, we found that, it gives very promising application potential in various detectors [8-10]. Hence, we adopted the paper based substrate and followed one step solution process for film synthesis of methyl ammonium lead iodide and other members of lead based halide family.

Introduction of paper as a substrate is one of the prime novelty of the thesis.This thesis work focus on new application potential of the perovskite halide series of material grown on paper as paper electronics based detectors; namely, gas detector, photo detector and radiation detector. Growth of perovskite halides using such substrates and making of paper electronic based device has been never introduced before to the best of our knowledge. Substrate induced specific morphology from such paper substrate is unique for perovskite halide system, which favors to make device for different detectors as will see in upcoming chapters.

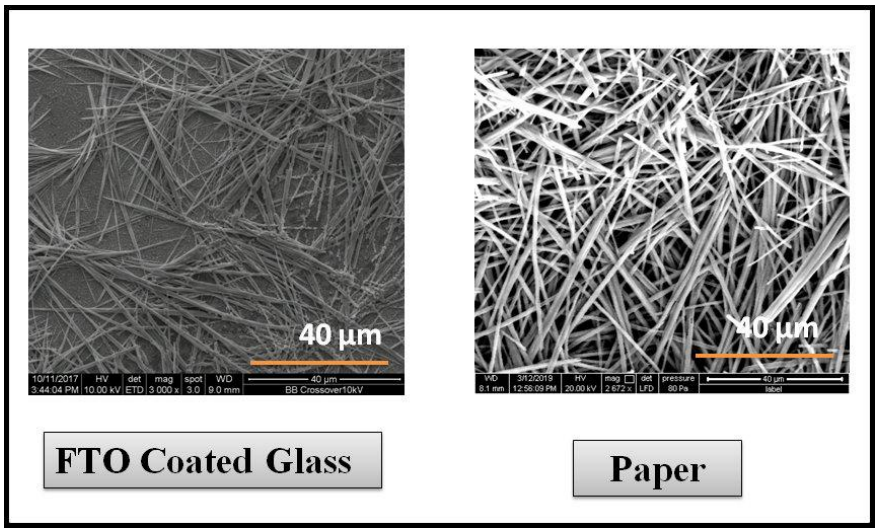

Figure 2.6: *Difference in compactness & uniformity of surface morphology of MAPI grown on two different substrates namely FTO coated glass and simple paper*

2.2.3 Synthesis of $CH_3NH_3PbBr_3$ / (MAPB), CH $(NH_2)_2PbI_3$ /FAPI and mixed Halide Microstructures by One Step Method:

MAPB microstructured film has been synthesized by equimolar mixing of lead bromide ($PbBr_2$) with methyl ammonium bromide (CH_3NH_3Br) at 1:1 molar ratio in dimethylformamide (DMF). Then different substrates spin and dip coated for ~1 min to dip coat in the solution. Then, these spin/dip coated substrates are kept at 120° C in an oven for ~ 20 minutes drying. This helps to form the of MAPB micro structures on the different substrates. Similar fashion was followed to synthesis FAPI. The lead iodide (PbI_2) and formamidium iodide (CH $(NH_2)_2I$)/FAI were mixed in DMF. Rest process is same (as shown in section 2.2.1) except annealing was done at 140°C.

For mixed halide film formation, mixed cation perovskite halide was synthesized by mixing of lead iodide ($PbBr_2$) 1 (M) in gamma butarolactone (GBL). After that methyl ammonium iodie (MAI) and formamidium iodide (FAI) were mixed in the PbI_2 solution in ratio of 3:2,

i.e (MAI: FAI=3:2) maintaining overall ratio between MAI/FAI and PbI_2 1:1 in the mixture/solution. We tuned the cation mixing as MAI and FAI at 3:2 ratio for its better optoelectronic property than other compositions. A commonly used paper then immersed for ~1 min to dip coat in the solution. Then, the dip coated paper finally is kept at 140° C in an oven for ~ 30 minutes for drying.

2.2.4 Bulk Single/Oriented Crystal Growth of Perovskite Halides:

Single crystals are uniform platform to study different physical properties like transport, carrier dynamics and very promising for application point of view. Since, single crystals are defect free, absence of grain boundary makes them preferable choice for superior performances in many applications like optoelectronic, radiation detector etc. Although there are wide use of thin films of perovskite halides in different photo voltaic and optoelectronic properties, but use of single crystal for studying different physical properties and applications is limited.

There are several strategies followed for bulk single crystal growth of perovskite halides – namely –i) solution temperature lowering method (STL method) ii) inverse temperature crystallization (ITC) method iii) anti solvent vapor assisted crystallization method iv) melt crystallization method [7,11].

We adopted the inverse crystallization temperature method because it is faster and relatively large crystals can be grown using this method. The mechanism of ITC method lies in balance between dissolution and precipitation. At lower temperature, the molecules are more attached to the solvent molecules completely. As temperature increases, the bonding energy deceases, more perovskite molecules concentrate in the solution. Nucleation occurs at some point when the solution become supersaturated, followed by crystallization. Choice of proper solvent is a key factor for this method [11].

It has been well accepted that FAPI holds better stability in comparison with MAPI [12]. So, we choose FAPI as a material to grow the single crystal.

The single crystals of $FAPbI_3$ are prepared using solution growth process with slight modification of standard inverse solubility mechanism. In this process,the nucleation is induced by the inverse solubility dependent on temperature in some organic solvents. As we already mentioned above that choosing proper solvent that plays a crucial role to form crystals in ITC method, we have used GBL as a solvent for its good solubility to the precursors (FAI and PbI_2) as well as remarkable solubility gradient with temperature.

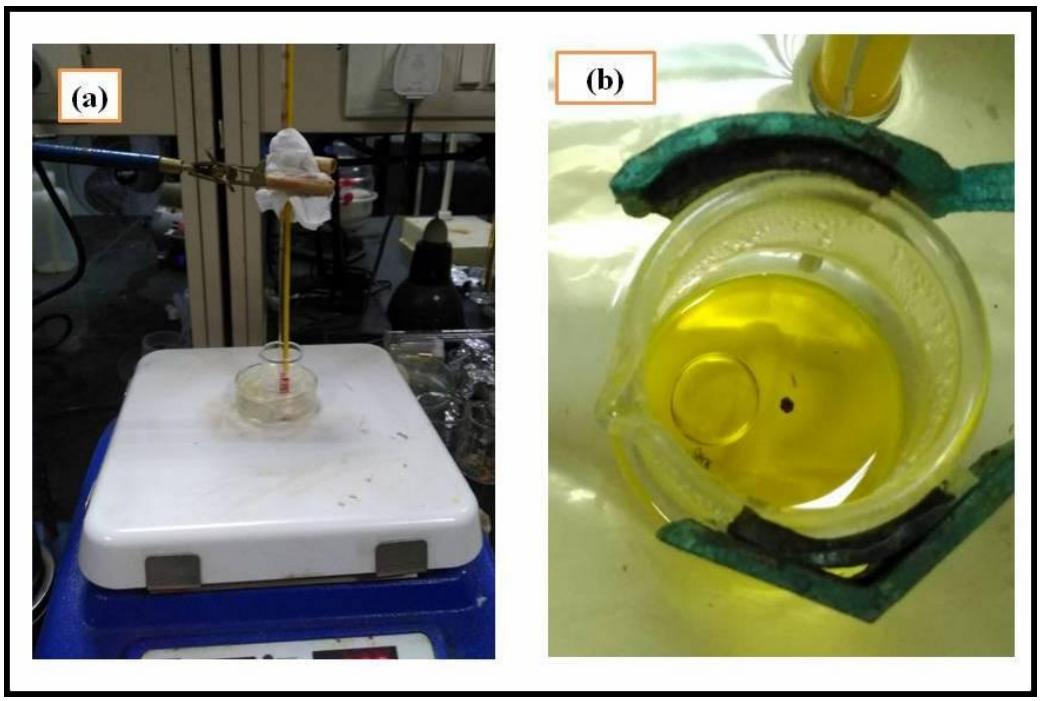

Figure 2.7: *(a) Experimental set up for growth of solution processed bulk crystals of FAPbI3/FAPI (b) Seed crystal of FAPI*

First equimolar FAI and PbI_2 are mixed in the GBL at 60°C under stirring until a clear solution is obtained. Then large single crystals were grown involving two steps: seed crystal preparation and large single crystal growth. First seed crystals were grown from the precursor solution maintaining uniform temperature at 110° c using oil bath. This process takes around 3 to 4 hrs. The seed crystals obtained around 2 mm x 2mm size. Then, one of seed crystals is picked up very carefully and that seed is placed on the similar solution maintaining identical temperature as shown figure 2.7. After 2 days, a large crystal of dimension ~ 5mm x 5 mm is obtained. The pictorial diagram has been shown in the following figure 2.8.

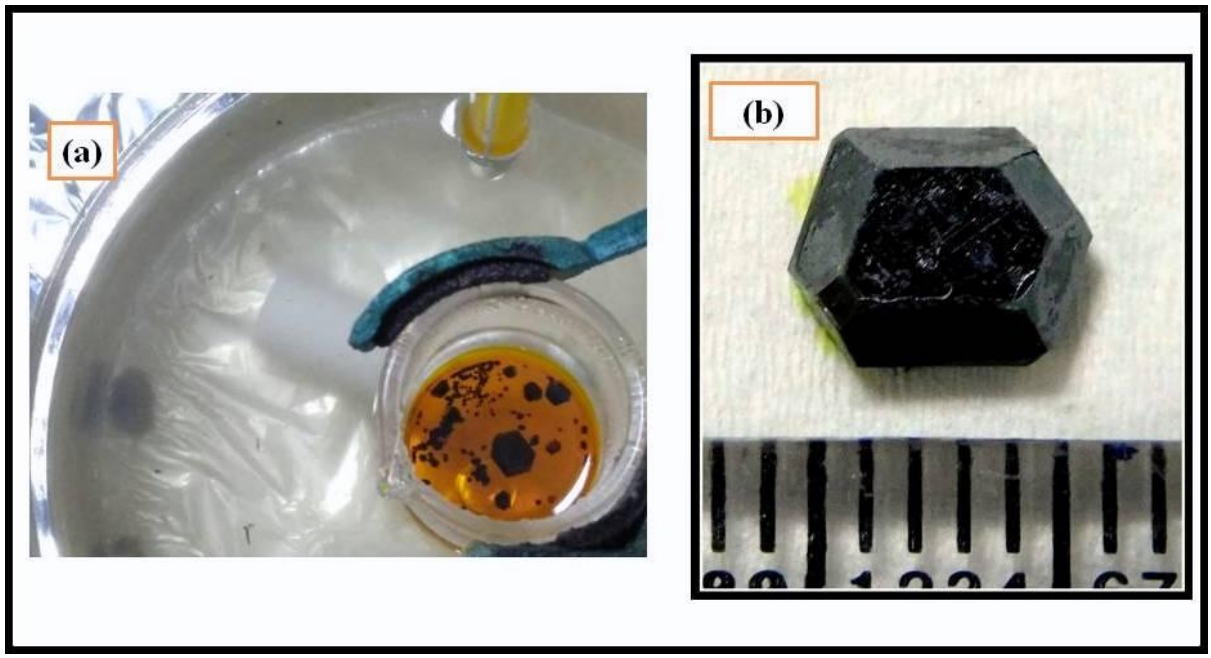

Figure 2.8: *(a) Typical growth process of bulk crystals of FAPI (b) Actual photographs of a as synthesized crystals*

2.3: Characterizations:

After synthesis of the samples, the characterizations are important to get insight about the material's quality, composition, surface morphologies and optical properties, so that one can get definite result. Since, our thesis is mainly focused paper based devices with these kinds of materials; the details characterizations based on only paper substrates will be described in the following.

2.3.1: Structural Characterizations:

X-Ray Diffraction Technique (XRD)

X-ray Diffraction is very often used technique to understand the crystallographic structure and phase of a material. In this thesis work we have used Panalytical X'PertPro XRD instrument having Cu(K_α) source with wavelength 1.5405 Å at an accelerating voltage of 45 kV and 40 mA current for analysis. This geometry that follows the system is the Bragg-Brentano geometry *(*θ-*2*θ*)* i.e. the sample holding stage is fixed while the X –ray tube rotates at -*θ*o/min and the detector rotates at a +*θ*o/min. The X−rays with sufficient energy penetrates into the solid sample and provide information about their crystallographic structures. The

detector which is used in this system is PIXEL detector, which has quite a low signal to noise ratio [13].

The as grown paper based perovskite halide samples are characterized by XRD system to get information about their crystallographic structure as shown in following figures.

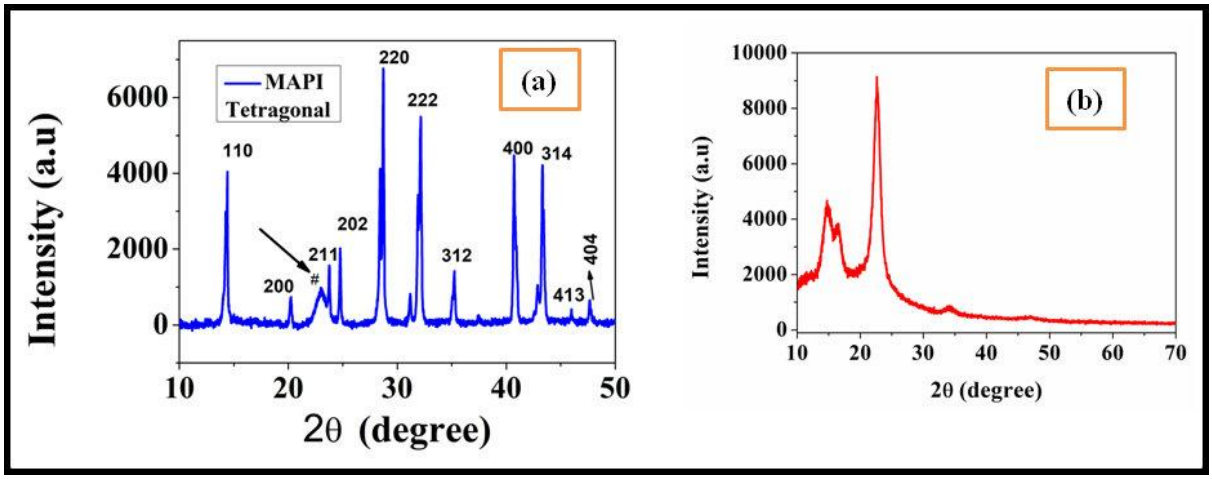

Figure 2.9: (a) *Fully indexed XRD of as grown MAPI film grown on paper. # mark coming from paper substrate. XRD shows tetragonal structure at room temperature (b) XRD of bare paper*

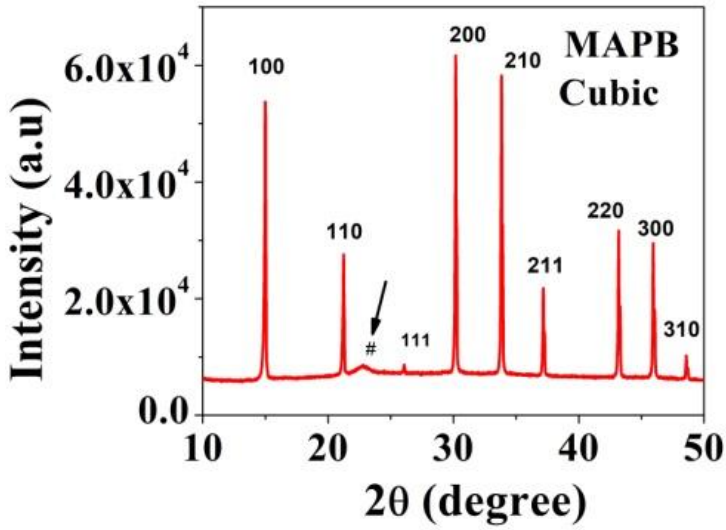

Figure 2.10: *Fully indexed XRD of as grown MAPB film grown on paper. # mark coming from paper substrate. XRD shows cubic crystal structure at room temperature*

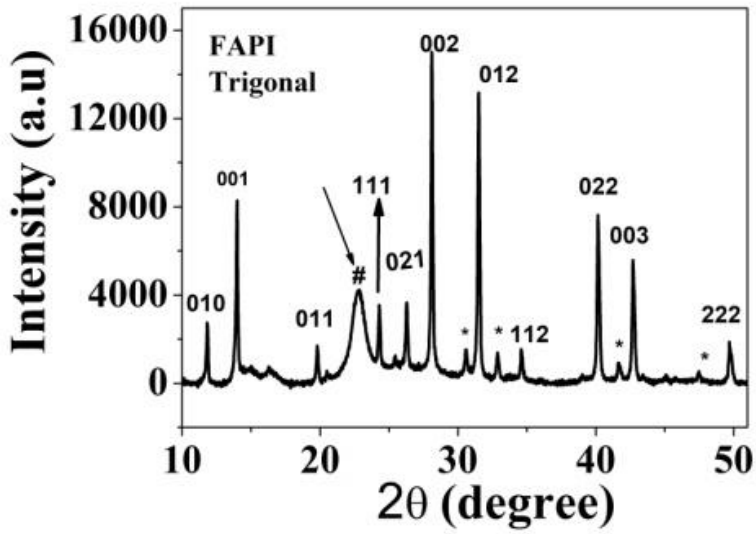

Figure 2.11: *Fully indexed XRD of as grown FAPI film grown on paper. # mark coming from paper substrate. XRD shows trigonal crystal structure at room temperature*

MAPI/paper shows tetragonal structure, where MAPB/paper shows room temperature cubic structure and FAPI/papers shows trigonal structure grown on paper at room temperature. The XRD of three samples has been shown in figures 2.9, 2.10, 2.11 respectively. XRD of the bare paper substrate has been taken to confirm the phase of material under research.

Morphological & Compositional Characterizations:

FESEM is the most used tool to fetch information about Morphology and topography of the as grown samples. It is an imaging technique based on electron beam that is scanned onto a sample, and scattered electrons are used to construct an image. The focused electrons emitted from the source and interaction with sample produces secondary electrons, back-scattered electrons, auger electrons, cathodoluminiscence and X-rays. A field emission electron gun is typically used as source to inject highly focused beam of electrons through an accelerating grid, condenser lens, objective aperture and scanning coils and finally through an objective lens and then scanned onto the sample, kept on a motorized stage. The beam is scanned over the sample in a raster pattern in synchronization with a cathode ray tube. Generally the secondary electrons are detected using an Everhart-Thornley detector [14]. Their intensity is proportional to the signal detected. The image obtained is black and white, corresponding to the intensity of the spot, which brings contrast to the image. SEM has a large depth of field (few mm) that allows a large amount of the sample to be imaged at once. It also has a very high resolution (1-10 nm) depending on the source used and the pixel size of CCD).

We have shown as grown paper based sample of three compositions along with their respective morphology as shown in figure 2.12. MAPI shows tetragonal structure with nano rod like (diameter ~300nm) surface morphology, MAPB shows room temperature cubic structure with micro cube/nano cube (~ 2-3 μm) morphology, and FAPI shows trigonal structure with the morphology of fibers like cellulose paper.

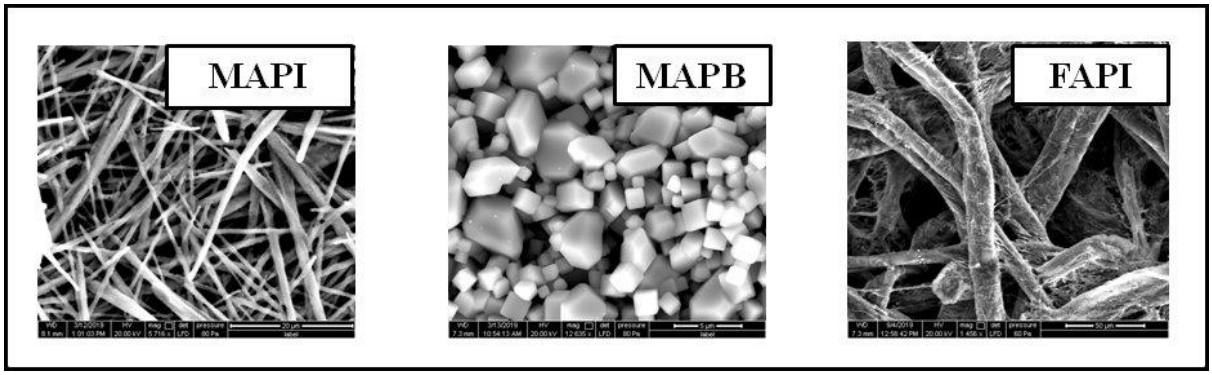

Figure 2.12: *Different surface morphology of different halide perovskites grown on paper. MAPI shows rod like structure, MAPB shows cube shape structure and FAPI fiborous structure*

EDX Analysis:

The X-Rays produced by the interaction of the primary electron beam with the sample are useful for elemental identification and is used for elemental quantification through EDX. The energy of X-Ray from each shell in an element is unique and provides as an accurate method for chemical analysis. Characteristic X-rays originates from electron transitions between core shells. An electron is first knocked out in order to create a vacancy, which gets filled up by X-ray emission. The number and energy of the X-rays emitted can be measured by an energy dispersive spectrometer. The specific energy of the X-ray peak has to be identified for each element. It is a very useful tool for elemental identification.

2.3.2. Optical Characterizations:

Optical characterization is non-contact method to investigate and analyze the optical properties of bulk and nano materials. We have utilized UV-visible spectroscopy to determine the optical band gap of perovskite lead halides. The photoluminescence spectroscopy has been utilized to investigate the emission and defects of perovskite halides.

UV-Visible Spectroscopy:

UV-Visible spectroscopy is one of the oldest and important tools to determine the absorption of light through the liquid or solid sample. The fundamental principle of UV-visible spectroscopy is based on electronic transition from a lower energy state to a higher energy state. A beam of light from UV-Visible source splits into different wavelength by diffraction grating. Then each monochromatic beam splits into two equal intensity beams by half mirrored device. One of the divided beams that go to sample named as sample beam with an intensity of I and other beam whichgoes to reference sample named as reference beam with intensity $I_0$are incident on the sample and a reference sample. The intensities of these light passes through the sample and reference sample are measured by electronic detectors and compared.

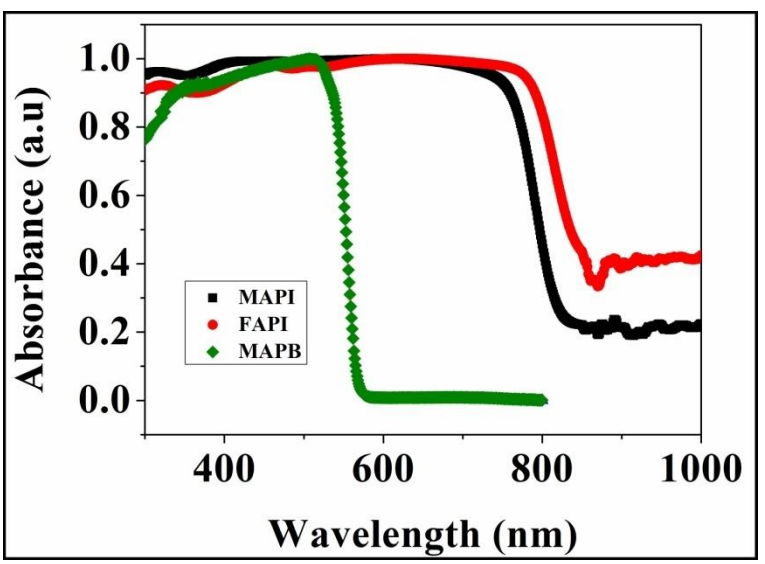

Figure 2.13: *UV-Vis absorption spectra of three different halide perovskites grown on paper substrate*

We have measured the UV-Visible spectra of solid paper based samples within range of 300-1000 nm by a spectrometer (PerkinElmer LAMBDA 750) in reflectance mode. The recorded absorption spectra have been shown in figure 2.13 and used to calculate the band gap of the paper based samples. In following table (table no 2.2) we have shown the materials and related band gaps of them.

Materials	Band Gap (eV)
$MAPbI_3$/MAPI	1.53
$MAPBBr_3$/MAPB	1.49
$FAPBI_3$/FAPI	2.3

Table 2.2: *Different halide perovskites and their respective band gaps*

Photoluminescence Measurements:

Photoluminescence measurement is a contactless, powerful method to probe the electronic structure of the material. In a typical photoluminescence experiment, a beam of light corresponding to the band gap energy or more than this is allowed to interact with the sample which absorbs and excites the electrons to jump into the conduction band from the valence band leaving behind equal numbers of holes in the valence band. These excited electrons stay in conduction band for very short time (lifetime of the electron), eventually

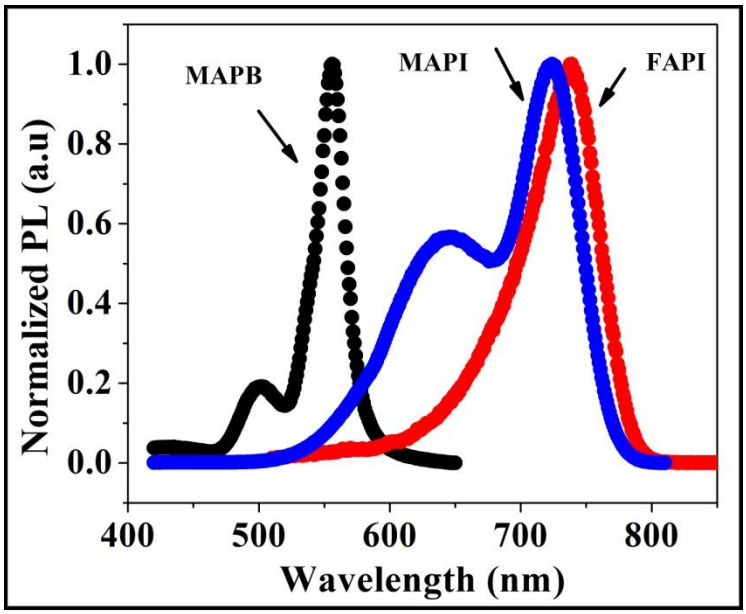

Figure 2.14: *Photoluminescence spectra of three different halide perovskites grown on paper substrate*

they recombine with photo generated holes. During recombination process, material gives the emission. The intensity and spectral content of this emission provides the material properties such as band gap level and impurities or defect levels. This technique has the highest potential to identify the extremely low concentration of intentionally or unintentionally created defect states which strongly affect material quality. We have performed

photoluminescence spectroscopy by spectrometer (Flurolog) for all materials where main observed peaks are band to band transition consistent with their band gaps. The MAPI has characteristics band to band edge emission peak is at 780 nm, MAPB is ~ 552 nm and FAPI shows its band to band transition ~795 nm as shown in figure 2.14.

2.4 Device Fabrications:

The novelty of this thesis work is, it focus on a new application potential of the solution processed perovskite halide series of material grown on paper as paper electronic based detectors; namely, gas detector, photo detector and radiation detector. Hence fabrication of device on paper is one of the important works. Single crystal based device was also made to perform experiment.

2.4.1 Details description of Device Fabrications:

All electrical and optoelectronic measurements were done using paper based devices with suitable channel lengths. The planner geometry is followed for electrical and optoelectronic measurements. As prepared perovskite halides coated paper was cut into small pieces (typical size of 1cm X 5mm) to form the device by thermal evaporation of two electrodes by metal masking. The typical channel length is ~1 mm for gas sensing and for optoelectronic measurements the channel length was made around 100 µm. Schematic of the paper devices are shown in figure 2.15. For radiation detection measurements, the opposite faces of the single crystals are metalized to make vertical device geometry with thickness ~ 2 mm.

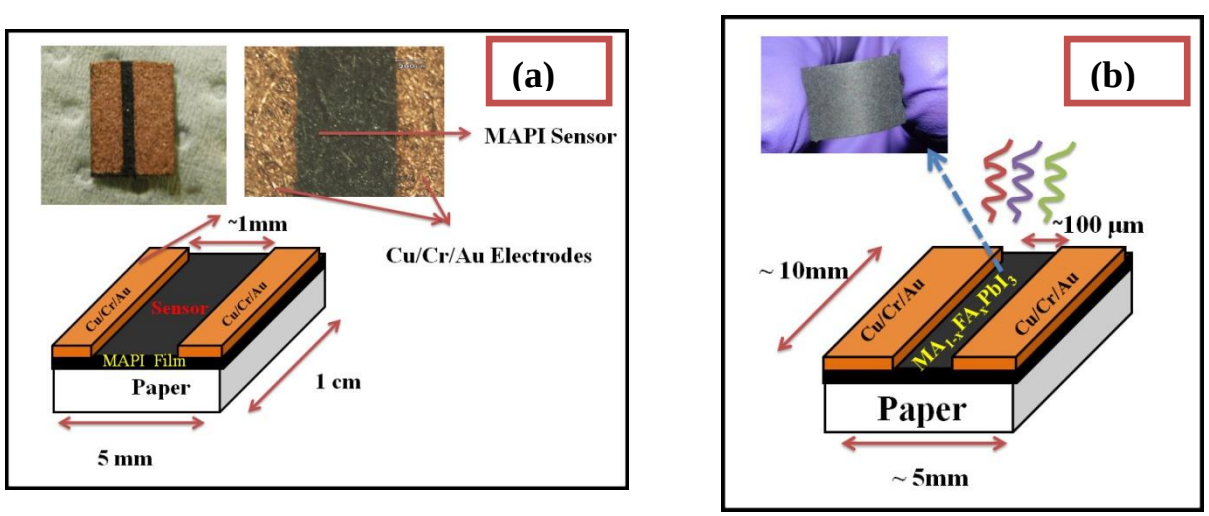

Figure 2.15: (*a) Schematic of paper based gas sensor devices along with actual photograph of halide perovskite MAPI (b) Schematic of paper photo detector using mixed cation ($MA_{1-x}FA_xPbI_3$) halide perovskite*

2.4.2 Metallization and Evaporation Chamber:

Metallization on paper based devices are done by thermal evaporation of Cu and Cr/Au pads in sequence through a metal mask in a customized chamber as shown in figure 2.16. All the devices under experiment have been metalized in this chamber. The body of this chamber is made up of stainless steel. It consists of (i) a port connected to high vacuum turbo pumping system, (ii) another port for gas inlet/outlet, (iii) three crucibles/baskets used for Cu, Cr and Au or another evaporation material, (iv) six electrodes each two are connected with one crucible to give power supply for heating the crucibles, (v) three Pt100 thermometer to measure the temperature of the crucibles, (vi) a transformer with adjustable rotor to supply power across the electrode for evaporating the materials, (vii) a sample holder mounted on a controllable rotating sample stage, (x) a movable mechanical shutter in between crucibles and sample holder and (xi) a door containing two view ports. On the top flange, there is provision for two electrical leads for applying bias across the sample electrodes. The chamber is

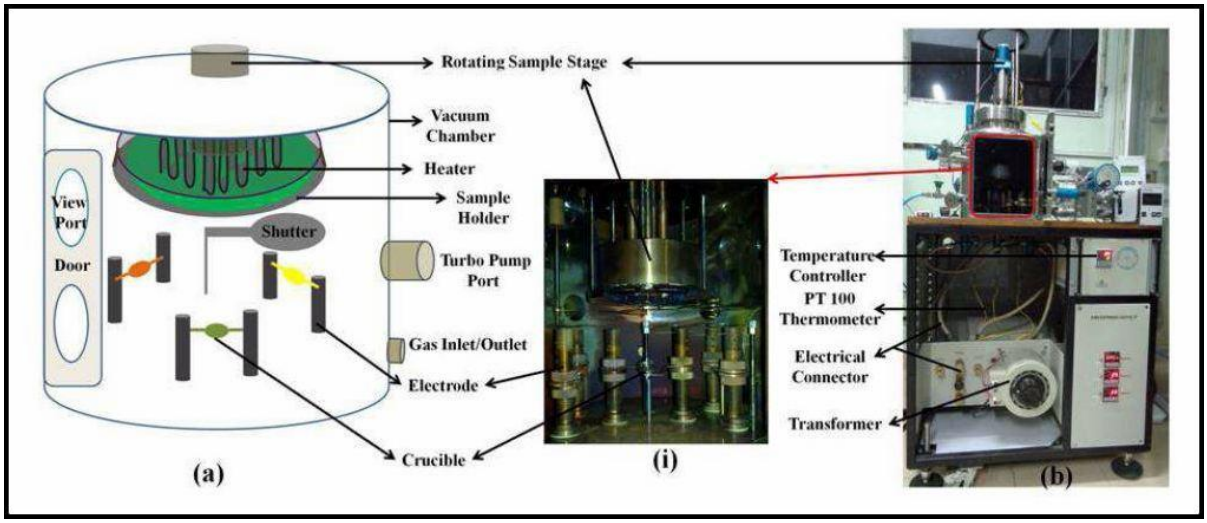

Figure 2.16: *(a) Schematic (b) Actual photograph of the deposition chamber for metallization of paper based devices used in this thesis* [15]

pumped with a Turbomolecular pump giving a base pressure of $\sim 4 \times 10^{-7}$ mbar. In this chamber three materials can be deposited consequently without breaking the vacuum. In our devices, metallization was done by thermal evaporation of Cu and Cr/Au pads in sequence through a metal mask to make the electrodes.

2.4.3 Choice of Electrodes:

A metal semiconductor junction becomes ohmic contact if the barrier height is zero at the interface. In this case carriers are free to move in and out of the semiconducting channel with negligible resistance across the contact. An ohmic contact is preferred because of easy flow of electron. We observed that copper (Cu) provides ohmic, whereas, gold (Au) electrodes show shotkey barrier. The reason behind ohmic contacts depends entirely on match of work function between electrode material and the semiconductor under measurement .We have seen that generally family of lead halide material (MAPI or MAPB) has better match with work function of Cu rather than Au[16]. So, we have chosen Cu as electrodes to make the contact ohmic. To prevent Cu electrode from oxidation, top ~10nm Cr/Au layer deposited on Cu electrode. For single crystal device, electrical contact pads were made on the opposite faces by metallization with Cu to make detector in vertical configuration. Typical photographs of halide perovskite based devices used in this thesis are shown in figure 2.17.

Materials	Work Function (eV)
MAPI/MAPB	~4.6
Copper (Cu)	4.53
Gold(Au)	5.1

Table 2.3: *Work Function of Halide Perovskites and respective electrodes for appropriate choice of electrodes*

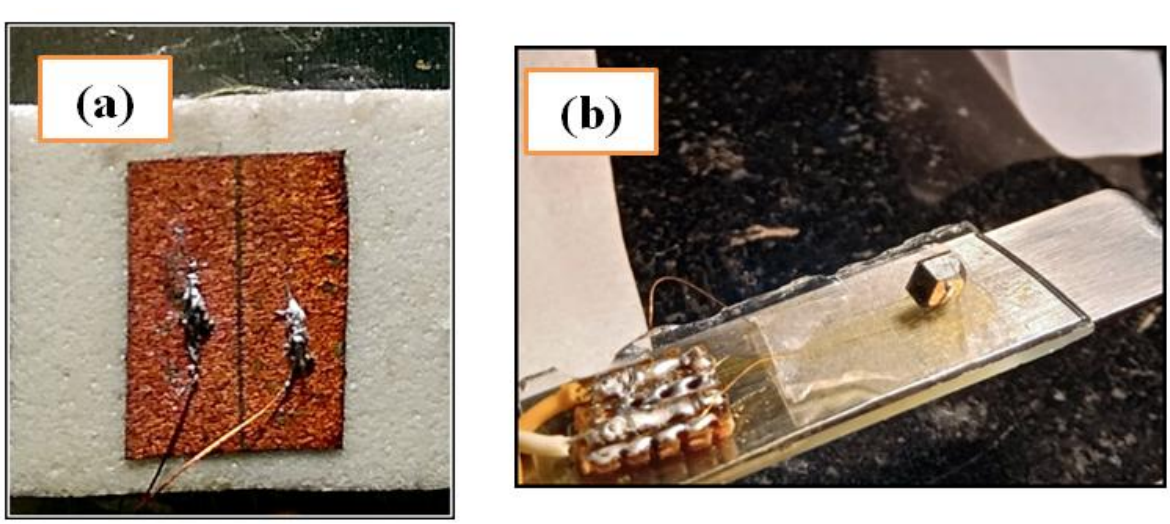

Figure 2.17: *Actual photograph of the (a) typical paper based device using halide perovskite (b) Bulk highly oriented crystal based device*

2.4.4 Contacts for Electrical Connections:

Electrical contacts was made on all the paper based thin film perovskite halide devices to utilize as detectors/sensors for gas sensing, photo and radiation detection. Electrical measurements on the detectors were done using 2 probe electrodes.

Typical contacts are made by putting small amount of silver paint into the metalized electrodes. But in our case perovskite halide, use of silver paste degrades the device performances to great extent. So, special care has been taken to make the contacts without compromising device performances. Electrical connection was made through customized spring loaded clips to avoid the photo and environmental degradation as sown in figure 2.18. In some cases indium shouldering has been used in the metal pads of devices instead of silver paint as indium contact does not require such kind wetting treatment for connection.

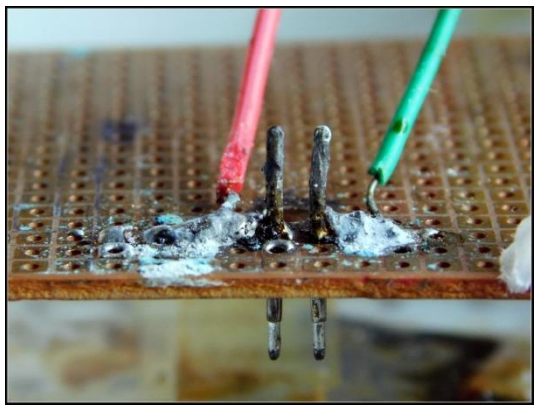

Figure 2.18: *Custom designed spring loaded clip for electrical measurements of paper based halide perovskite devices*

2.5 Experimental Set Ups and Related Measurements:

2.5.1 The Gas Sensing set UP for electrical Measurements:

A custom made set- up was developed to characterize the gas sensing properties of the materials and the sensor was placed in test chamber. The whole set-up is consisting of two different chambers. One of them is used as mixing chamber and another one test chamber. All of them are made of stainless steel. The test chamber can be pumped down to a pressure of 10^{-6} mbar by a turbo pump. The test gas was calibrated by volumetric method and compared with a commercial ammonia meter. The schematic and the actual experimental set up is shown in figure2.19 & 2.20 respectively. During the experiment, controlled amount of NH_3 gas was mixed with known volume dry Nitrogen (N_2) gas in the mixing chamber, which allows controlled testing for very low concentration of NH_3 gas. The flow rate was controlled

by a mass flow controller. $I-V$ and $I-t$ measurements were done using a Source-Meter employing a two probe configuration and custom-developed computer programs. All sensing measurements were performed at room temperature (27ºC). Spring loaded clips were used for making contact to the electrodes of the paper based sensor to prevent the moisture effect of silver paint.

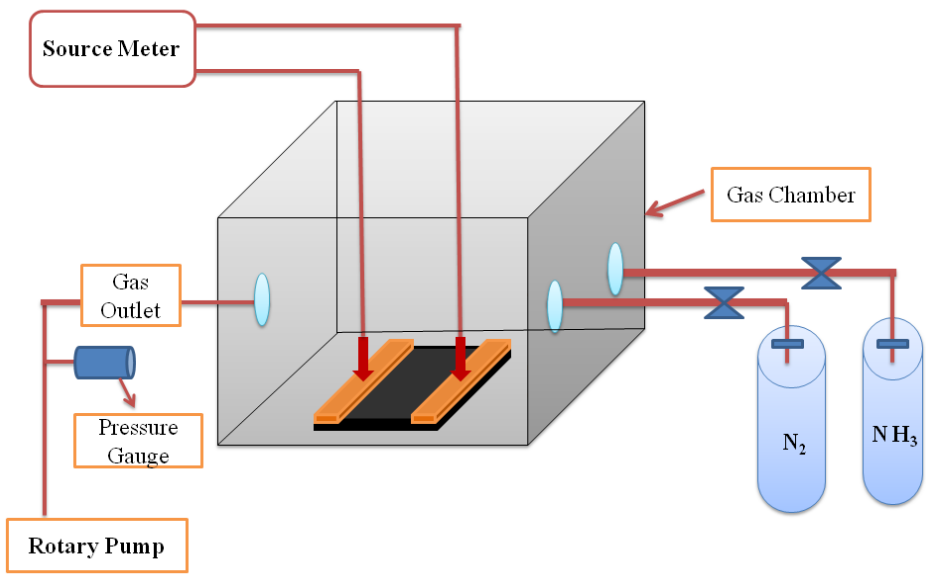

Figure 2.19: *Schematic of gas sensing measurements using halide perovskites used in this thesis*

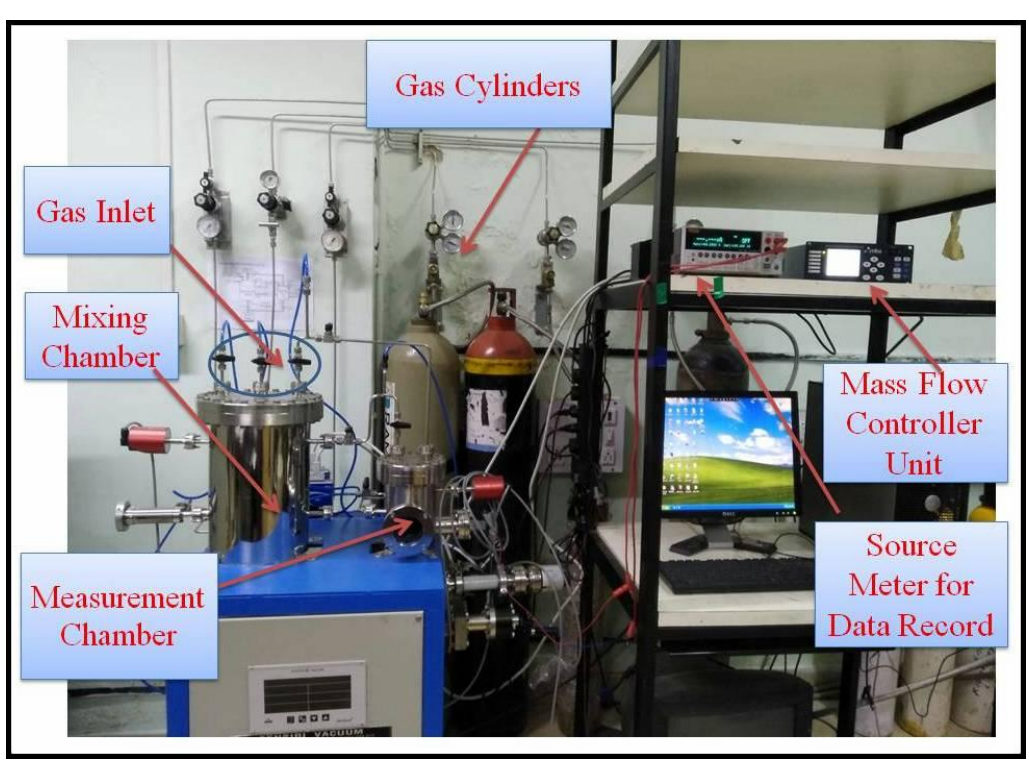

Figure 2.20: *Actual photograph of the customized gas sensing SET UP for measurement*

2.5.2 The Optoelectronic set-up:

The optoelectronics measurements enable us to get insight the information about interaction of light with matter. In a typical optoelectronic set up consist of –i) light source ii) suitable dispersive medium iii) monochromator iv) detector to measure the response.

Opto-electronic studies were performed using a standard Xenon light source (Zolix @ 150 watt) with tunable wavelengths by the monochromator in the range 300-1100nm. A xenon light source characteristic has emission lines beyond 800nm, which results in a low minimum inlight intensity at certain wavelengths. The system in the wavelength range up to 1100nm was calibrated using a Si detector with NIST traceable calibration. The illumination was turned ON and OFF by optical chopper. Power of the illuminated light falling on the sample is measured by putting a power-meter in placeof the sample. By measuring the total illuminated area on the sample and power of illumination, we have calculated the power density of illumination. A schematic of the experimental setup is shown in Fig. 2.21. The real set up is shown in figure 2.22.

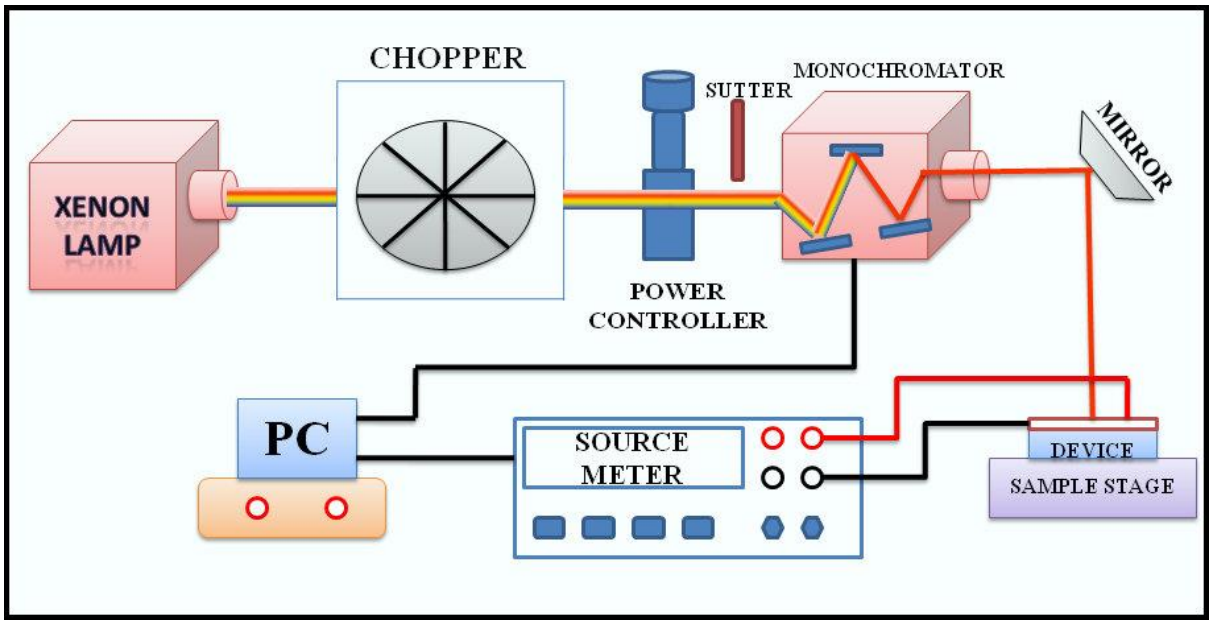

Figure 2.21: *Schematic of optoelectronic/photo response measurements using halide perovskites used in this thesis*

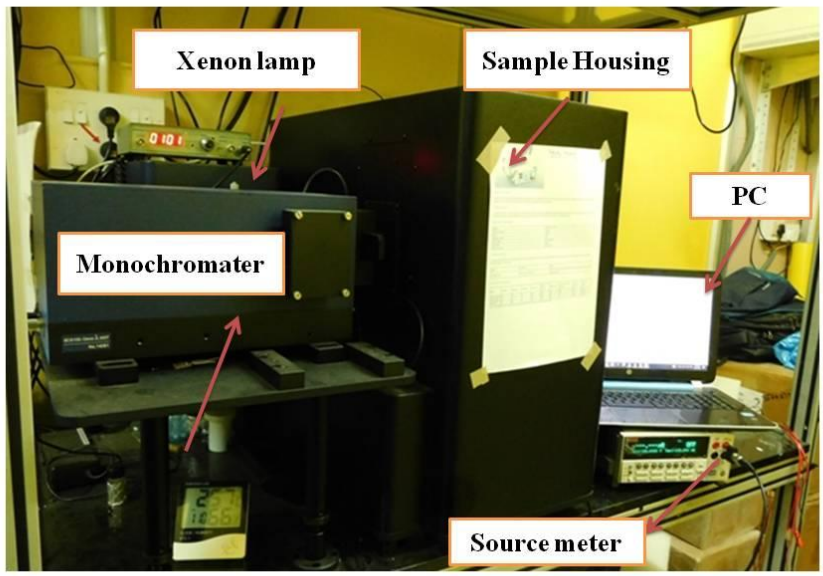

55

Figure 2.22: *Actual photograph of the photo response measurement SET UP for measurement*

The electrical measurements were performed employing two probe configurations of the paper based devices. The data were taken by source meter with chopper modulated illumination. Custom made lab-view program has been used to record the current-voltage $(I-V)$ and current-time $(I-t)$ curves in dark condition as well as under illumination through GPIB interface. These measurements enable us to get the photo current as function of wavelength and illumination intensity that is used to calculate the spectral Responsivity.

2.5.2.1 Customized Test Chamber for Optoelectronic measurements:

As discussed previously, the perovskite halides are prone to degradation under humidity which largely affects the device performances, we designed a custom made test chamber for controlled experiment protecting from moisture. The chamber was made of stainless steel consisting one optical window with high transparent quartz glass. Vacuum during experiment was used up to the order $10^{-3} mbar$ to prevent the samples from moisture; high transitive quartz glass was used to pass the light through the chamber. Also, dry Nitrogen (N_2) gas was injected to protect the environment any residual moisture during the experiment. A detail of the test chamber has been shown in figure 2.23.

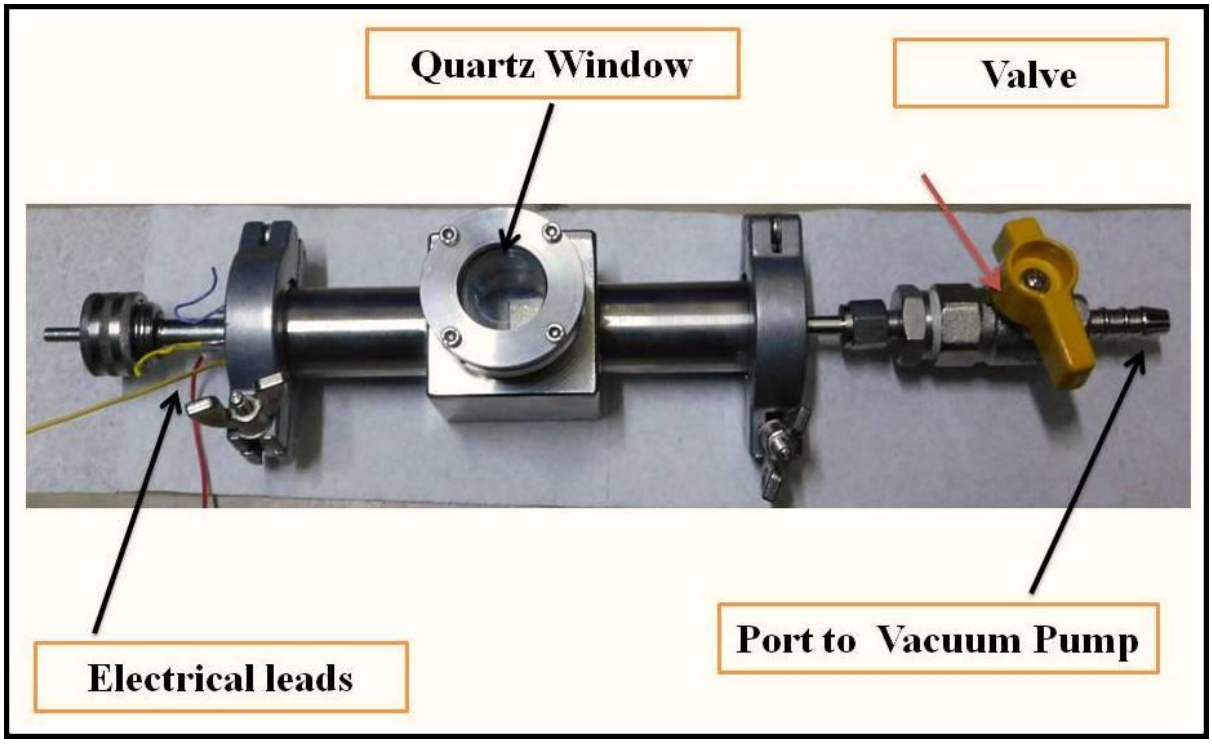

Figure 2.23: *Custom designed chamber for measuring photo response in vacuum to mitigate the effect of moisture*

2.5.3 Gamma Ray Detection Measurement:

For tracing the gamma ray using perovskite halide samples under experiment, we used two types of radiation sources with different activities. The high active source was of Co-60 with current activity ~ 1KCi contained safely in a sealed chamber. The chamber was specially designed to protect the radiation from such a radioactive source. In the top of the chamber there is adjustable insertion inside which the device is mounted that to be inserted into the radiation. The adjustable hook is controlled through programmable software, that allows the devices to be put into the radiation chamber for different exposure time and controls the motion of the devices inside the radiation. The electrical leads are made through the hook for online electrical measurements. The source detector distance was around 8 cm. To control the radiation flux on the sample, lead plates with different thickness was used to attenuate the radiation. In figure 2.24 we have shown the description of the chamber. We mention that the facility of such high energetic & radio-active gamma source is a national facility at by UGC-DAE-CSR Kolkata and not easily available throughout the country.

For low activity detection we have made a source –detector geometry and radiation was impinged to the sample with radioactive source with different activity. We have tested micro

curie level source to test our limit of detectivity of our devices. Like other properties as described above, the $I-V$ and $I-t$ measurements were done using a Source-Meter with a custom developed program employing two probe configuration. All detection properties were carried out at room temperature.

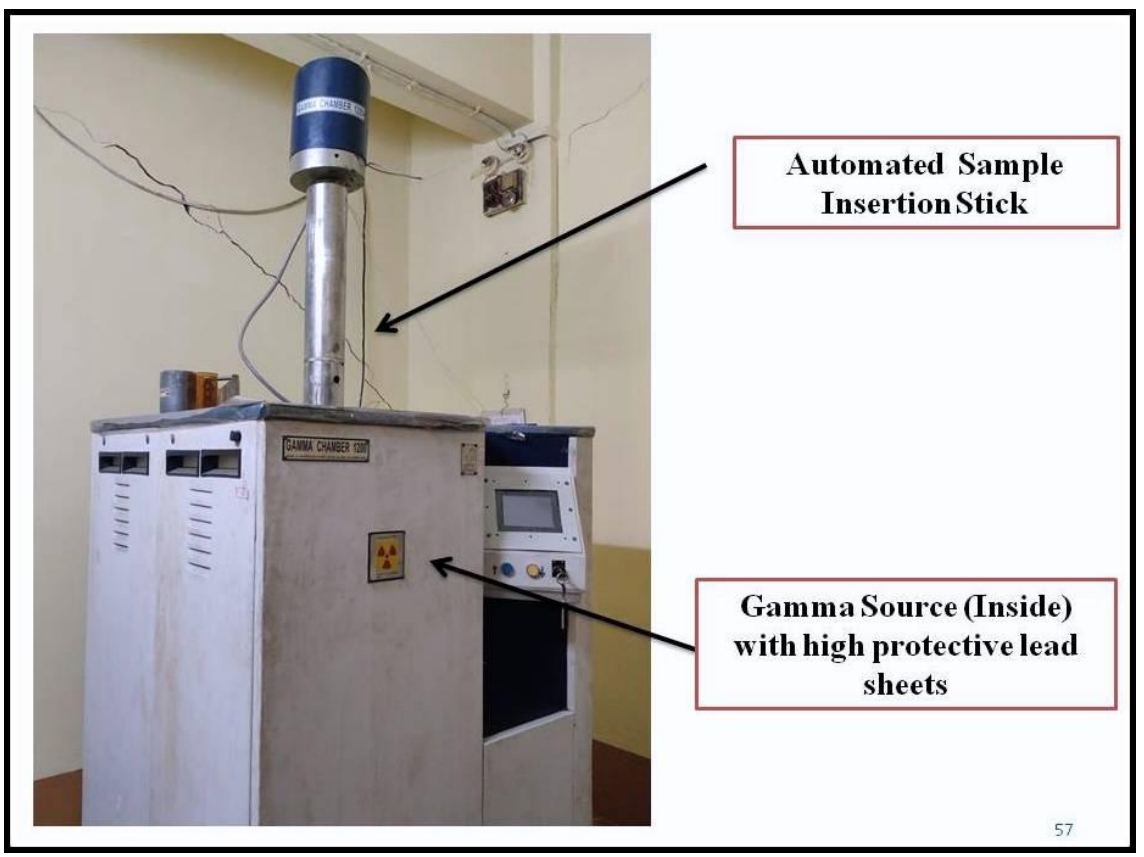

Figure 2.24: *Actual photograph of the gamma ray chamber (Co-60 source) and SET UP for measurement*

2.6 Remarks & Challenges:

One of the major challenges of this thesis was to get compact films with better coverage. Such uniform coverage has been achieved by introduction of paper as a substrate .Such paper grown materials are used to fabricate as devices which also new for perovskite halides. Also metallization on such paper substrates is an important challenge and making of paper electronic based device for different detectors is the novelty our research.

2.7 Conclusions:

In this chapter of thesis, synthesis of large class of materials under lead based perovskite halide (altering cation, anion) has been provided by a solution processed common synthesis route. It has been shown that different nano and microstructure thin films of perovskite halides can be grown tuning different growth parameters. Introduction of paper as a substrate is one of the prime novelty of thesis which not only provides compact film with specific surface morphology. Growth of perovskite halide using paper substrate is a completely new observation. Also growth of good quality single crystal of perovskite halide has been provided.

The paper grown films are characterized by several characterization tools like XRD, SEM, EDX, UV-Visible and Photoluminescence spectroscopy. This analysis provides us information about crystallographic phase, purity, surface morphology, band gap and emission. Such paper grown materials are used to fabricate as devices which also new for perovskite halides which essentially probes these kind of emerging materials as compatible with paper electronics. Also metallization on such paper substrates is an important achievement. The subsequent measurements like optoelectronics, electrical etc using paper electronics based perovskite halides will be provided in the next few chapters in the thesis.

References:

2.1 Zhao, Y.; Zhu, K. *Chem. Soc. Rev*. *45*, 655, 2016

2.2 Shaowei Shi, Yongfang Li, Xiaoyu Li and Haiqiao Wang, *Mater. Horiz.*, 2, 378, 2015

2.3 Wei Wang, Moses O. Tade´a and Zongping Shao, *Chem. Soc. Rev.*, 44, 5371, 2015

2.4 Teddy Salim, Shuangyong Sun,Yuichiro Abe, Anurag Krishna, Andrew C. Grimsdalea and Yeng Ming Lam, *J. Mater. Chem. A*, 3, 8943, 2015

2.5 Tze-Bin Song.et.al; DOI: 10.1039/c4ta05246c

2.6 Jin-Wook Lee and Nam-Gyu Park, *Mrs Bulletin* ,40, 2015

2.7 Shuigen Li, Chen Zhang , Jiao-Jiao Song , Xiaohu Xie , Jian-Qiao Meng , and Shunjian Xu, *Crystals* 8, 220, 2018,(11-12)

2.8 Avisek Maity ,A.K.Raychaudhuri,Barnali Ghosh ; *Scientific Reports* (2019) ,9,1-10

2.9 Avisek Maity, A.K.Raychaudhuri,Barnali Ghosh ; *Journal of Physical Chemistry C* ,(2021), 125, 19, 10646–10652

2.10 Avisek Maity,Chandni Das, A.K.Raychaudhuri, Abhijit Saha,Barnali Ghosh; *Journal of Physics D: Applied Physics*, (2021), 54, 455104

2.11 Jie Ding and Qingfeng Yan, 10.1007/s40843-017-9039-8

2.12 Li.Z; Yang , M.; Park,J.; Wei,S.;. Berry,J.; Zhu,K. Solid-State Alloys, *Chem. Mater. 28*, 284−292. 2016

2.13 PANanalytical B. V. Lelyweg, 1, 7602 EA Almelo, The Netherlands.14

2.14 R. F. Egerton, "Physical Principles of Electron Microscopy: An Introduction to TEM,SEM and AEM", Springer, 2005

2.15 Rabeya Basori, Ph.D thesis, submitted to Calcutta University 2015.

2.16 R. Jeyakumar and Atanu Bag, *Solar Energy*, 221, Pages 456-467, 2021

Chapter 3

Methyl Ammonium Lead Iodide as Paper Based Visual Ammonia Gas Sensor: Potential Applications as gas sensor

In this chapter of thesis we have investigated a new application potential of halide perovskites namely methyl ammonium lead iodide (MAPI) as an active gas sensor material. We also investigated a new simple technique to trace ammonia based on visual color change which works like pH papers on disposable basis. The as fabricated visual sensors are grown in flexible substrate like paper even in large area for enhanced scalability in cost effective manner. Moreover is workable at room temperature with very high selectivity, sensitivity and exhibit very low detection limit down to ~10ppm. It acts as a quick and easy method to detect hazardous gases at work places. The subsequent reason behind the color change has also been discussed in this chapter. For real time usage of the sensor, we have developed a prototype in the form of a wrist band (named as: 'Ammo Watch'. So it can be extremely useful when people working in any environment prone to ammonia for their safety! A patent has been granted in this issue.

3.1 Introduction:

Perovskite halides are one of the most sensational and well researched classes of emerging materials since last decade for its unprecedented application potentials. High absorption coefficient, band gap tunability, long diffusion length make them outstanding candidate for photovoltaic and optoelectronic applications as we discussed also in introduction section [1]. Among them methyl ammonium lead iodide perovskites is mostly attracted because of its outstanding application potential in the area of solar cell and optoelectronics like photo detector, light emitting diode (LED) etc. There are still some interesting areas of application which are not explored much. In this thesis chapter, we have explored a new application potential of methyl ammonium lead iodide (MAPI) in the area of gas sensor as solid state detector with a new detection technique.

Realization of thin film gas sensors for efficient and cost-effective detection of toxic gases has gain considerable current interest [2-4]. Most of the reports available on thin film based gas sensors are electrical signal based and would need a peripheral arrangement for detection of the gas [5-7]. It is envisaged that if a color change sensor can be made where a visual detection can detect the hazardous gas in ppm level that would make it extremely easy to use as well as cost effective as it would need no electronics peripheral as well as need of trained operator can be obliterated. As examples, color change sensors based on papers are widely used for pH measurements as well as for measurements of glucose level in urine [8]. However, such easy to use sensors are not available for hazardous gases till date.

In this chapter of thesis, we describe such paper based color change visual sensors can be made from lead based perovskite halide, MAPI for easy and rapid detection of ammonia gas at room temperature. The sensor is thus cheap and disposable. Since the sensor needs no electrical read–out and no external peripherals, it is field useable without need for trained operators. The innovation involves effective utilization of MAPI as an active material for solid state gas sensor which has not been utilized before for effective gas sensing.

One of the most hazardous environmental pollutants in the atmosphere is ammonia (NH_3). Detection of the presence of NH_3at a low level is most desirable as the presence of the gas can occur in several areas like refrigeration, food processing and storage, environmental protection, chemical technology, etc[5-6]. Up to now most NH_3 sensing materials are metal-oxide semiconductor systems that are based on electrical sensing or optical detection and often suffer from low selectivity, room temperature operation and slow response/recovery

rate and poor detection limit [9-12]. In that context investigation of new materials like perovskite halides for NH_3 detection at room temperature using paper with new detection technique based on visual color is an important innovative step forward.

In this chapter, we have studied/discussed in detail paper based visual gas sensing property and sensor characteristics of perovskite halide $MAPbI_3$ (MAPI).This lead based perovskite change its pristine color in presence of NH_3 gas very quickly. The detailed sensor properties of the visual gas sensor have been discussed in this chapter. The reason behind color change has also been investigated through series of experiments using spectroscopic and structural characterization tools as gas sensor.

3.2Gas Sensor Fundamentals:

In a very simple and native way of speaking, a gas sensor is composed of a receptor and a transducer. The receptor is generally provided by a material and compositions of materials which changes its physical and /or chemical properties (dielectric constant, work function, mass etc) or emits light or heat upon interaction with the target gas. A transducer is a device which used to transform such an effect into an electrical signal. In a typical semiconductor gas sensor is generally, the material is used as receptor and sometimes acts as both receptor and transducer. However the overall components of a gas sensor, and the fabrication we will discuss in subsequent section. The schematic of the typical gas sensor is shown in the following [13].

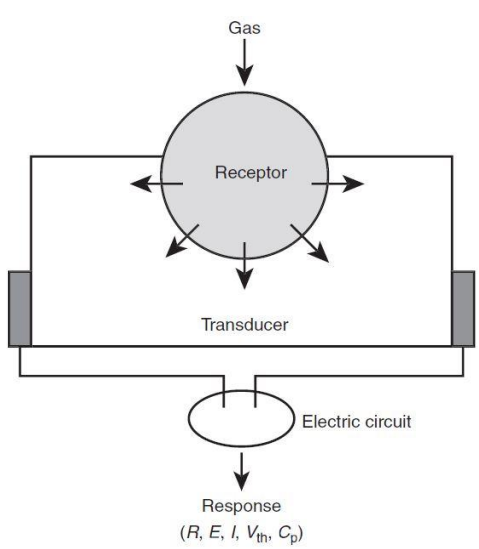

Figure 3.1: *Basic principle of gas sensor; gas sensor in a nut shell [13]*

3.3Classification of Gas Sensor:

Solid-state gas sensors are generally operated on basic of the interaction between gas particles with surfaces and adjacent volumes. Different physical parameters, commonly, resistivity, electrochemical potential, the density, and/or the optical properties are altered upon gas exposure.

To classify the gas sensor, several approaches can be used according operations on diverse principles. Taking into transducer mechanism, gas sensors are classified into several categories. The following table summarizes the different classes of gas sensor and their operating principles.

Sl No	Class of Gas Sensors	Operating Principles & Measured Quantities
1	Electrochemical (chemiristor)	Change in Voltage , Current , Capacitance/Impedance • Voltametry • Potentiomentry
2	Electrical	• Metal Oxide Conductivity • Electrolyte Conductivity • Work Function
3	Mass Sensitive	Change in the weight, amplitude, phase, frequency • Quartz Crystal Microbalance • Surface Acoustic Wave Propagation • Cantilever
4	Magnetic	Change in paramagnetic gas properties
5	Optical	Change in light Intensity, Color or Emission Spectra • Absorbance • Reflectance • Refractive Index • Light Scattering
6	Thermometric	Change in temperature, heat flow, heat content • Thermoelectric • Pyroelectric • Thermal Conductivity

Table 3.1: *Existing gas sensors & their principle of operations[xx]s*

However, on basis of absorption and interaction of materials with target gas molecules, we can classify the gas sensors into two other sub categories.

They are- I) Physical Sensor II) Chemical Sensor

In Physical sensor no chemical reaction takes place at the receptor, and the signal is a result

of a physical process, such as mass, absorbance, refractive index or conductivity change. Chemical sensors are based on chemical reaction between target molecule and receptor.
Interaction of target gas with the sensing material is one of the key factors determining the sensing behaviour of a material. Apart from external parameter like temperature, in general there are other several parameters related to material and substrate used to grow the film that affect the gas sensing. Among them grain size, porosity, film thickness, surface geometry, film texture, active surface area are the major parameters to determine the sensitivity /response of gas sensing material.

3.4 Ammonia as Toxic Gas & Necessity of Ammonia Gas Sensor:

Ammonia (NH_3) is generally treated as one of the toxic pollutant in environment with characteristic of pungent smell. From above table we can see that several sectors from which ammonia gas can be emitted and hence development of ammonia gas sensor is extremely important.

- **Ammonia Sources:** Ammonia is emitted from agricultural process. It is generated by the decomposition of animal manures. NH_3 contributes significantly to the nutritional needs of terrestrial organisms by serving as a precursor to food stuffs and fertilizers. NH_3, either directly or indirectly, is also a building block for the synthesis of many pharmaceuticals.
- **Effect of Ammonia:** Ammonia is toxic and caustic. Generally, an acceptable level of NH_3gas is 8-h exposure limit at 25 ppm and a short-term (15 min) exposure level at 35 ppm [14].Sustained exposure may cause severe problem on human health. Ammonia gas is a severe respiratory tract irritant. It can even be fatal if the inhaled gas has NH_3 above an acceptable limit of 500 ppm for 30 minutes. Brief exposure to concentrations above 1,500 ppm can cause pulmonary edema, a potentially fatal accumulation of fluid in the lungs [14].

3.5 Existing Ammonia gas sensors and their detection methods:

Existing gas sensors used to trace the ammonia is mostly metal oxide based (MOS) and operated at elevated temperature. Although metal oxide are preferred for their limited sensing range, good response but suffers from many disadvantages like high temperature operation, high power consumption, poor precision etc. Therefore, lots of effort is going on investigate to develop sensors to trace ammonia (NH_3) which are high sensitive, room temperature

operable, high response with excellent selectivity tuning growth process, surface modification, engineering with other materials and dimensionality. As nanostructure enhances the adsorption of the target gas due to higher surface area than their bulk counterpart, 1D nanostructure are also being incorporated to improve the performances of existing ammonia gas sensors[15]. Reports are available on fictionalization by carbon nanotube (CNT) (both single wall and multi wall CNT) on metal oxide semiconductor to enhance the response. Common metal oxide NH_3 gas sensors are WO_3, SnO_2, In_2O_3 but all works at temperature range typically between 50°C to 300°C[15]. Very few reports are available on room temperature gas sensor based on mainly PANI that too has poor sensitivity as compared to metal oxides. Along with this, all these sensors are based on electrical detection method which needs read out instruments. Not only ammonia sensors, most gas sensors are electrical based, few are optical. The description of sensing components, sensor fabrication and mechanism of sensing followed by typical electrical gas sensors (mainly metal oxides (MOS)) will be subsequently discussed in the next chapter. (Chapter 4).In following chart we are listing the different detection methods for detection that gas sensors follows (mostly metal oxide based).

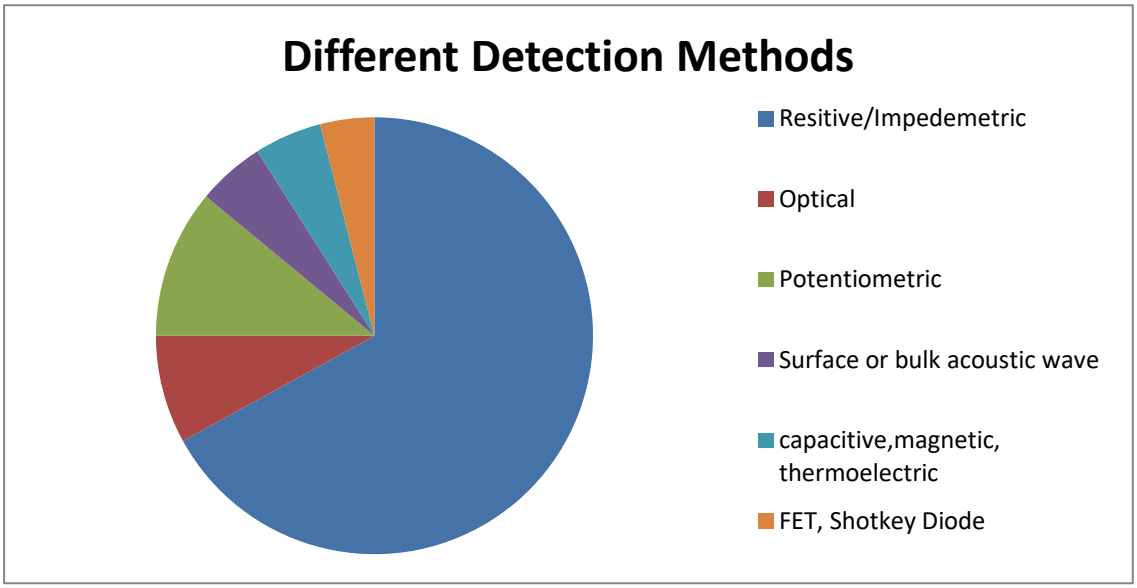

Figure 3.2: *Different Techniques for detection of ammonia gas*

Thus innovation and development of new gas sensor materials along with novel, easy detection method to trace ammonia working simultaneously room temperature operable and cost effective manner would be extremely rewarding. In following section we are going to describe a novel, cheap detection technique to trace ammonia by family of lead based

perovskite halides which can be addressed as new material for solid state ammonia gas detector.

3.6 Experiments and Measurements:

In this chapter of thesis we have studied the visual gas sensing property shown by methyl ammonium lead iodide ($CH_3NH_3PbI_3$/MAPI) using cheap paper substrate. Details of synthesis and characterization of paper sensor has been described in chapter 2 (section 2.3). Then this solution processed paper grown material are cut into several pieces with similar size (typically $1\ cm \times 1\ cm$) to form the devices which are used to test the ammonia sensing property. Still for sake of convenience, we are putting surface morphology of bare paper and MAPI coated paper in figure no 3.3.

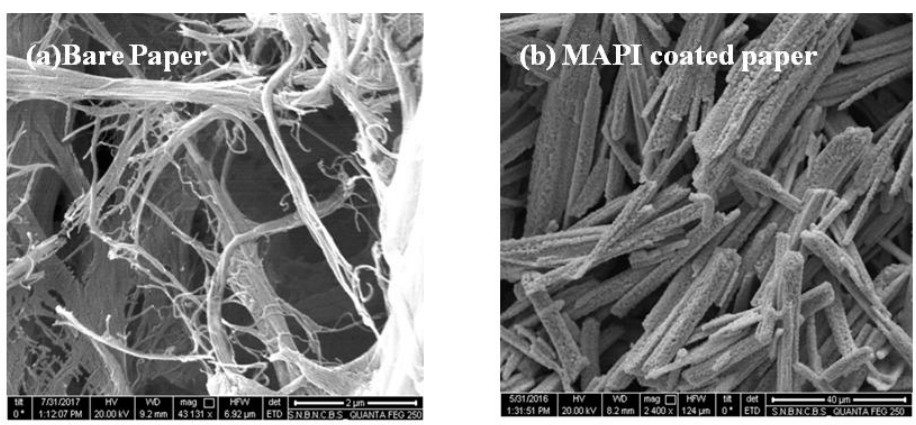

Figure 3.3: *FESEM Images of a) bare paper and b) MAPI thin film grown on paper*

The main experiment in case of visual sensing is to measure the response time to change the pristine color.

The experiment was carried out in a custom designed test chamber with controlled gas environment. Initially the test chamber was purged by injecting nitrogen (N_2) gas for a sufficiently longer time. Then calibrated amount of NH_3 (with a given concentration) was injected into the chamber. The calibration was done by using volumetric method.

3.7: Ammonia gas induced visual color change by methyl ammonium lead iodide perovskite halide:

We show here, a quick, easy method of ammonia detection by simple visual color change method by paper based solution grown lead based perovskite halide MAPI. The paper grown lead based perovskites (hybrid halide) change its color in presence of ammonia gas as shown in figure 3.4. Since, sensor is fabricated on paper, hence very cost effective.

The color of the paper sensor made from the material changes on exposure to NH_3 gas and can be detected visually as shown in figure. MAPI changes from its original black to yellow color. The color change effect shown by methyl ammonium lead iodide has been observed at room temperature.

The necessary response time to change the color in presence of NH_3gas has been recorded in a video camera during the experiment. From video we got the necessary response time to change the color of the sensor.

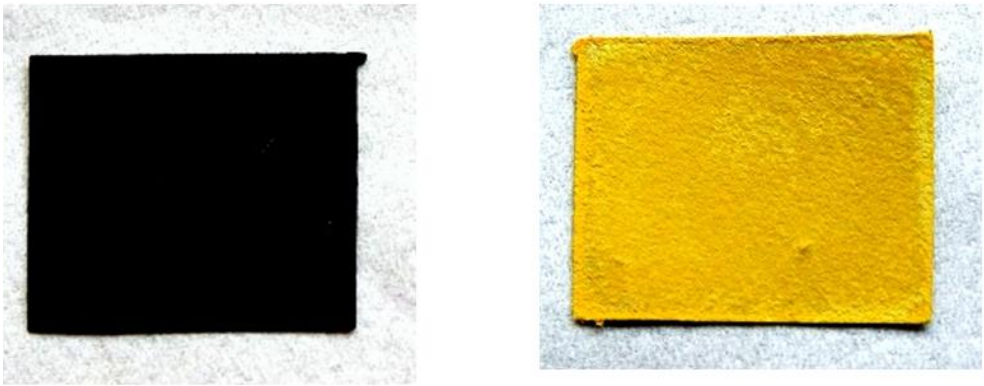

Figure 3.4: *Color change response of the MAPI Sensor: a) represents the original black color of the unexposed film. b) Represents the yellow color of the film in presence of NH_3 gas.*

It is also noteworthy that this color change phenomenon occurs in presence of NH_3 gas both in open atmosphere and as well as closed test chamber with suitable injection of NH_3.

3.8 Detailed Study of Visual Sensor Characteristics:

Such kind of simple visual colorimetric detection technique further motivated us to explore further to study the detailed characteristics of this visual gas sensor. We extended our study to explicitly characterize the detail gas sensor characteristics using MAPI. In following section we have discussed the sensing characteristics of MAPI based paper sensor.

3.8.1 Investigation of concentration dependent Response Time :

It is important to study the response (here response time) of a gas sensor as a function of concentration of target gas. It carries the information about dependency of sensor performance on concentration. We investigated the response time for color change at different NH_3 gas concentration by injecting NH_3 gas in the test chamber and response was similarly recorded through video camera as discussed earlier. Figure 3.5 shows the dependence response time (respective time to change the color) $\dot{t}$ of the MAPI paper sensor for different gas concentrations. It can be seen that for concentration of only 10 ppm the visual sensor changes its color within a response time of around 12 sec. Bare paper had no response of

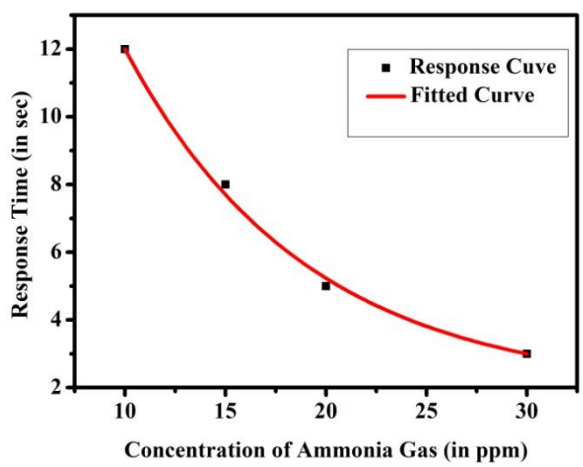

Figure 3.5. *Dependence of the time response of the paper sensor to different concentrations of NH_3 gas at room temperature*

color change when exposed to NH_3 gas. Also below 10 ppm concentration of NH_3 gas, the color change effect did not occur. It has also been clearly observed as shown in figure 3.5 that the MAPI sensor exhibits a faster response when exposed to higher concentrations of NH_3 gas. The response time τ shows an exponential dependence on concentrationc such that,$\sim \exp(-c/c_{0)}$ (c_0 being a constant) so that with increase of the NH_3 concentration the response time quickly decreases, at high concentration (~20-25ppm) when it approaches a danger level, the senor quickly turns color within 4-5 sec and gives a visual warning.

3.8.2 Selectivity of the paper sensor to Ammonia Gas:

Selectivity is one of the major characteristic properties of a gas sensor. Selectivity of the visual sensor was tested by injecting different other hazards gases like Methane (CH_4), Nitrous Oxide (N_2O), Carbon dioxide (CO_2) etc in the test chamber each up to a concentration of 500 ppm for long time (~ 15 minutes or more). No visual color change had been observed in all these cases. This strongly suggests the visual gas sensor is highly selective to the NH_3 gas only. MAPI decomposes in presence of NH_3 and this does not happen with other gases. This ensures that the paper sensor has high level of selectivity towards NH_3.

3.8.3 Effect of Humidity

Since perovskites are known for their degradation it is crucial to check the perovskite sensor response on humidity. Stability under exposure to moisture is an important parameter for its usability in an open atmospheric condition where there may be a likelihood of the moisture affecting the sensor. This effect of humidity on MAPI sensor was investigated in a controlled way by subjecting the sensor paper in the test chamber with different percentage of relative humidity (% RH). It was observed that no color change happened during exposure to humidity for RH range from 10% to 90%. In figure 3.6 we have shown photographs of the sensor paper when exposed to three different relative humidity (13%, 43% and 76%) as

Figure3.6: *Photograph of paper sensor in atmosphere of varying humidity as shown by the RH meter reading.*

a) At relative humidity 76% b) At relative humidity 43% c) At relative humidity 13%

shown by the RH meter. The pristine black color of the sensor is maintained irrespective of the relative humidity (exposure time ~180 sec). In humid condition the sensor can response to visual color change when the sensor paper is exposed to NH_3 gas.

3.8.4 Stability towards storage and shelf-life

A number of sensor papers were stored in a vacuum desiccator. Temperature range tested between 20ºc to 35ºc for storage as well as for experiment. For testing the visual performances, one strip was taken out at interval of 15 days and then exposed to only 15ppm of NH_3 gas in the test chamber and response time was measured. We continued it for 180

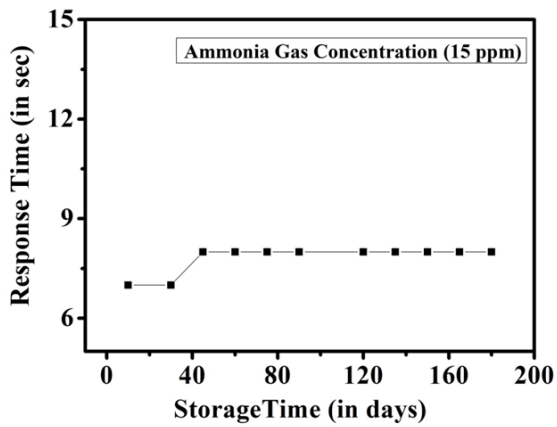

Figure 3.7: *Stability of the sensor against long term storage. Sensing study was performed at room temperature upon exposure to NH_3 gas of fixed concentration 15 ppm.*

days. The data are shown in figure 3.7. It can be seen that the response time of the paper sensor leading to visual color change (from black to yellow) is nearly constant after an initial small change (that occurs within about first 40 days). This small change in the response time however, does not affect its utility. The relatively high shelf -life and almost constant detection performance of the sensor can be concluded as usability of MAPI as standalone stable sensor for NH_3gas at room temperature.

3.9. Discussions:

3.9.1 Investigation of Color Change:

The primary results on color change of MAPI on exposure to NH_3 indicate that there could be a phenomenon of conversion of corresponding lead based halide of the pristine perovskites since the converted color is similar to lead iodide (PbI_2). To rule out hypothesis and to get better insight we performed optical spectroscopic measurements.

- **Evidence from UV – Visible spectroscopy**

The UV-Visible spectroscopy on pristine (unexposed) perovskite halides film of MAPI, exposed NH_3 film and corresponding lead halide film i.e. PbI_2 was done and has shown in figure 3.8 respectively. The exposed film exhibits a very different optical absorption than that

of unexposed /pristine one. For all cases data were taken in absorbance mode with solid sample attachment.

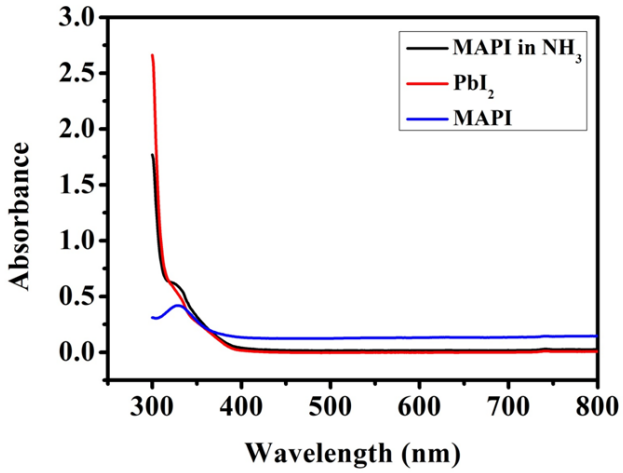

Figure 3.8: *Comparison of UV-VIS absorption of unexposed pristine MAPI on paper, NH_3 exposed MAPI and PbI_2 film on paper.*

MAPI film starts to absorb around 750-800 nm and strongly absorbs for wavelength below 500 nm. But in contrast the film exposed to NH_3, the absorbance of the film is nearly zero in the visible region and it starts to absorb only in the UV region for wavelength below 400nm. Comparison with the absorption spectra of the PbI_2 film shows that the NH_3 treated MAPI film has similar absorption spectra as that of the PbI_2 film. Identical nature of absorption spectra of exposed films and the lead iodide film suggests a firm evidence of our hypothesis.

- **Evidence from PL spectroscopy:**

To check further we performed PL spectroscopy for pristine MAPI film, NH_3exposed MAPI film, and corresponding Lead Iodide film. Like absorption spectra, in case of PL, we recorded the spectra of pristine, NH_3treated and corresponding lead halide films.

PL spectroscopy shows the pristine (unexposed) MAPI film has PL peak around 785 nm and for exposed film, the PL spectra displays a peak around 532 nm and which is identical with the spectra obtained from $PbBr_2$ film (as shown in figure 3.9) at 532 nm PL peak. In comparison of the PL spectra of the NH_3treated film with that of the PbI_2 films shows striking similarity of the two

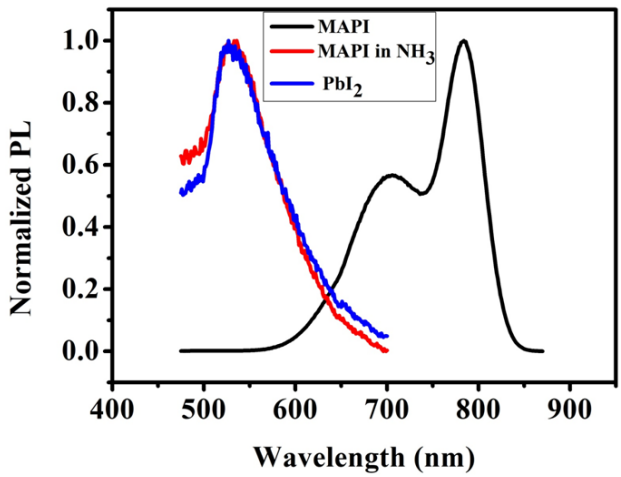

Figure 3.9: *Comparison of PL spectra of unexposed pristine MAPI on paper, exposed MAPI (to NH_3) and PbI_2 film on paper.*

and again establishing that the dominant phase of the MAPI film on exposure to NH_3 gas is indeed due to distinct color of PbI_2 phase. Distinct PL spectra of three different materials along with exposed condition and respective halides has been shown figure 3.9.

- **Confirmation from structural study:**

In order to detect any structural change occurred in MAPI film during NH_3 exposure, we also performed the XRD of the NH_3 exposed MAPI film on the paper. Figure 3.10 shows the comparison of XRD patterns between the unexposed MAPI film and NH_3 exposed MAPI film and also the XRD pattern of a PbI_2film on paper. The XRD pattern of the MAPI film changes substantially after the film is exposed to the NH_3 gas. It can be easily seen from

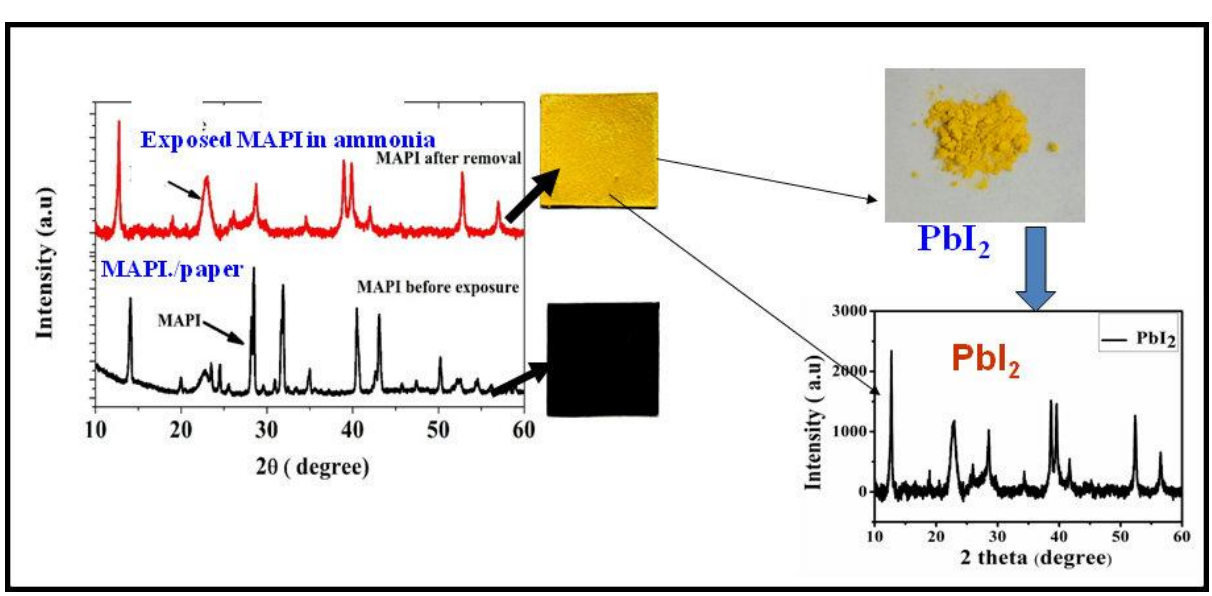

Figure 3.10: *Comparison among XRD data of unexposed pristine MAPI on paper, exposed MAPI (to NH_3) and PbI_2 film on paper*

figure 3.10 that the XRD pattern of the gas exposed MAPI becomes comparable to that seen in the PbI_2 film and most of the peaks of the two XRD pattern (marked by arrow) match. This observation further establishes the identity of the new phase obtained from MAPI after NH_3 exposure. The new phase formation or structural transformation of PbI_2 during interaction with ammonia and dependency of structural change under ammonia gas concentration.

3.9.2Novelty and Utility of such gas sensor for detection of ammonia:

Novelty of Solid state visual gas sensor using perovskite halide:

- Fast response (~ 5 sec)
- VISUAL color change with Ammonia gas
- PAPER based
- Disposable (like pH paper)
- Workable at room temperature
- High sensitivity :~10 ppm
- High selectivity: yes
- Humidity insensitive
- Shelf life 6 months or more in dry storage condition
- Cost effective

The effective invention of this chapter mainly focuses on few aspects. Firstly, use of perovskite halide as active material for explicitly solid state gas sensor to detect ammonia has not been reported previously to the best of our knowledge [16]. On the other hand, use of cellulose paper for fabrication of perovskite halide material as sensor is also an innovative approach.

Most common applications of cellulose-based materials are as dielectric for capacitors and super capacitors, permeable membranes in liquid electrolyte batteries or just the physical support of energy storage devices, organic thin film transistor (TFT) arrays inkjet-printed sensors [17].

But paper based gas sensor for perovskite halide is a new invention and reported no where before us. Another approach, the method of detection of tracing gas sensor is quite unique. It just based on a simple color change, which is relatively simple and easy detection technique to trace a toxic pollutant.

As a visual sensor to assess the immediate extent of danger of presence of the NH_3 in an ambience, this is a desirable feature. The sensor takes nearly 10 sec (~ 10 ppm NH_3) to respond and this will not lead to detrimental exposure. On the other hand when the concentration is relatively high (~20-25ppm) and it approaches a danger level, the senor quickly turns color within 5 sec and gives a visual warning. For any operator in a hazardous environment this will give an immediate danger signal.

The ability of the cheap easy to make paper based perovskite halide visual sensors to trace of NH_3at room temperature at high selectivity and high sensitivity (~ 10ppm) without any added electronics or need of any extra gadget, will have big impact and is of great practical relevance in areas of application where quick sensing is needed that no undue exposure will occur to NH_3.

3.10 Technological aspects of this new approach towards gas senor:

In recent past, an appreciable interest is being noticed on translational research from the new, novel invention of scientific observation in laboratory.

An attempt towards translational research utilizing novel application potentials aims at bringing the knowledge from research to the market**.** It includes protection of new technologies by means of patents and copyright**,** promoting the technology and encouraging potential industrial partner to use to technology. Moreover, technology transfer supports worthy combination of the cutting-edge knowledge and the entrepreneurial spirit and it is important in the scene that it helps on developing early stage intellectual property into tools for direct use by the research community, or into bases for new platforms, products, or services to be made into products for public use.

Since, we have found several novel aspects of solid state gas sensor under study:

i) new detection method to trace ammonia gas,
ii) usage of new materials to detect ammonia as a sensor,
iii) paper based disposable technology with room temperature operation
iv) Stand alone

All these innovative aspects can be translated into modern commercial/industrial research through technology transfer.

Social impact: Development of prototypes/device using Visual color change based ammonia gas sensor (<10ppm)for stand - alone use for hazards gas detection in an open/ close atmosphere down to 10ppm level/based on ammonia gas sensing can be useful in Environment protection and health care sector.

Patent and Copyrights: This proof of concept has been applied for Indian patent and **patent has been granted (Grant No- 316234, India** *(31/07/2019)*) and also designed as prototype. The idea had been patented in the name of "**AMMONIA GAS SENSOR AND A METHOD FOR MANUFACTURING THE SAME"**. The objective of the invention was to develop an ammonia gas sensor which would be adapted to trace the atmospheric ammonia in open or closed environment by a simple color change effect, without using any other instrumental arrangements or facilities [18].

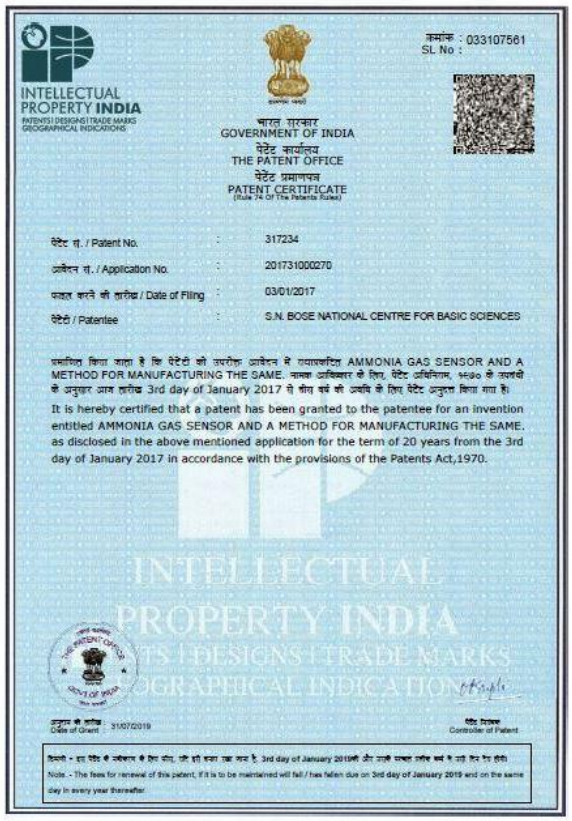

Figure 3.11: *Certificate of granted patent from Indian patent office* (*Grant No- 316234)*

Prototype Development: After protecting the new proposed technology through patent, it is important to develop prototype in the form of a product for real time use. We have proposed several approaches to design the prototypes in form of strip or roll. However, we have adopted in the form of watch named as "Ammo-Watch" to make more sound in view of practical use of the sensor. Some schematics along with our developed prototype have been

shown in figure 3.12(a) The developed prototype could be used in the wrist with slot of sensor can be put in use and throw basis. This kind of prototype might be useful for routine use in areas like food sector, healthcare sector for practical use in disposable manner. Moreover it can be used in the form of roll also as shown in figure 3.12(b).

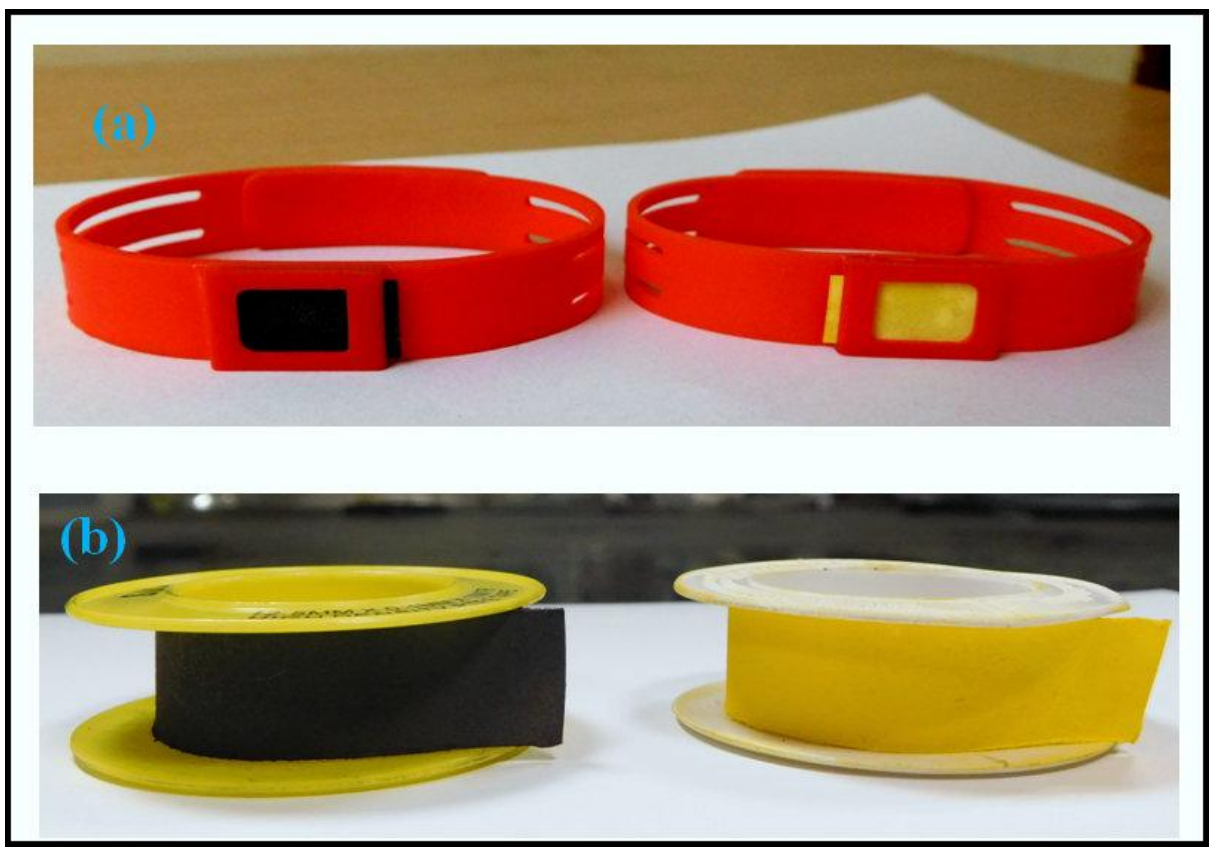

Figure 3.12: *Lab developed prototypes (a) in from of watch called "Ammo-watch" & (b) Prototyped developed in form roll (blue ones are pristine MAPI & yellow ones are exposed)*

Batch Production: Next to prototype development, we have synthesized the sensors in batch for large scale growth. We have developed a batch of 100 sensor strips and also grown it in a relatively large paper (4-5 inch) to enhance scalability. These sensors are ready to be used in the stage of field testing. The developed batch production has been shown in figure 3.13.

Figure 3.13: *(a) Large scale growth for a batch of 100 sensors b) Grown on a large paper substrate for enhancing the scalability 5 inch) to enhance scalability.*

3.11 Conclusion:

In summary, we have explored a new application potential of halide perovskite methyl ammonium lead iodide in the area of solid state gas senor which is completely new in case of perovskite halides. The sensor is paper based using solution growth route and operable at room temperature. Since the sensor is easy to fabricate and being a visual color change sensors; does not require any other extra equipment for its operation. Thus the sensor can be used as rapid and selective detection of ammonia in a cost effective manner. It has been proposed that NH_3gas induced decomposition of material to the lead halides give rise to the color change of the material during interaction with NH_3. This proof of concept has been utilized for prototype development; a patent has been filed and granted. Thus this work establishes that methyl ammonium lead iodide could act as new generation room temperature (unheated) solid state NH_3 sensor with new detection method which is compatible with paper based technology.

However, the electrical detection method could go beyond visual limit and can be probed as very high sensitive (~ ppb) towards ammonia detection. We will discuss ammonia gas detection property of the same material methyl ammonium lead iodide ($CH_3NH_3PbI_3$) by electrical read out of lead halide perovskite using paper electronics in next chapter.

References:

3.1 Wei Wang,a Moses O. Tade´a and Zongping Shao, *Chem. Soc. Rev.,* 44, 5371, 2015

3.2 Moseley,P.T. *Meas. Sci. Technol*.28, 0822001, 2017

3.3 Meixner, H., Gerblinger, J., Lampe, U., Fleischer.M. *Sensors and Actuators B*,23,119-125,1995

3.4 Timmer, B. & Olthuis ,W., Berg, A.V, *Sensors and Actuators B,* 107,666–677, 2005

3.5 Wang, J., Wei, XW., Wangyang, PH., *Nanoscale Res Lett.* 10, 461,2015

3.6 Lee, S.K., Chang, D., Kim, SW. *J Hazard Mater* 268,110–114,2014

3.7 Chen, T.Y., Chen, H.I., Hsu, C.S., Huang, C.C., Wu, J.S., Chou, P.C., Liu ,W.C., *Sensors and Actuators B* 221, 491–498, 2015

3.8 Dong ,Y. et al; Nanoscale 4 ,3969 ,2012

3.9 Wang, L. et al;. *ACS Appl Mater & Inter,* 6, 14131–14140 ,2014

3.10 Zhihua, L., Xucheng, Z., Jiyong, S., Xiaobo, Z., Xiaowei, H., Tahir, H.E., Holmes ,M., *Sens. Actuators B:Chem.* 226**,** 553–562,2016

3.11 Lee, K., Scardaci ,V., Kim, H.Y., Hallam, T., Nolan, H., Bolf, B.E., Maltbie, G.S., Abbott, J.E., Duesberg ,G.S., *Sens. Actuators B: Chem.* 188 , 571–57,2013

3.12 Yavari, F., Chen, Z., Thomas, A.V. , Ren, W., Cheng, H.M. , Koratkar, N.;*Sci. Rep.*,1, 166 ,2011.

3.13Handbook of gas sensor, *Properties, Advantages and Shortcomings for Applications*, Volume -1 Ghenadii Korotcenkov, DOI 10.1007/978-1-4614-7388-6

3.14[Dataset] Occupational safety and health guideline for ammonia, U.S department of health and human services, National Institute for occupational safety and health, 1992

3.15Handbook of gas sensor *Properties, Advantages and Shortcomings for Applications*, Volume -2 Ghenadii Korotcenkov, DOI 10.1007/978-1-4614-7165-3

3.16 Maity, A.; Ghosh, B.. *Sci. Rep. 8,* 1-10, 2018

3.17 Yang Lin, Dmitry Gritsenko, Qian Liu, Xiaonan Lu, and Jie Xu; *ACS Appl. Mater. Interfaces* 8, 20501−20515, 2016

3.18 Patent : Avisek Maity, Arup Kumar Raychaudhuri, Barnali Ghosh; Ammonia gas sensor and a method for manufacturing the same; *Grant No- 316234, India (31/07/2019)*

Chapter 4

Sub ppm Detection of Ammonia Gas by Methyl Ammonium Lead Iodide (MAPI) Perovskites using Paper Electronics: Detection beyond visual limit

In this chapter of thesis we have explored the detection capability of methyl ammonium lead iodide (MAPI) beyond its visual limit. We studied the detailed gas sensing property of methyl ammonium lead iodide based sensor to trance ammonia gas using electrical read out. Gas sensing activity has been studied down to sub ppm level by fabricating paper electronics based gas sensor. The sensing parameters like sensitivity, stability; selectivity has also been discussed in great detail. We also compared the response among other semiconductor gas sensors. A proof of concept of prototypes and its social impact of such high sensitive gas detection has also been briefly discussed.

4.1. Introduction:

In previous chapter (chapter no-3) of this thesis, we have introduced perovskite halide namely methyl ammonium lead iodide (MAPI) as an active material for new generation of solid state room temperature ammonia gas sensor (by visual detection) beyond its wide application in solar cell. The as fabricated paper based perovskite halide sensor is able to detect ammonia by simple visual color change method at room temperature(sensitivity ~10ppm).This phenomenon /observations immediately raise the issue of tracing the ammonia gas beyond the visual limit like, ultra high sensitivity; down to sub ppm level by the perovskite halide. To rule out the possibility, one must adopt among those methods which are faster as well as well as high sensitive than process of visual color change. The time scale for tracing the gas should be less than that time scale of visual sensing and the sensor should be high sensitive (~ sub ppm) compare to visual sensor (~ few ppm). We have adopted the electrical technique because electronic process is faster as well needs less complex instrumental arrangements than optical spectroscopic technique.

In this chapter, we have shown an innovative idea of fabricating paper electronics based ammonia sensor using electrical read out from methyl ammonium lead iodide to trace ammonia which is much faster than visual technique and one can go below down to sub ppm level (~ppb) through noise limited detection. The paper based electrical sensor made of perovskite halides MAPI is operable at room temperature using paper electronics. The proof of concept of paper based electrical readout based ammonia sensor has also been patented (application no: 201831001993).

Typical existing ammonia gas sensors based on electrical detection are; metal-oxide semi-conductors (MOS), reduced graphene oxide (RGO) etc, and needs elevated temperature for operation. Very few reports are available on room temperature ammonia sensors based on Polyanyline (PANI) which are also in the detection range of environmental monitoring [1]. On other hand, in recent days, high sensitive sensors for specific gases are considered as very useful tool to detect markers for several diseases via exhaled human breathe analysis for early disease detection. Several reports are available that shows correlation between specific diseases and exhaled breathe [2-3]. Ammonia is well known biomarker for chronic kidney disease [4]. Such high sensitive, low level detection limit (~ ppb level) of our electrical sensors could extremely lift up the potentiality of lead based perovskite halides as viable non invasive tool for human breathe analysis in bio-medical industry in future where often sub

ppm detection capability is required. Moreover, being paper electronics based sensor; this would have an excellent credibility because of its cost-effectiveness, disposability and flexibility. Not only for ammonia, there is no report on gas sensor based on paper electronics except ours to the best of our knowledge using halide perovskites [5].This electrical sensor can be operable at ~1V DC with an output current in the range of few nA, that makes these sensors compatible with paper electronics with low power consumption (nW) in contrast with the metal oxide sensors where typical power consumption is mill watt (mW) range.

In this chapter we have systematically described the electrical nature of sensing ammonia by perovskite halide; methyl ammonium lead iodide (MAPI) based solid state sensor made on paper working at ambient temperature. We have shown that MAPI based sensor can go down to sub ppm (ppb) level through noise limited detection capability. Finally we have proposed a brief discussion about proof of concept of prototypes and its social impact of such high sensitive gas sensor.

4.2 Influencing Factors for Semiconductor Gas sensors using electrical read-out:

In previous chapter we had shown that, fundamental sensing mechanism of any gas sensor lies on the interaction between target gas and the sensing material. There are primary factors that directly influence the mechanism process like nature of adsorption, temperature, nature of sensing material etc. Apart from this surface geometry, thickness of the sensing layer etc are the other factors to determine the sensing process. [6]

The basic and general structure of the as typical as fabricated semiconductor electrical (chemi resistive type) gas sensors consist of –

an insulating substrate with heater (for working at elevated temperature to heat up the sensor)

sensing material (as a receptor and/or transducer)

suitable electrodes for read out the sensor resistance

In following figure (figure no- 4.1) we have shown a basic structure of semiconductor gas sensor.

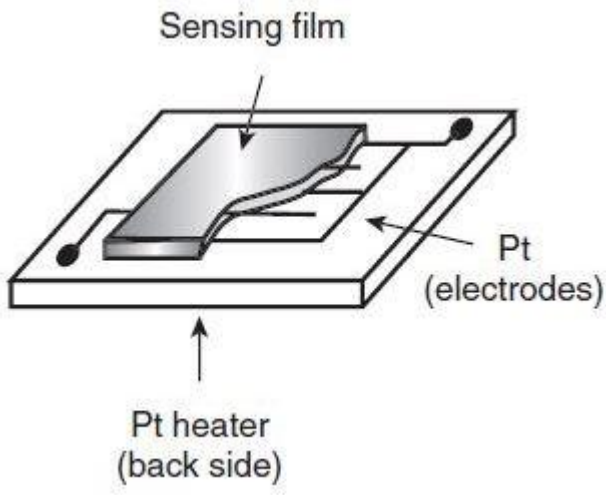

Figure 4.1: *Schematic of an electrical read out based gas sensor [6]*

Novelty of our work from conventional metal oxide based semiconductor

(1) The sensor device uses paper electronics which is uncommon from metal oxide grown sensor films

2) It works at room temperature thus needing no heating platform which is strong contrast with conventional metal oxide sensor

3) Also high sensitivity down to ppb level solely from one particular sensor material without any material engineering is a good achievement.

4.3 Experimental Procedure & Device Fabrication:

To study the electrical response of the lead based perovskite halides in presence of ammonia, we used thin films of MAPI grown on cellulose paper and fabricated paper sensors using paper electronics. The as grown paper sensors are used to form device for investigation of electrical response of the sensors in presence of ammonia gas. Synthesis of MAPI on paper with surface morphology, and details fabrication process has been discussed in chapter 2 (in section 2.3 & 2.4) along with synthesis of other perovskites. All measurements have been performed at room temperature.

The experiments consist of measurement of following quantities:

Sensor current (I) at a fixed bias(V) as a function of ammonia gas concentration with time typically known as $(I-t)$ measurement

The $(I-V)$ characteristics at unexposed condition and in presence of ammonia gas

It is important to recap some fundamental characteristics of electrical gas sensors:

Response/ Sensitivity: Sensor response represents the change in resistance of the gas sensor with respect to the initial resistance of the device when exposed to different gas. It is often defined as the –

$$S = \frac{R_0 - R_g}{R_0} = \frac{\Delta R}{R_0} \qquad \ldots\ldots\ldots\ldots\ldots\ldots\ldots \quad (4.1)$$

where R_g and R_0 are the resistances of the sensor when exposed to gas and without gas.

$\frac{\Delta R}{R_0}$ may be positive or negative depending on resistance change on exposure to gas.

Response time: Response time is the time taken by the sensor to reach its stable output value when subjected to a step change in input.

Selectivity: refers to characteristics that determine whether a sensor can respond selectively to a group of target gases or even specifically to a single target.

4.4 Ammonia Gas Induced Electrical Response by Methyl Ammonium Lead Iodide:

4.4.1 Electrical properties of the gas sensor before exposure:

It is very crucial to check the electric nature $(I - V)$ of the pristine films for any gas sensor before exposure to gas. The base resistance of any gas sensors is an important quantity and desirable to be reproducible with a stable value. The pristine electrical characteristics of the gas sensor have been studied using Cu electrode. The data in figure 4.2 elucidates that the sensor shows a linear behaviour. The average base resistances of the sensor are found to be ~5GΩ. A number of devices have been tested for checking the reproducibility of the base

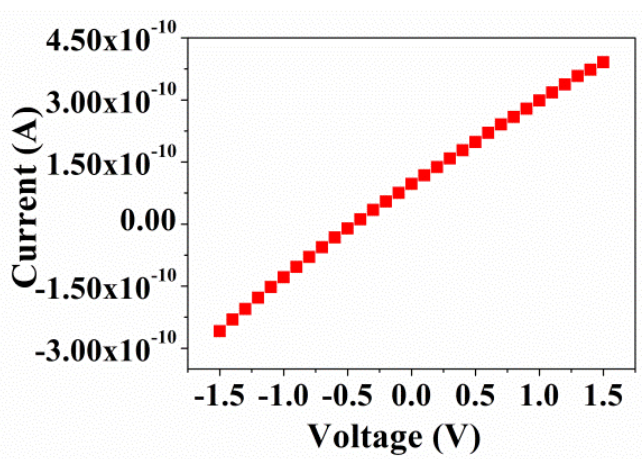

Figure 4.2: *Current-Voltage relationship of pristine MAPI ammonia sensor grown on paper*

resistances of the sensors. In figure no 4.3(a) we have shown the variation of the resistances for number of devices for MAPI. It has been observed that typical base resistance of the MAPI paper sensor varies from 4.5 GΩ to 7.5 GΩ depending on the details of the fabrication method and sensor size. We have also checked the stability of the pristine sensors (MAPI) films towards storage (in a vacuum desiccator). It has been found that resistance of the films varies typically within ~ ±0.5 GΩ (10% of the average device resistance) over a storage period of 100 days. The data has been shown in figure 4.3(b).

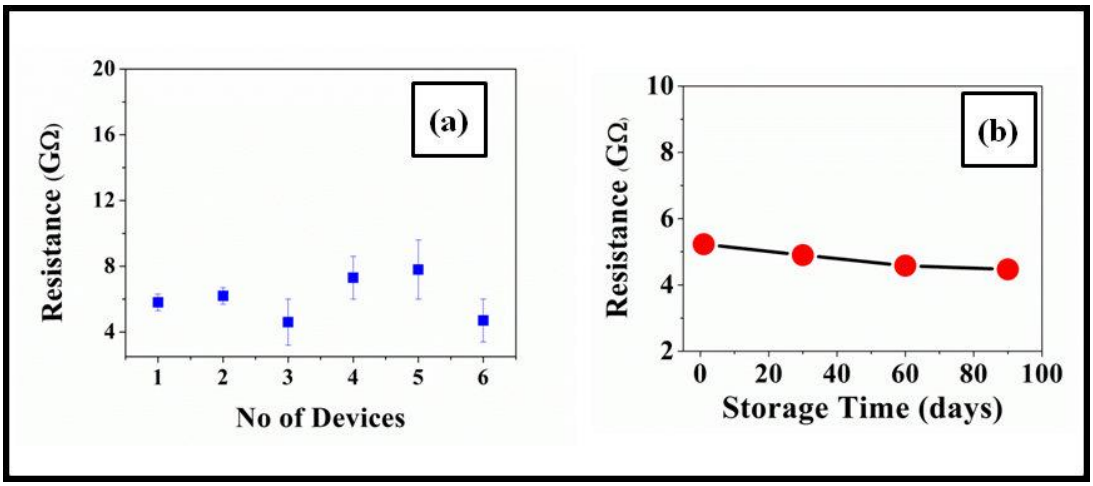

Figure 4.3: *(a) Variation of base resistance for number of six devices (b) Average base resistance over a period of 100 days*

4.4.2 Ammonia gas sensing property by electrical read out:

The electrical response of paper based MAPI sensors/devices at ambient temperature has been recorded at different concentration (ppm) of NH_3 noting the current change of the devices in presence of the ammonia. In previous chapter (Chapter no-3) we had shown that MAPI has detection limit of 10 ppm for visual detection.

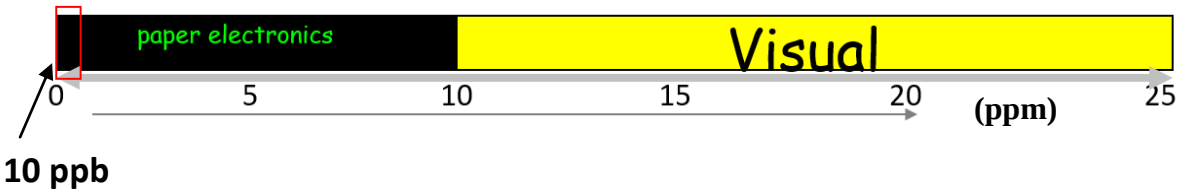

Figure 4.4: *Schematic of detection limit of two different detection methods. The shaded region describes the high sensitive detection limit down to ppb level*

In the schematic of figure 4.4 indicates about the sensitivity of the MAPI sensor with ppm level of ammonia gas. The yellow portion indicates the visual limit of the sensor, the visual

sensing limit ~ 10ppm. Simple sensor paper is sufficient for visual sensing (explained in details in chapter 3). Whereas, for sensing below 10 ppm using MAPI sensor, one need to make device using paper electronics and to take electrical readout. The sensitivity can go down to ~ 10 ppb (noise limited). The electrical measurements as well as sensors characteristics will be discussed in this chapter in following sections.

4.4.3 Electrical Nature /Characteristics of the Lead based halide perovskites on exposure to ammonia

The study of current –voltage *(I-V)* relationship during NH_3 exposure would be important to understand the interaction of ammonia gas with the family of perovskite halides. We have recorded *(I-V)* characteristics of the sensor at exposed condition as compared to the pristine (before exposure to NH_3 gas) one. In figure 4.5 the data for a fixed concentration (20 ppm) has been shown for MAPI. The significant current increment has been observed during exposure to NH_3. The *I-V* curve remains linear on exposure, only the slope changes as the resistance comes down. This observation also proves that the nature of the contact is not affected by the gas exposure and it remains ohmic.

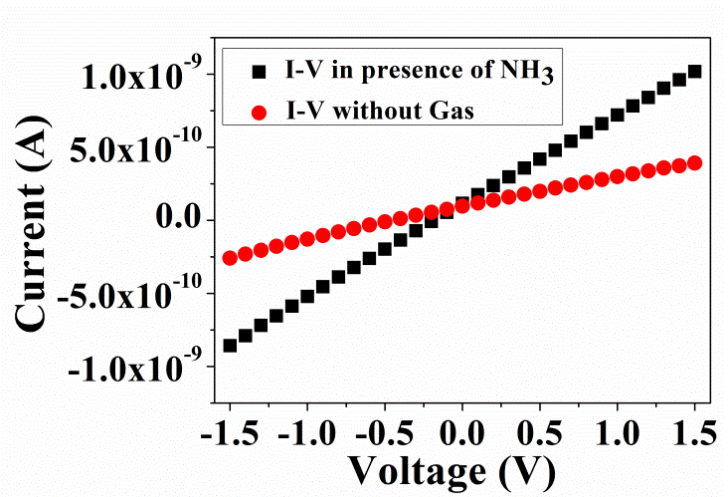

Figure 4.5: *Comparison of the current –voltage (I-V) characteristics of the sensor both exposed and unexposed condition*

4.5 Details Study of Sensor Characteristics of MAPI based paper sensor :

It is interesting to examine/study/explore such the sensor characteristics in detail for further insight. We extend this study with MAPI based electrical paper sensor for its higher sensitivity.

4.5.1 Sensitivity Study of the Sensor for Exposure to Low Concentration of NH_3 (≤ 10ppm):

The MAPI based sensors were tested for exposure to NH_3 gas at low concentration below ≤ 10ppm (in dry N_2 base gas).The MAPI sensor was placed into the test chamber (as shown in figure 2.19 in chapter 2) for investigation of its sensitivity towards low concentration.

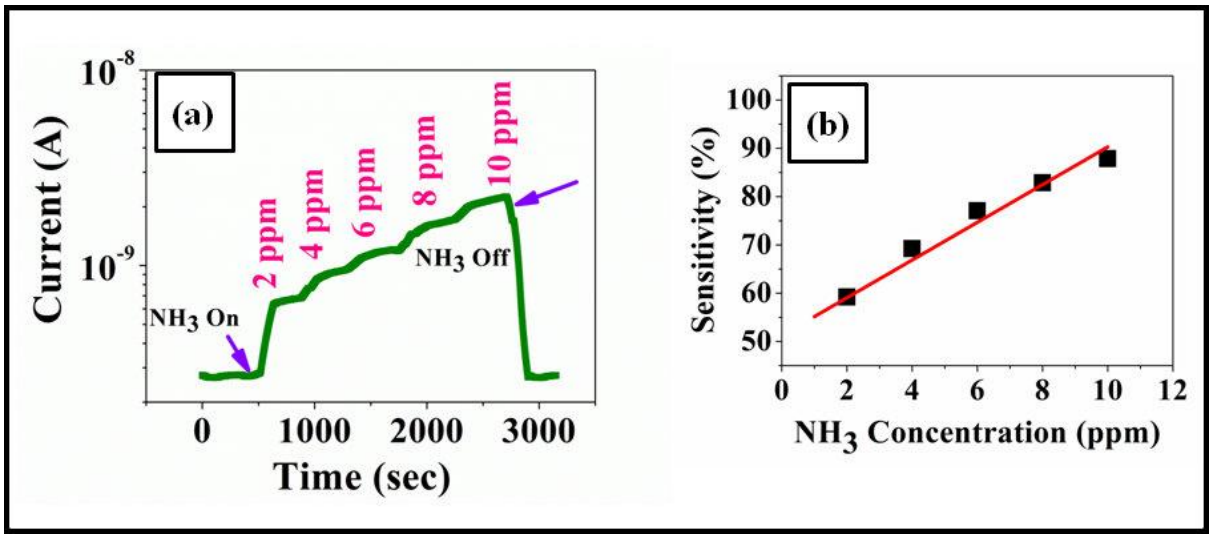

Figure 4.6 (*a) Current response of a typical paper based ammonia gas sensor using MAPI (b) Sensitivity of the sensor as a function of ammonia gas concentration*

The initial test condition was set up by repeated purging and evacuation of the test chamber by flowing dry nitrogen. A base atmosphere of dry nitrogen with known moles is created in the chamber. A calibrated amount (moles) of ammonia (NH_3) was then admitted. It has been observed that the current starts increasing with injection of NH_3 from an initial base current (bias =1.5V). The test gas was admitted by steps of 2 ppm. The data on a representative device are shown in figure 4.6(a). After a concentration of 10 ppm was reached the chamber has been pumped out and dry N_2 was purged. This leads to recovery of the initial / base condition and the current through the device prior to the gas exposure is restored. It has been observed that the device current changes by nearly one order of magnitude with only 10 ppm NH_3 gas. The sensitivity of the gas sensor as calculated by formula is shown in figure 4.6(b) as function of ammonia gas concentration. The sensitivity increases linearly with increase of gas concentration [5].

4.5.2 Reproducibility and Stability of the Response:

Reproducibility is a useful parameter for sensor characteristics. We have also performed for several cycles to study the repeatability / reproducibility of the sensor. It has been observed that even after repeated cycles of exposure and recovery, for a fixed concentration (10 ppm) the current response level of the sensor has not changed significantly. Average response i.e.

(sensitivity for a fixed ppm) of the sensors for a fixed ammonia concentration (10 ppm) is found to be 86.8±1.1 (%) for 10 cycles. The current response data for a typical sensor of 10 cycles has been shown in figure 4.7(a). We see from the data, beyond initial few cycles, the response stabilizes to within 10% after repeated cycling.

Stability is another key parameter for any gas sensor. To test the stability, a collection of sensor papers were stored in a pumped desiccator. At an interval of 30 days one strip was taken out and then exposed to only a fixed concentration (10 ppm) of NH_3 gas in the chamber and sensitivity of the sensor was measured at room temperature. This was continued for a period of 150 days. The data are shown in figure 4.7(b).The decrease of the sensor response at 10 ppm NH_3 concentration for storage over a period of 150days is < 5%. After some initial degradation over 3 weeks the sensor response stabilizes within 2%-3%. A good shelf -life and almost constant sensing performance of the sensor shows that the paper electronics based MAPI sensor qualifies as a stable sensor for NH_3 gas at room temperature [5].

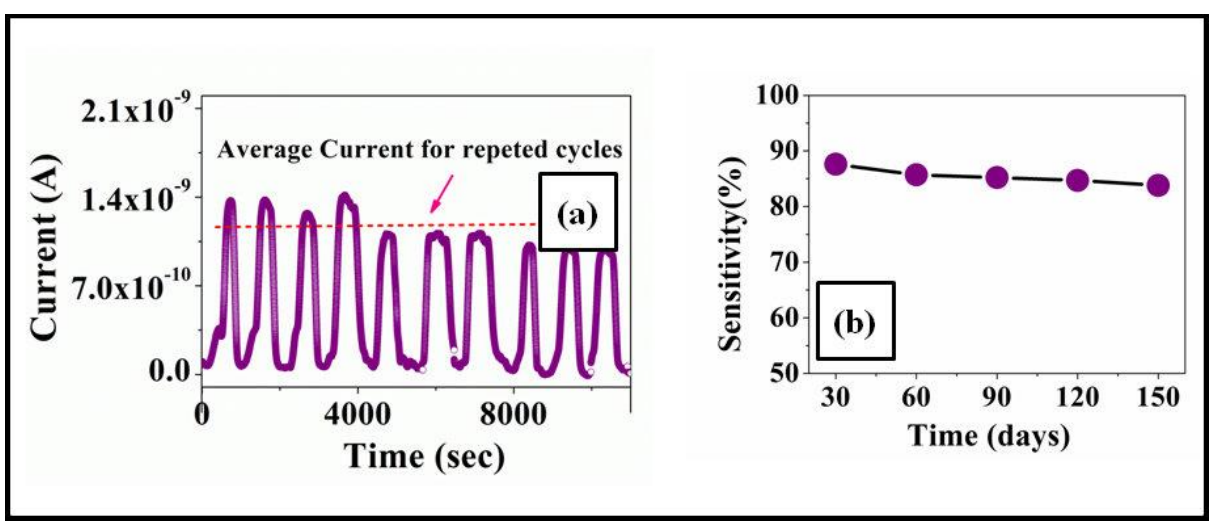

Figure 4.7. *(a) Repeatability of a particular sensor for 10 cycles for a fixed concentration of 10 ppm NH_3 gas (b) Stability study of the sensor for a fixed concentration of 10 ppm NH_3 gas*

4.5.3 Effect of humidity on sensing property:

It is more crucial for gas sensors to check the effect of humidity on sensing. This effect of humidity was studied by injecting water vapor in the test chamber by keeping the other parameters fixed. The amount of water vapor was measured by a humidity meter. This allowed controlled injection of the relative humidity (% RH) into the chamber effectively. A fixed NH_3 concentration (10 ppm) was then admitted. We have shown the response of the

sensor to 20 ppm NH_3 in different relative humidity ranging from 20% RH to 80% RH in figure 4.8.

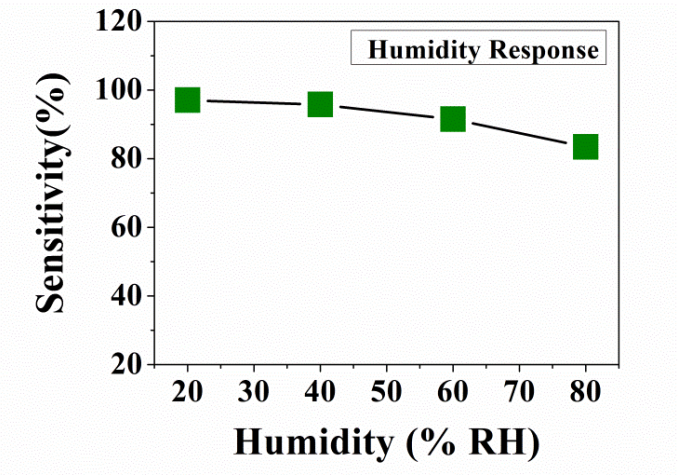

4.8 Dependence of the response of the senor on humidity (Test carried out for fixed concentration of 10 ppm of NH_3 gas)

It has been observed that sensitivity decreases, although by a small measure, with increase of humidity in this range. The change of sensor response in the range of observed humidity is nearly 15%. An uncertainty in response of about 15% would imply an uncertainty of about 10ppm in NH_3 concentration. If an uncertainty of 10 ppm is acceptable no humidity control is needed. For precise NH_3 concentration determination as needed for breath analysis with an uncertainty of better than 1ppm a humidity control in the test chamber to better than 20% of RH will be necessary.

4.5.4 Selectivity of the paper sensor:

Since selectivity is another prime requirement of any gas sensors, we studied the selectivity for MAPI based paper sensors. High selectivity is also very important for practical use. The all sensors were test both in toxic gases like (NO, NO_2) as well as other organic volatiles including methanol, IPA, TCE etc. We observed that the response towards NH_3 is substantially higher than other species of test gases which immediately suggests high selectivity of the sensors towards NH_3. The data has been shown in figure 4.9.

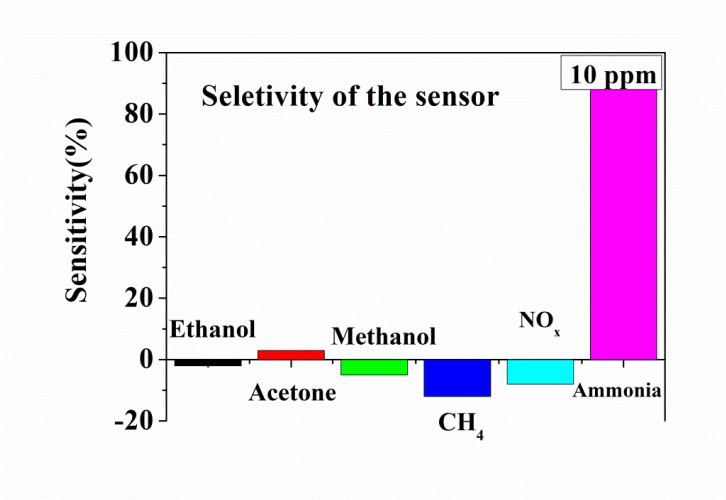

Figure 4.9: *Selectivity of the sensor to NH_3 gas (fixed concentration of 10 ppm) and other organic volatiles (saturated vapors)*

4.5.5 Noise Limited Detectibility down to ppb Level:

Detection capability well below ppm level or sub ppm level of any sensor could be extremely advantageous for medical diagnostic and clinical application in addition with environmental sensing as we discussed in introduction section of this chapter. Since, the paper based halide sensors show a very high response towards ammonia, we have tried to estimate their lowest detection capability by noise limited current of the devices. From the sensitivity curve as a function of ammonia concentration and extrapolation from the curve allows us to get an estimation of noise limited detection limit of the sensors. Noise limited detection for any kind of detector actually signifies lowest minimum ability of detection depending upon what we are detecting. In following we have discussed the method of noise limited detection by our MAPI based paper sensor.

The measured rms noise in the current for a given MAPI based sensor is ± 1.6 pA. The noise in current has been shown in figure 4.10. The change in current for a given device is ≈ 0.15 nA for 1 ppm gas concentration from the extrapolation curve. From the current sensitivity at 1 ppm we get current noise limited detectability of the sensor is around ± 10 ppb. Such high level detection would extremely be an effective probe to utilize these materials in real field applications like, exhaled breathe analysis as a non invasive tool for early diagnosis of chronic diseases. This proof of concept has been used to file a patent (patent file no-201831001993) and a prototype has been proposed. The technological aspects of these high sensitive sensors have been described in detail in following section of this chapter.

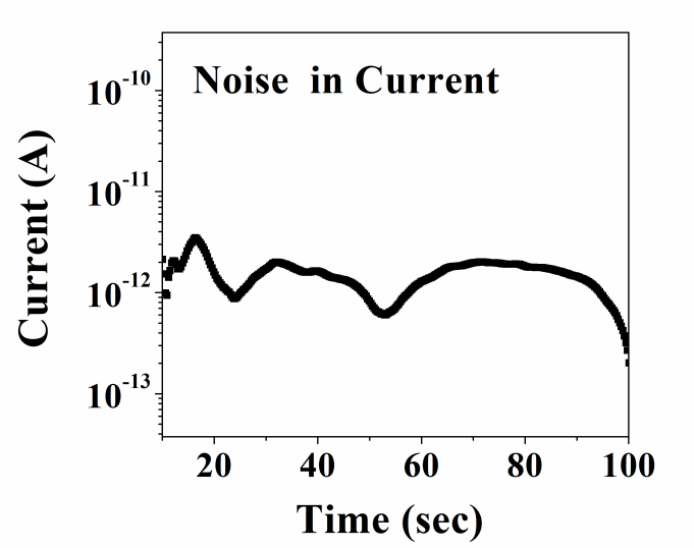

Figure 4.10 *The current noise of the sensor*

4.5.6. Effect of Bending on Gas sensing Property:

Since our sensor are paper based (hence being flexible) it is good to check mechanical flexibility for portable substrates .Flexibility of the paper sensor has been studied by checking sensitivity at different bending condition by varying bending radius. The data for two different bending radii for a fixed concentration of NH_3 has been shown in figure 4.11. From figure 4.11 it has been observed that our paper sensor is capable to detect NH_3 gas at bend condition also. Sensing performance is not much affected due to bending. At higher bending radius there is very small decrement of sensitivity as effective exposed area to target gas (NH_3) has been reduced. A change around 10% has been observed due to highest bending (bending radius ~ 4mm).

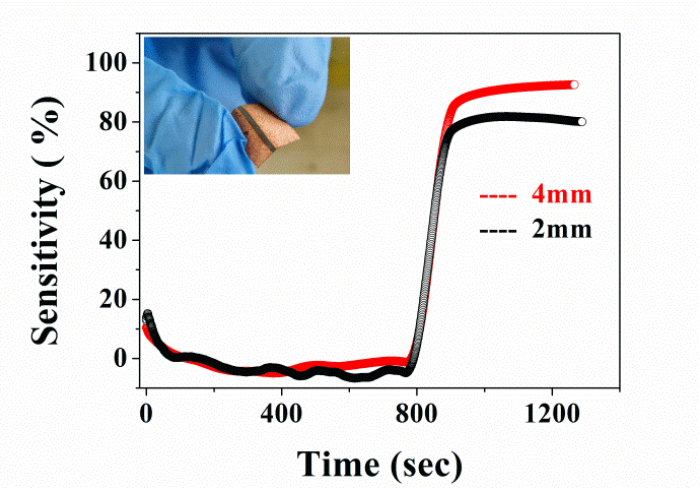

Figure 4.11 *Performance of the sensor at different bend condition i.e the flexibility test of the sensor*

4.6 Discussion:

4.6.1 Comparison with other existing ammonia gas sensors

The ammonia gas sensor we described here is an unheated sensor. All measurements of sensing were carried out at room temperature (27ºC). Usually known NH_3 sensors, such as metal oxide based sensors require elevated temperature [200º -500ºC] for operation although often show adequate sensitivity. The heated operation immediately raises the requirements of operational power. In heated NH_3 gas sensors based on metal oxide as active materials the typical sensitivity ~25% at NH_3 concentration 1000 ppm at operation temperature 200^0C. Very few materials such as PANI based NH_3 sensors are reported that operates at room temperature. But these sensors suffer from significantly less sensitivity (e.g, sensitivity of 30 % at 200 ppm)[7-9].In comparison to other sensors in available reports; here based on paper based sensors and using lead based perovskite MAPI as active material have much higher sensitivity, selectivity and relatively fast response at room temperature. Since there is no need of heating for operation, the operational power requirement for lead perovskite gas sensor using MAPI is only around few nanoWatt (nW). Such low operational power requirement makes it compatible with most portable electronics that are also cloud compatible. The sensor with MAPI is also cheap to fabricate being paper based and due to utilization of a low cost, and simple solution based fabrication process. In next chapter (chapter5), a details study and explanation/mechanism as well as series of experiments using halide perovskite family related to gas sensing (both visual/electrical) has been discussed.

4.6.2 Technological Aspects of this Invention:

As discussed in previous chapter, there is a considerable interest in translational research which aims to bring the laboratory invention to product development. This study shows us several new aspects in the arena of novel gas sensor devices using electrical read out

Electrical sensor made of emerging material, methyl ammonium lead Iodide (MAPI): A solid state gas sensor. The salient features are –

Salient Features:

- Sensor grown on paper,
- High Sensitive
- Highly Selective
- Cost Effective Fabrication
- Very low (sub ppm) detection limit (~10 ppb by noise limited detectibility)

- Disposable Technology
- Compatible with low power paper electronics
- Room Temperature Operation

This proof of concept led us to file a patent entitled as "**A PAPER BASED AMMONIA GAS SELECTIVE SENSOR WITH ELECTRICAL READ OUT AND A METHOD FOR MANUFACTURING THE SAME**". Patent pending application no- 201831001993 has been filed on 17/01/2018.First examination report (FER) has been submitted on August 2021[10].

4.6.3 Proposed Prototype and social impact of research:

Sub ppm level (below 1 ppm) detection capability by MAPI based through current noise promotes us to think of a prototype that could be used as exhaled breathe analysis where ammonia emitted from breathe is extremely low level (~ few ppb). High sensitive sensor can be used as markers for renal disease and chronic kidney diseases (CKD). Even during dialysis of a patient exhaled NH_3 can used to check the efficacy of the dialysis. To detect real time response from such cases it is important to boost up the current level of the sensor from nano level to micro/ mili level so that it can be detected easily by cost effective circuits like using OPAM-128. For this we propose a sensor array based on MAPI using inter digital electrode. So, this kind of low power (nW) paper electronics based device using simple solution processed fabrication would make it viable for large scale use in disposable manner. The proposed prototype name is **"Ammo Read".** This array based sensor is designed could have potential to detect sub ppm capability for real time practical usage will be useful in environment protection as well as health care sector.

4.7 Conclusions:

In summary we have demonstrated, like visual detection to trace ammonia (NH_3), electrical readout based sensors can be made from lead based perovskite halide MAPI which can detect beyond visual limit. The electrical sensors is also based on paper which is an important achievement towards paper electronics for next generation solid state gas sensing devices using lead based halide perovskite MAPI as active material for gas sensors. The electrical sensor is operable at room temperature and solution processed; hence very cost effective as well as disposable compared to existing electrical ammonia gas sensors. The sensor can detect down to sub ppm level by the noise limited detection which suggests them as proposed applications in exhaled breathe analysis as a non invasive tool for detection of several chronic

diseases as cheap , disposable manner making it useful in health care sector. The proof of concept has been patented. The processing related to technological aspect of such new innovation has also been initiated. The nano watt power requirement also makes it very much compatible with low power electronic. Thus this study can pave the pathway of solid state ammonia gas sensor using new active material with suitable process of technology transfer for rapid and selective detection of ammonia using low power paper electronics.

References:

4.1 Maria Vesna Nikolic, Vladimir Milovanovic , Zorka Z. Vasiljevic and Zoran Stamenkovic, *Sensors* 20, 6694, 2020

4.2 Capuano,R. *et al.,. Sci. Rep., 5*, 16491, 2015

4.3 Haick.H; Broza. Y. , Mochalski. P., Ruzsanyi V., Amann. et A., *Chem Soc Rev*, *43*, 1423–1449 2014

4.4 Sawicka K.; Gouma P.; and. Simon S, *Sens. Actuators, B*, *108***,** 585-588, 2005

4.5 Avisek Maity ,A.K.Raychaudhuri,Barnali Ghosh ; *Scientific Reports*,9,1-10, 2019

4.6 Handbook of gas sensor *Properties, Advantages and Shortcomings for Applications*, Volume -2 Ghenadii Korotcenkov, DOI 10.1007/978-1-4614-7165-3

4.7Tai, H., Yuan, Z., Zheng, W., Ye, Z., Liu , C. , Du ,X.; *Nano Express*, 2016, DOI: 10.1186/s11671-016-1343-7.

4.8Kumar , L. , Rawal , I. , Kaur , A. , Annapoorni, S. ; *Sensors and Actuators B*, 240, 408–416, 2017

4.9Samà , J. et al.. *Sensors and Actuators B*, 232, 402–409, 2016

4.10 Patent : Avisek Maity, Arup Kumar Raychaudhuri, Barnali Ghosh; A paper based ammonia gas selective sensor with electrical read out and a method for manufacturing the same; [*File no- 201831001993, India (2018)*]

Chapter 5

Understanding of gas sensing mechanism by family of lead based organic perovskite halides (ABX_3: A=MA, FA; B= Pb; X=Br, I): Experiments & Simulations

In this chapter we have further extended the gas sensing behaviors to trace ammonia using family of lead halide perovskites. Highly sensitive and highly selective room temperature ammonia (NH_3) gas sensors (both visual and electrical) can be made from family of Perovskite Lead halides with different anions and cations that could go down to sub ppm level (by noise limited detection) using cheap paper electronics. It has been show how the qualitative nature of sensing capability towards NH_3 by lead based perovskite halides ($CH_3NH_3PbBr_3$/MAPB & $CH(NH_2)_2PbI_3$ /FAPI) remains same under alteration of the cation and anion in $CH_3NH_3PbI_3$ (MAPI). Based on experiments, a generalized sensing mechanism has been proposed followed by family of lead (Pb) halide perovskites. The proposed mechanism has been substantiated by molecular dynamics simulations as well that also helps to realize the difference of speed of response among all three lead based halides.

5.1 Introduction:

In last two chapters (chapter 3 & 4) of the thesis, we have introduced Methyl Ammonium Lead Iodide ($MAPbI_3$/MAPI) as active material for new generation of solid state room temperature ammonia gas sensor. At the same time the visual colorimetric method for tracing ammonia we described a completely new gas detection technique using organic perovskite halide as described in chapter 3. The as fabricated paper based perovskite halide sensors are able to detect ammonia by simple visual color change method at room temperature [1]. In chapter 4 we had shown that the same paper based sensor could detect down to sub ppm level using electrical read outs as electrical detection is faster [2]. The sensor works at room temperature for both detection techniques (i.e visual and electrical sensing). Also the high resolution noise limited detectivity was also an important step forward towards of paper based electronics.

Thus excellent capability of MAPI of ammonia gas detection based visual (color change) as well as electrical sensor raises the question whether the family of lead perovskite halides (ABX_3; B=Pb) as a family of compounds (with different "A"-site cations as well as halide anions) also could act as NH_3 gas sensor irrespective of different crystal structure and surface morphology. It would be an innovative extension of our two previous works (both visual & electrical by MAPI) to study/investigate the sensing behavior of other halide perovskites so that the family of halide perovskite could serve as a common platform for new generation solid state gas sensor.

We have grown different halide materials by altering "A" site 'cation' and halide 'anions' keeping "B" site cation fixed and studied the gas sensing property using compounds $MAPbBr_3$ /(MAPB) and $FAPbI_3$ (FAPI) along with $MAPbI_3$/MAPI

We have systematically studied the sensing behavior of MAPB and FAPI based paper sensors (both visual and electrical) and compared the response along with MAPI. This comparative study allows us to get insight about sensing response both qualitative and quantitative extent shown by lead based halide perovskite family.

The $MAPbI_3$ (MAPI) has a tetragonal crystal structure; $MAPbBr_3$ (MAPB) has cubic structure; whereas, $FAPbI_3$ (FAPI) has trigonal structure with electronic band gap of 2.3 eV, 1.6eV, and 1.52 eV respectively [3-4]. It has been observed that the qualitative nature of sensing towards NH_3 gas remains the same for all three perovskites irrespective of their

differences in and electronic and crystal structures. All three lead based perovskite halides exhibits color change effect in presence of NH_3 gas. Beyond visual limit all the sensors are capable to trace NH_3gas by electrical read outs down to sub ppm level by its noise limited detection. In this chapter of thesis, we have established that the family of lead based perovskites halides as a general platform for value added gas sensing using paper electronics working at room temperature and also studied different aspects of gas sensing by them in great detail.

The common nature of sensing shown by the lead based halide perovskites motivated us to investigate whether a common sensing mechanism lies behind it. We proposed a mechanism for gas detection by the family of lead halides and in addition to experimental support; we also have performed molecular dynamic (MD) simulations to validate the proposed mechanism. This simulation supports the color change as well as electrical resistance change that lead to sensing operation. The proposed mechanism is based on preferential adsorption of NH_3 molecules on the surface of the perovskite halides and in strong contrast with the gas sensing mechanism of common metal-oxide gas sensors [5].

The notion of this chapter is to establish the response of the lead based halide perovskites family towards NH_3 gas sensing in a universal fashion and to develop them as a common platform for solid state NH_3 gas sensor working at room temperature with cost effective and disposable, paper based technology as a viable alternative to metal oxide gas sensors.

5.2 Experimental Procedure and Simulation Methods:

To study the visual and electrical response of the lead based perovskite halides in presence of ammonia, the thin films of MAPI, MAPB and FAPI was grown on paper and fabricated paper sensors. The as grown paper sensors are used to form device for investigation of electrical response of the sensors in presence of gas. Synthesis of lead based perovskite halides on paper with their respective surface morphologies and details fabrication process have been discussed in great detail in chapter 2. For sake of convenience we have shown the structural and morphological characteristics here in following figure 5.1. Similar experimental measurement procedure [$(I-V)$and$(I-t)$] was followed as discussed in previous chapter (chapter 4) for electrical response.

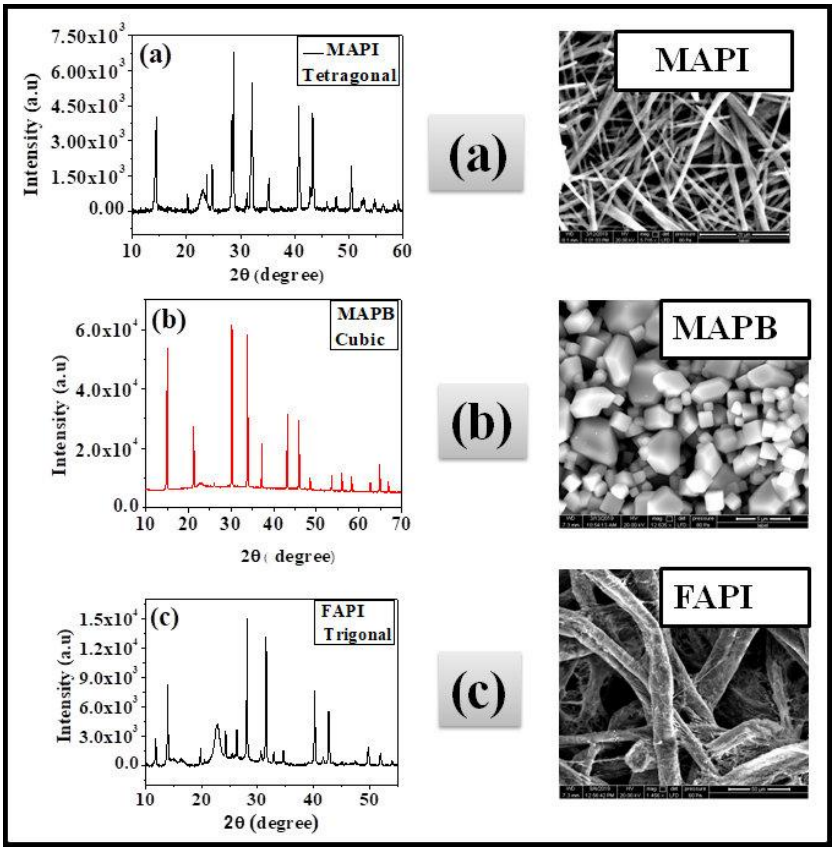

Figure 5.1.*XRD & FESEM images of pristine a) MAPI b) MAPB c) FAPI film grown on paper*

Molecular dynamics: Molecular dynamics (MD) simulation was performed using Quantum Espresso® DFT software package with BURAI GUI (graphical user interface). We have optimized the MD simulation for both MAPI as well as MAPB geometries with 10^{-6} electron convergence threshold. We have simulated (110) plane of MAPI and (100) plane of MAPB because in XRD pattern shows preferential orientation of the plane in the film. We have used ultra- soft pseudopotential(USPP) with PBE exchange and correlation functional. Starting potential was chosen as atomic and starting wave-function was chosen as atomic+random. We have chosen wave function energy cut-off as 50 Ry and charge-density energy cut-off as 400 Ry. We have simulated for 10 no of steps and time-step has been chosen to be 10.3353 A.U (in Ry) (i.e. ~50 x 10^{-17}s).

5.3 Ammonia gas induced visual color change by family of lead based perovskite halides:

We show here, similar to MAPI other lead based halides, like FAPI & MAPB also capable to trace ammonia by simple visual color change method using paper based solution grown

films. So all paper grown lead based perovskites (hybrid halide) change their color in presence of ammonia gas. We have also shown qualitative nature of visual sensing remains same under alteration / substitution of cation and anion keeping B site cation (Pb) as fixed. As we already pointed out in introduction that, though we have discussed about the MAPI based sensor (visual and electrical) in two previous chapters we put the results of MAPI here for the sake of completeness and this will help us to compare with others.

The color of the paper sensors made from all the three materials change on exposure to NH_3 gas and can be detected visually as shown in figure 5.2. FAPI changes to yellow from their original black color similar to MAPI whereas the pristine orange color of MAPB changes to white in presence of NH_3 gas. Hence all three materials under lead halide perovskites show the color change effect at room temperature.

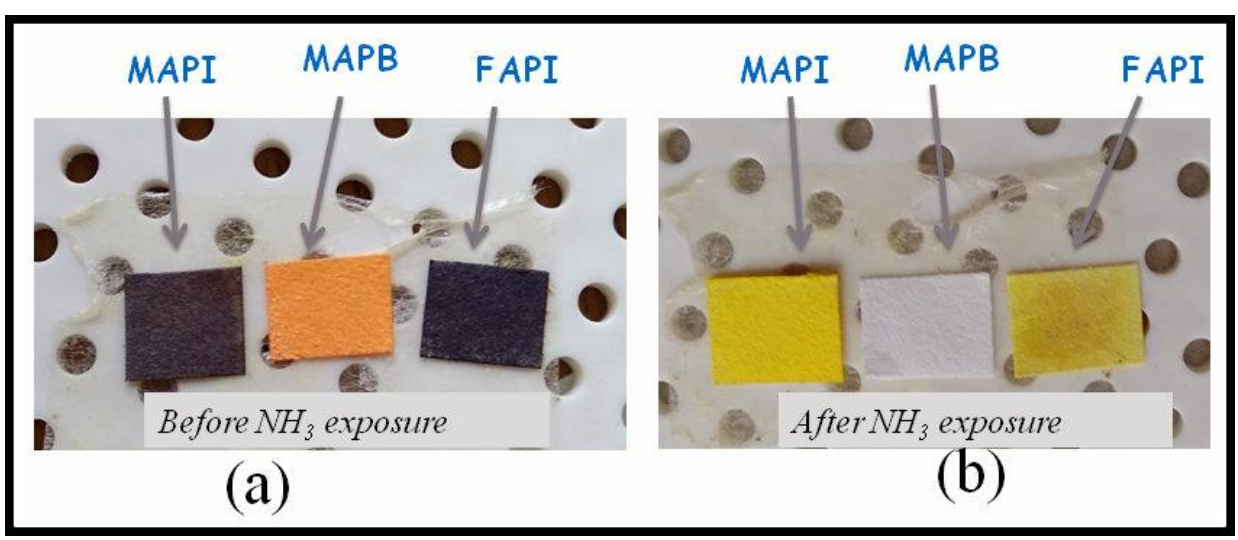

Figure 5. 2. *Photographs of MAPI MAPB, FAPI films (a) before NH_3gas exposure (pristine films) (b) after NH_3gas exposure*

To get insight more about visual response, we had carried out the experiment of all three micro/ nano structured films (MAPI, MAPB and FAPI) in identical environment at room temperature. All the three films were cut into identical size, shape and had been grown in same environment and exposed to equal concentration of NH_3 and recorded the experiment in a video camera. From video we got the necessary response time to change the color of all three sensors. All compounds, irrespective of cation/anion substitution are able to detect NH_3 gas visually though the response time is different. It has been observed that for a fixed concentration (~80 ppm), among all three, MAPI shows very instantaneous response (< 1 sec), where MAPB has response time ~ 2 min and FAPI has higher response time (> 4 min)

for complete change of the color from their pristine one as recorded from the video camera i.e. response time (τ) for MAPI $_{visual}$< MAPB $_{visual}$ < FAPI $_{visual}$.

It is also noteworthy that this color change phenomenon occurs in presence of NH_3 gas both in open atmosphere and as well as closed custom made test chamber with suitable injection of NH_3.

5.3.1 Visual Sensing by Inorganic Halide Perovskite:

It also has been observed that not only in 'organic (hybrid)' perovskite halide, the visual color change phenomenon occurs in 'inorganic' lead based perovskite halide also. We tested with inorganic cesium lead bromide ($CsPbBr_3$) film which has pristine yellow color. The yellow color changes to colorless in presence of NH_3 gas that could imply similar visual detection method for tracing NH_3gas like other organic lead based perovskite halides. The photographs of both pristine (unexposed) and NH_3 gas exposed films are shown in figure 5.3 [5].

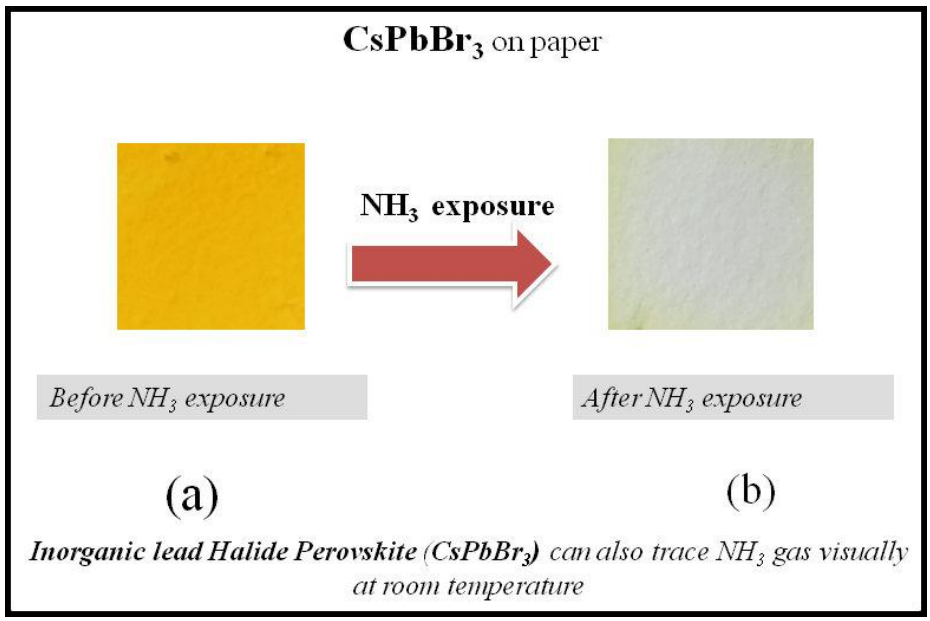

Figure5. 3. *Photographs of $CsPbB_3$ film (a) before NH_3gas exposure (pristine film) (b) after NH_3gas exposure*

5.4 Gas Induced Electrical Response of Family of Perovskite Halides:

5.4.1 Ammonia Gas sensing property by electrical read out:

The electrical response of all three paper based sensors/devices at ambient temperature has been recorded at different concentration (ppm) of NH_3 noting the current change of the devices in presence of the ammonia. In previous chapter we had shown that MAPI has lowest

visual detection limit (10 ppm for MAPI). For that reason we recorded the current response below 10 ppm for MAPI only. For other two cases we recorded down to 20 ppm concentration as their visual limit is relatively much higher than MAPI. The current response of the MAPB and FAPI based devices at different concentration has been shown in figure along with response of MAPI separately. The sensitivity is defined as like previous-

$$S \equiv \frac{[(R]_0 - R_g)}{R_0} = \frac{\Delta R}{R_0} \qquad 5\ldots\ldots (1)$$

where R_g and R_0 are the resistances of the sensor when exposed to NH_3 gas and without gas (base resistance) respectively.

It has been observed for all three cases the current starts increasing with injection of NH_3 for from an initial base current (bias =1.5V). It is noticed that like visual sensing performances of lead based perovskite halides as discussed above (section- 5.3), MAPI shows the highest electrical response. For other two sensors, the response of MAPB towards NH_3 is higher than that FAPI which is also consistent with their visual sensing performance as shown in figure 5.4(a). For a fixed concentration of 20 ppm, the electrical sensitivity of MAPI is *S*~96%, for MAPB *S*~ 82 % and for FAPI *S*~ 65% i.e. electrical sensitivity, MAPI $_{electrical}$ > MAPB $_{electrical}$ > FAPI $_{electrical}$. The typical sensitivity curve for all three sensors has been shown in figure 5.4(b).

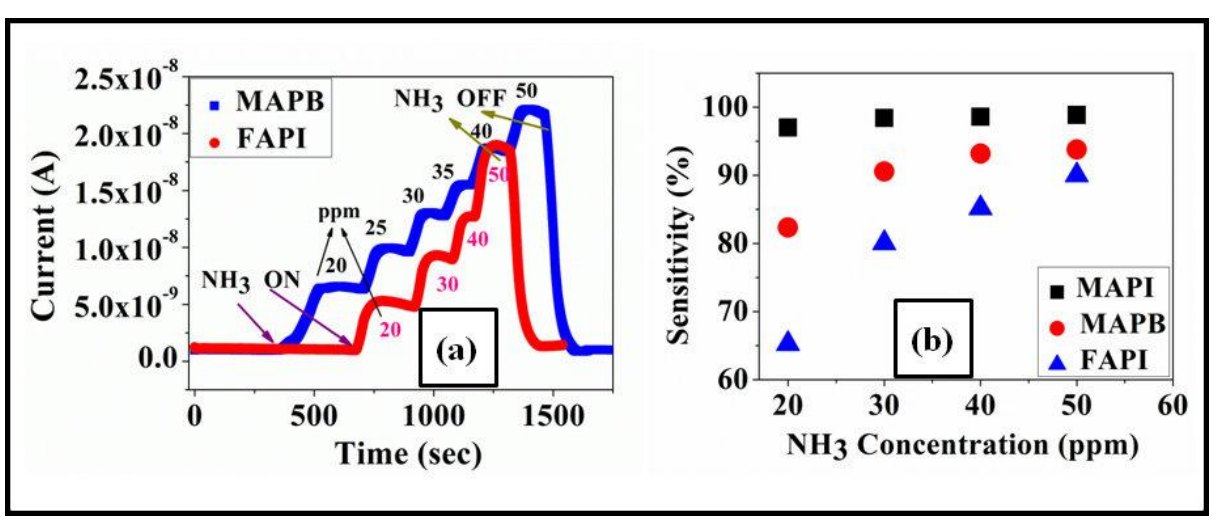

Figure 5.4. *a) Current response of MAPB and FAPI paper based sensors b) Current response of MAPI sensor c) Comparison of sensitivity of MAPI, MAPB, and FAPI based sensors at ambient temperature (up to 50 ppm)*

5.4.2 Electrical Nature /Characteristics of the Lead based halide perovskites before and during exposure to ammonia

The base resistance of the any gas sensors is a useful quantity. The pristine electrical characteristics of the gas sensors have been studied using Cu electrode. The data in figure 5.5 elucidates that all the sensors show a linear behavior. The average base resistances of the sensors are found to be ~5GΩ for MAPI, for MAPB~0.8 GΩ, and for FAPI it is ~0.4GΩ. Among the sensors MAPI shows higher resistive nature at unexposed condition for similar/identical device geometry. A number of devices have been tested for checking the reproducibility of the base resistances of the sensors.

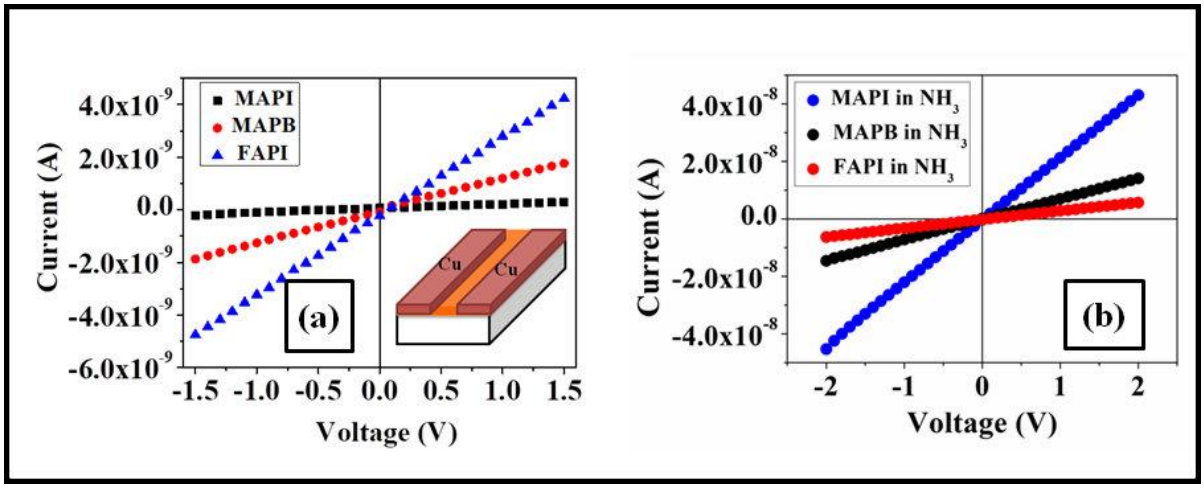

Figure 5.5 *a) I-V Characteristics of pristine MAPI, MAPB and FAPI paper sensors (paper electronics) along with schematic of the device b) I-V Characteristics MAPI, MAPB and FAPI paper sensors during exposure in NH_3*

The study of current –voltage *(I-V)* relationship during NH_3 exposure would give the insight about interaction of ammonia gas with the family of perovskite halides. We have recorded *(I-V)* characteristics of all three sensors at exposed condition as compared to the pristine (before exposure to NH_3 gas) one. In figure the data for a fixed concentration (20 ppm) has been shown for all three cases. Like MAPI significant current increment has been observed during exposure to NH_3 for other lead based halides also. In all three cases the *I-V* curve remains linear on exposure, i.e ohmic. From the $(I-V)$ curves it can be seen that even at a bias of $V = 1V$ the device the maximum current is in lower resistance MAPI sensor which is < 20 nA. It is much lower in the other two sensors so that the power consumption of the sensors at 1V is < 20nW.

This result on difference in sensitivity is important to understand the sensing mechanism which will be discussed in detail in later section.

We have also calculated the noise limited detectability from the current response data for all the sensors. Calculated results indicate that MAPI (10ppb) has much higher electrical sensitivity compare to other two i.e. MAPB (300ppb) and FAPI (500ppb), the schematic in fig also demonstrates that detectability. This sub ppb detection capability could extend the usage of these materials in case of medical fields like exhaled breathe analysis etc. It is noteworthy that for all three paper based lead perovskite halide sensors, operable at ambient temperature show much faster response compared to those observed in typical metal oxide based sensors.

To get a clear and concise view and for better clarity of overall sensing behavior towards ammonia by family of lead halide perovskites (by both visual and electrical detection) we have plotted different sensing regime for all the perovskites in a single graph as shown figure 5.6. Also to correlate the visual and electrical detection, the sensing parameters and characteristics for both sensing method have been listed in table [5].

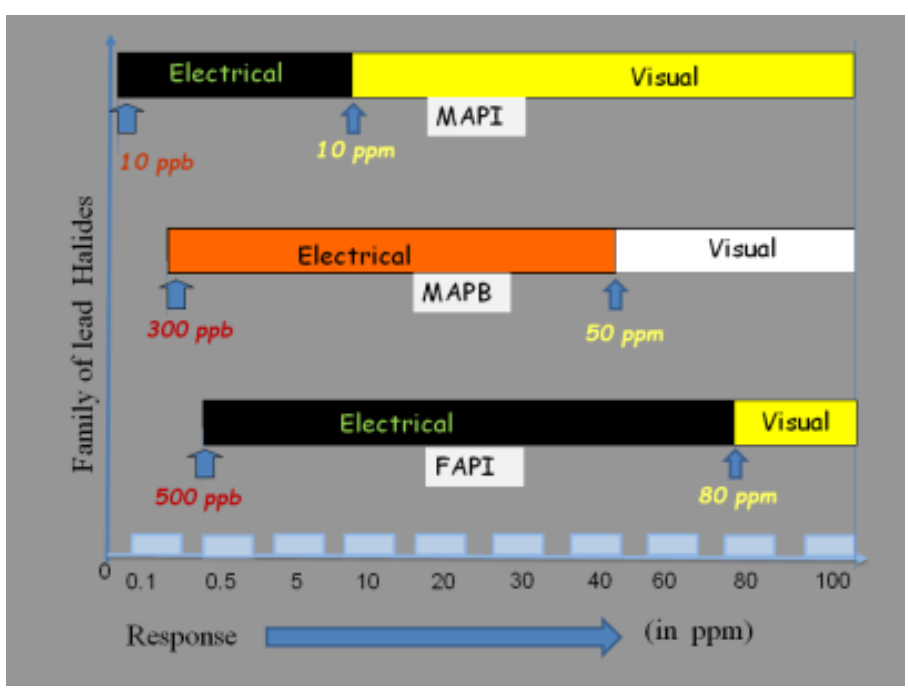

Figure 5.6.*Schematic of sensitivity scale of perovskite lead halide paper sensors (MAPI, MAPB and FAPI)*

5.4.3 Selectivity & Stability of the sensors towards storage:

High selectivity & storage stability are important parameters of gas sensor for practical use. The sensors were tested both in toxic gases like NO as well as other organic volatiles including methanol, Isopropyl alcohol/(2 Propanol) , Trichloroethylene(TCE)etc. For both sensors (MAPB & FAPI), the response towards NH_3 gas is much higher than other species of test gases immediately suggests high selectivity of the sensors towards NH_3 gas. The data is given in figure 5.7(a).Selectivity of MAPI has already been described previous chapter.

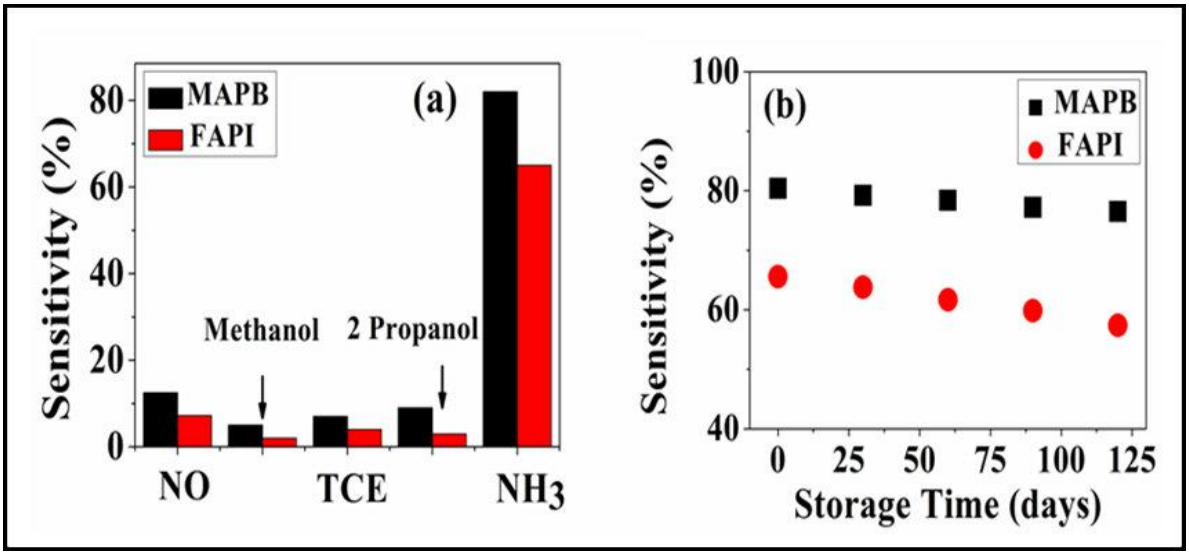

Figure 5.7. *(a)Selectivity of the sensors (MAPB & FAPI) towards NH_3gas (20 ppm) and other organic volatiles (saturated vapors) (b) Long term stability of the sensors for a fixed concentration (20 ppm)*

Stability towards storage has been tested for both sensors for a time period of 120 days with 30 days interval. The test has been done for a same concentration (20 ppm NH_3 gas) for both the sensors. Data is given in figure 5.7(b). It has been observed that MAPB shows longer stability than FAPI because FAPI has a tendency to slowly degrade towards a polymorphic δ phase from its black (α) phase which has less sensitivity. Sensing performance i.e sensitivity of MAPB sensor degrades around 5% after 120 days whereas for FAPI degrades ~ 12%. However this decrement of sensitivity does not affect its utility.

5.5 Understanding the gas sensing behavior by Family of Halide Perovskites:

Response by lead based perovskite halides towards ammonia in a qualitative similar fashion opens up a very basic aspect that does the lead based perovskite family follow a general sensing mechanism? Is there any common mechanism behind the similar nature of response shown by them? It is worthwhile to investigate the sensing mechanism towards NH_3 and the

nature of interaction during NH_3 exposure by the family of perovskite halides. We have tried to understand this via both experiment and MD (molecular dynamics) simulation.

5.5.1 Temperature Dependence of Sensitivity:

To appreciate any differentiation in the sensing mechanism as compared to shown by typical metal oxide semiconductors (MOS), we first performed temperature dependent sensitivity of the lead based perovskite based sensor (electrical). If charge transfer mechanism similar to typical metal oxide semiconductor is responsible here for sensing NH_3, then current response is expected to increase at elevated temperature due to reduction depletion width at grain boundaries. In contrast, we observe that the sensitivity reduces as the temperature of operation is enhanced in perovskite lead halides paper sensors. We performed the experiment using MAPB sensor for its better structural stability at higher temperature and noticed the sensing behavior of MAPB film from room temperature (27°C) to a moderate temperature (60°C) on exposure to 20 ppm NH_3 gas. The data are shown in figure 5. 8. The decrease in sensitivity is about 2%/K. We would see later on that this decrease of sensitivity has its origin in energy for NH_3 adsorption on the sensor material.

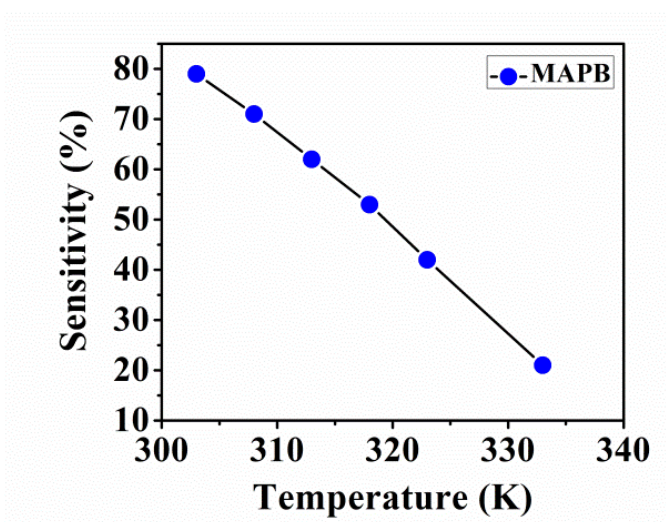

Figure 5.8: *Sensitivity of MAPB sensor as a function of temperature.*

5.6 Proposed sensing mechanism &correlation with color change:

The unusual temperature dependency of sensing performance by lead halide perovskite indicates a different insight to mechanism of gas sensing by lead halide perovskite. The basic

difference in mechanism for perovskite based gas sensor lies in the chemical reaction that occurs in presence of ammonia give rise to distinct color in comparison with conventional metal oxide based semiconductor gas sensors where mechanism is only dominated by selective physio adsorption of target molecules in the surface of the materials. The prominent yellow colors (for MAPI & FAPI) and white (for MAPB) strongly indicates a chemical reaction to a conversion of lead iodide (for MAPI & FAPI) and lead bromide (for MAPB) during interaction of ammonia. Thus the post exposure products must contain corresponding lead halides .Thus; the primary results on color change on exposure to NH_3 gas suggest decomposition of the perovskite halides during chemical reaction to lead halides which have distinct and characteristic colors. This is also supported in electrical observation. The Pb halides in general show higher conductivity due to higher ionic conductivity leading to reduction in resistance of the sensor on exposure to NH_3 gas. To validate and correlate the color change we propose a general sensing mechanism followed by family of lead halide perovskites and substantiated by molecular dynamics simulations and spectroscopic evidences.

The proposed basic mechanism for gas sensing for NH_3 gas in the general halide class of perovskites ABX_3(A=MA, FA B=Pb, X= Br,I) is given the generalized equation:

$$\mathbf{CN_{(2-i)}\,H_{(6-j)}\,PbX_3 + NH_3 = CN_{(2-i)}\,H_{(6-(j+1))}\uparrow + PbX_2(s) + HX\,(g)\uparrow + NH_3\,(g)\uparrow} \qquad 5\ldots..(2)$$

For $MAPbI_3$& $MAPbBr_3$ (i=1; j=0) give rise to following equation

$$\mathbf{CH_3NH_3PbX_3 + NH_3 = CH_3NH_2\,(g)\uparrow + PbX_2(s) + HX\,(g)\uparrow + NH_3\,(g)\uparrow} \quad \mathbf{(X=I,Br)}\ (2a)$$

For $FAPbI_3$ (i=0; j=1) that converts to the equation as follows

$$\mathbf{CH\,(NH_2)_2PbI_3 + NH_3 = CH(NH)\,NH_2\,(g)\uparrow + PbI_2(s) + HI\,(g)\uparrow + NH_3\,(g)\uparrow} \qquad (2b)$$

The above proposed reaction indicates that only solid reaction product that is left behind post exposure is PbX_2, (PbI_2 for MAPI & FAPI and $PbBr_2$ for MAPB) other reaction products being gas they leave the reaction environment. For MAPI and MAPB the volatile products are methylamine (CH_3NH_2), hydroiodic acid (HI) and hydrobromic acid (HBr) respectively. For FAPI these are fomamidine ($CH(NH)NH_2$), and hidroiodic acid (HI) . The formation of the PbX_2 on the surface of the sensor thus can explain the color change in the sensor material [5].

Below we describe results of both spectroscopic and electrical the experiments that had been performed to validate the proposed reaction mechanism and detection of PbX_2 as the primary color change agent similar to MAPI as discussed in chapter 3.

- **UV – Visible spectroscopy**:

The UV-Visible on pristine (unexposed) perovskite halides films of MAPB and FAPI, exposed NH_3 films and corresponding lead halide films i.e. $PbBr_2$ and PbI_2 were done and are shown in figure 5.9(a) and 5.9(b) respectively. For both cases the exposed film exhibits a very different optical absorption than that of unexposed films. For the MAPB the pristine (unexposed) film starts to absorb around 575 nm whereas, the exposed film starts to absorb around 385 nm which shows very similar nature

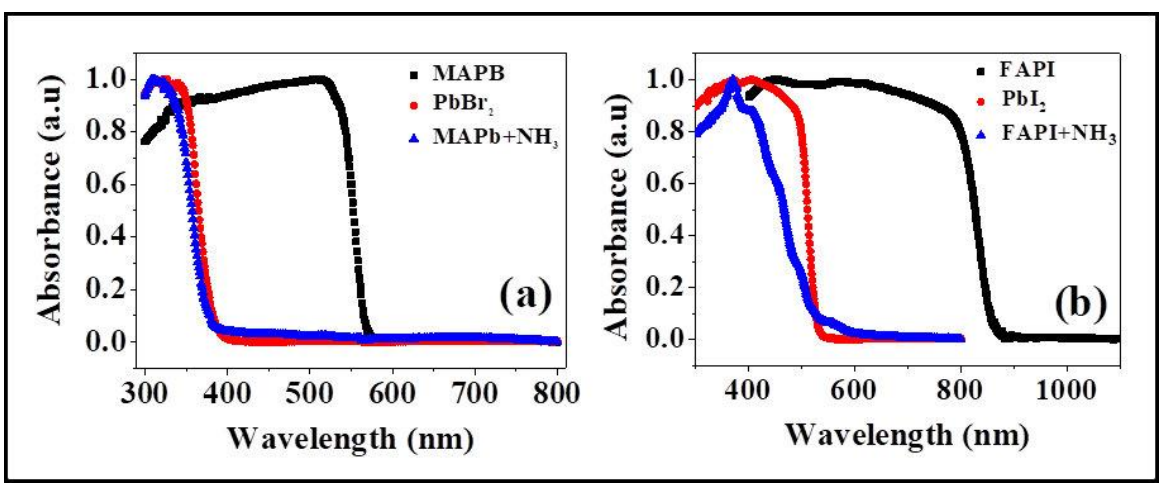

Figure5. 9 *a) Comparative study of UV spectra among pristine (before exposure), exposed MAPB and lead bromide ($PbBr_{2)}$ film b) pristine (before exposure), exposed FAPI and lead iodide (PbI_2) films respectively*

to $PbBr_2$ film. For both cases data were taken in absorbance mode with solid sample attachment.

In case of FAPI also, where pristine FAPI (unexposed to NH_3 gas) has substantially different absorption spectra than exposed NH_3gas film whereas, PbI_2 has identical absorption edge like exposed FAPI film.

For both cases identical nature between absorption spectra of exposed films and the corresponding lead halide films suggests a firm evidence of our hypothesis.

- **Photo- Luminescence (PL) spectroscopy:**

The PL data are shown in figure 5.10(a) and 5.10(b). The pristine (unexposed) MAPB film has a PL peak around 557 nm and the exposed film show a broad PL peak around 470nm and which is identical with the spectra obtained from $PbBr_2$ film (figure 5.10a). In case of FAPI (figure 5.10(b), the original (unexposed) film has a PL peak around 790 nm which is very different from the exposed FAPI film. Exposed FAPI film shows PL peak around 514 nm which is comparable to the PL spectra of PbI_2 film. Thus PL spectra also justify our hypothesis.

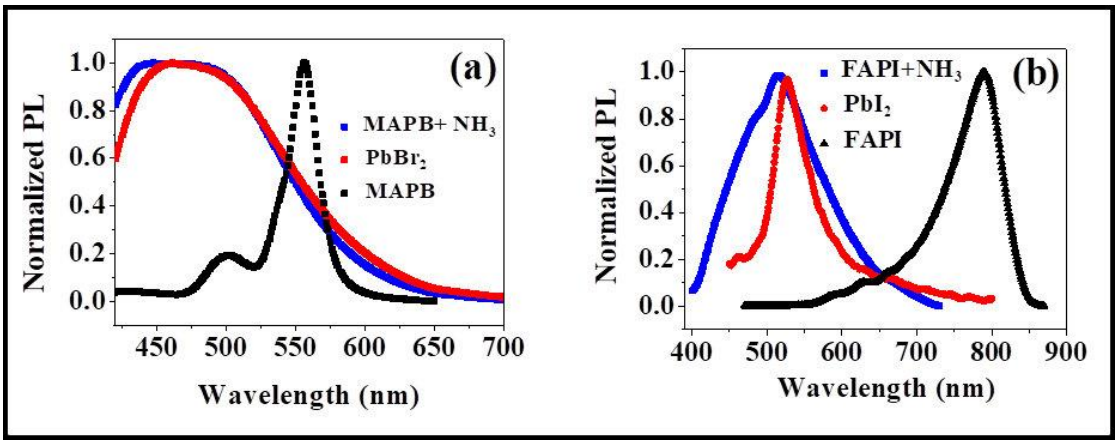

Figure 5. 10. *a) Comparative study of PL (photoluminescence) spectra of pristine, exposed MAPB and lead bromide ($PbBr_2$) film b) pristine, exposed FAPI and lead iodide (PbI_2) films respectively*

- **Electrical transport in the sensor films :**

Exposure of the films led to the formation of PbI_2 and $PbBr_2$ as have been observed from optical absorption and PL experiments. We argue that the enhancement of current in the sensor when it is exposed to NH_3 gas also occurs due to formation of PbI_2 and $PbBr_2$ which have less resistance likely due to the fact that they are also ionic conductor along with electronic conduction [6].We measured I-V characteristics of the sensors on the unexposed and fully exposed condition and compared the results with those performed on lead halides. From figure 5.11(a) and 5.11(b) it can be seen that the I-V characteristic of exposed MAPB is analogous to that of $PbBr_2$ where the current and conductance are higher. Similarly the I-V characteristic of exposed FAPI is similar to that of PbI_2 which show higher current. These results clearly establish that on exposure to NH_3 gas there is formation of lead (Pb) halides.

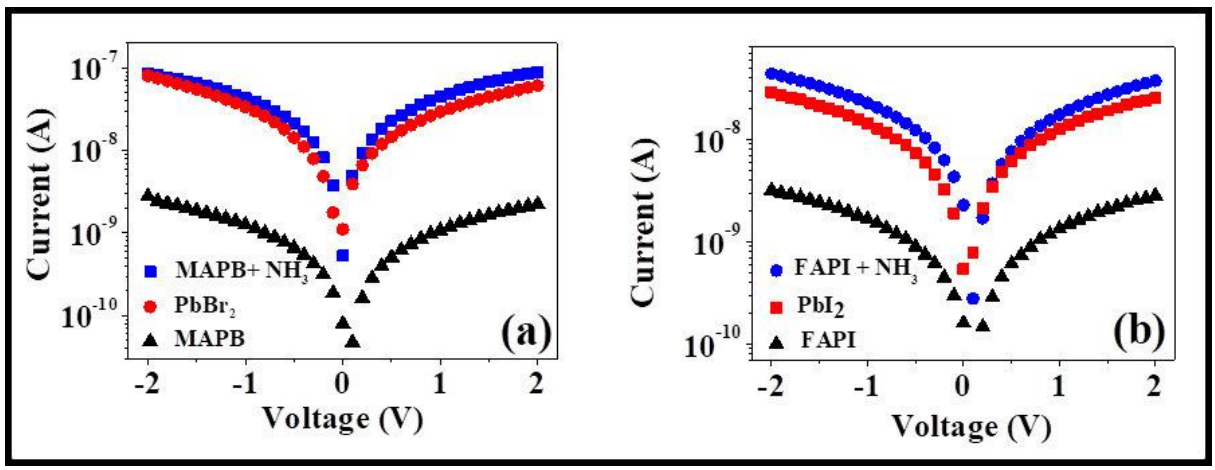

Figure 5.11. *Comparative study of I-V characteristics between a) pristine $PbBr_2$, exposed and unexposed MAPB film b) pristine PbI_2, unexposed and exposed FAPI film*

5.7 Understanding of the proposed mechanism by MD simulation:

To understand further about the proposed mechanism on basis of preferential adsorption of NH_3 molecules for gas sensing we have performed MD simulation of NH_3 gas adsorption on (110) plane of MAPI and (100) plane of MAPB as explained in the section 5.2 of this thesis.

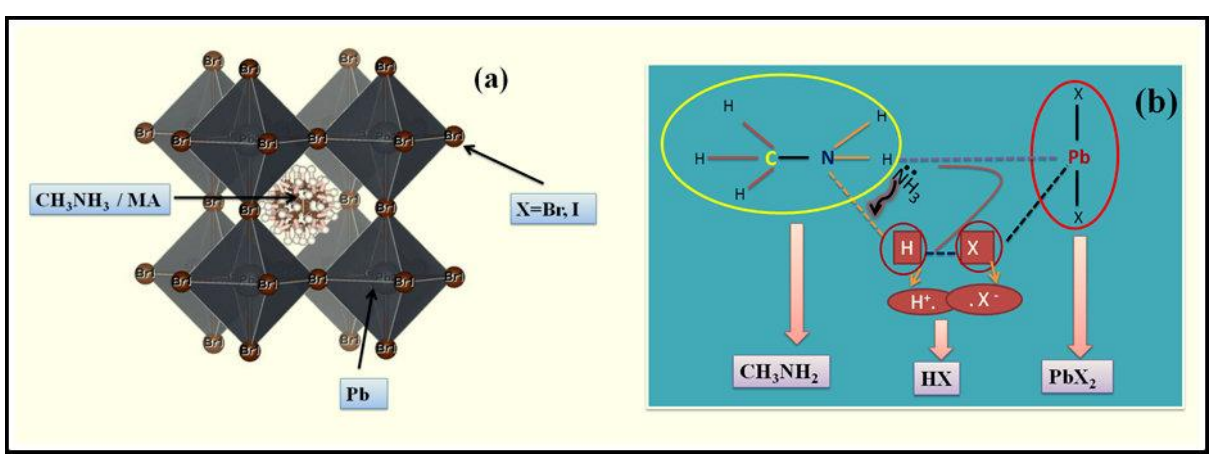

Figure 5. 12.*a) Schematic of the structure of the perovskite halides and b) mechanism of interaction with NH_3 and respective breaking of bonds to form the lead halides*

The schematic structure of the perovskite lead halide is shown in Figure 5.12(a). The corner sharing array of $(PbX_6)^{4-}$ octahedra make the basic structure. For simulation, we have placed one ammonia molecule at the edge of lead and bromine. We have chosen lead and bromine atom because they are heavier with respect to other atoms and therefore during thermal fluctuation their position will not change significantly. The NH_3 has a lone pair of

electrons which break the $(PbX_6)^{4-}$ octahedra and gets shared between H^+ and X^- forming HX and PbX_2 (see equations 2(a) and (b)).

The energy required for making the reaction self-sustainable arises from the exothermic nature of the reaction as given from the energy calculation of the adsorption energy ($E_{adsorption}$) for surface attachment of NH_3 on MAPX surface :

$$E_{adsorption} = E_{surface+NH_3} - (E_{surface} + E_{NH_3}) \qquad 5\ldots\ldots\ldots(3)$$

A snap shot of the MD simulation of the attached NH_3 molecule to MAPI and MAPB surfaces are shown in Figure 5.13. Adsorption energy ($E_{adsorption}$)for MAPB is$\approx 1.6eV$ whereas for MAPI is$\approx 4.5\ eV$ at 300K. The higher value of adsorption energy corroborates our observation of higher sensitivity of MAPI than MAPB at room temperature further. For MAPI the energy is nearly temperature independent (decrement ~0.004%/K) but for MAPB it decreases significantly at the rate of ~1.3%/K. This decrement in $E_{adsorption}$ leads to the decrease of sensitivity of MAPB during heating (see figure 5.8). The important role of the adsorption energy in enhancing the sensitivity can be appreciated.

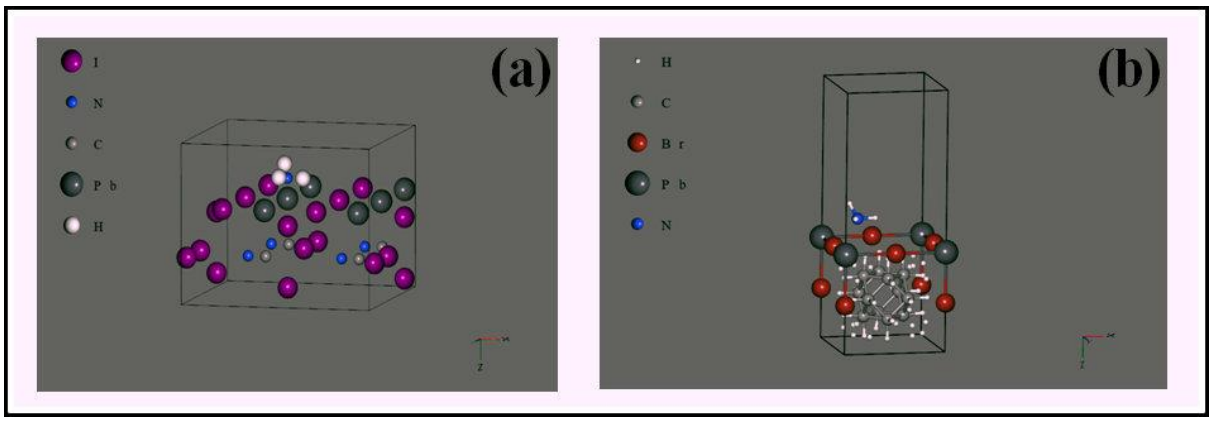

Figure 5.13. *A snap shot of the MD step for attachment of NH_3 molecule to a) MAPI b) MAPB surface.*

MD results also show an important phenomenon that has direct consequence on the higher sensitivity as well as response speed in MAPI compared to those in MAPB. The MD results show that during interaction with NH_3 there is transient temperature rise in a relatively short time scale (MD steps) as shown in Figure 5.14. The heat release due to exothermic nature of the reaction (which also makes it self-sustained) leads to the localized temperature rise. This temperature rise is useful to understand the mechanism in terms of bond breaking. Thus

during chemical reaction ammonia acts as heat source and helps to break the weak hydrogen bonds in A site cation (N-H bond) connected with the $(PbX_6)^{4-}$ octahedra [schematic has been shown in figure 5.12(b)] . The NH_3 has a lone pair of electrons which then gets shared between H^+ and X^- forming HX and PbX_2 (see equations 2(a) and (b)).Thus post exposure solid product left only lead halides. As shown in Figure 5.14 the temperature rises quickly to a high value in MAPI (compared to that in MAPB) preferably for higher adsorption energy leading to rapid and more efficient decomposition of the parent compound. This in turn gives rise to higher sensitivity and rapid response in the MAPI based sensor compared to other sensors.

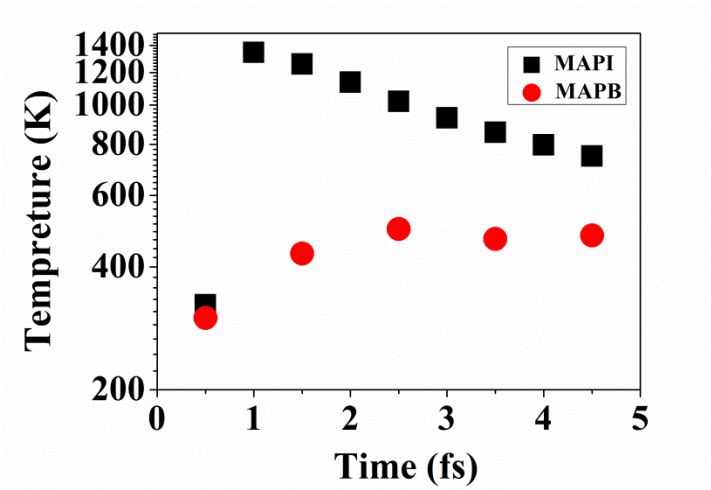

Figure5.14. *Local transient temperature rise during reaction as revealed by MD simulation for MAPB and MAPI.*

The discussion above shows that the NH_3 gas sensing mechanism by family of lead based perovskite halides is very distinct from that seen in conventional metal oxide gas sensors. The mechanism is explained in terms of surface attachment of NH_3 molecule and resulting chemical reaction**.** Good surface attachment of NH_3 is predominant factor for faster reaction and hence sensitivity among lead based perovskite halides. Role of NH_3 in driving the reaction leading to formation of PbX_2 also imparts specificity of the sensor to NH_3 gas[5].

5.8 Conclusions:

In summary we have demonstrated that high sensitivity and high selectivity ammonia gas sensors (both visual and electrical) can be made from family of perovskite lead halides with different anion and cation. The solution processed sensors are made on paper and operable at room temperature. We established that response towards NH_3 gas is qualitatively independent of substitution/alteration of cation or anion; surface morphology, crystal structure, and

electronic band gap although there are quantitative differences following a general reaction mechanism. The cation and anion substitution, surface morphology in perovskite halides (lead based) could extensively modulate the sensitivity /response towards NH_3gas.

It has been proposed that the sensitivity (as well as specific selectivity) of the lead based perovskite halide family to NH_3 gas arise from the fact that the material decomposes to the respective lead halides during interaction with NH_3 that give rise to the color change as well as reduction of resistance of the material. The quantitative difference in response has been substantiated by preferential adsorption of ammonia molecules and established by molecular dynamics simulations This work shows that the lead based perovskite halide family could provide a general platform for room temperature (unheated) solid state NH_3gas sensor which is also compatible with low power paper electronics.

References

5.1 Maity, A and Ghosh, B;. *Sci. Rep.*, 8, (2018), 1-10

5.2 Maity,A, Raychaudhuri, A.K , Ghosh, B; *Sci. Rep*., 9, (2019) ,1-10

5.3Valerio D'Innocenzo, Ajay Ram Srimath Kandada,Michele De Bastiani, Marina Gandini,†and Annamaria Petrozza, *J. Am. Chem. Soc.*,136, 17730−17733, 2014

5.4 Sneha A. Kulkarni,Tom Baikie,Pablo P. Boix, Natalia Yantara, Nripan Mathews, and Subodh Mhaisalkar, *J. Mater. Chem. A*, 2,9221, 2014

5.5 Avisek Maity, Saikat Mitra ,Chandni Das, Sohel Siraj, A.K.Raychaudhuri, Barnali Ghosh; *Materials Research Bulletin*,136, 111142, 2020

5.6 Oberschmidt',J and Lazarus,D.; *Physic.Rev.B.*21, 5813-5821, 1980

Chapter 6

Paper Electronics based stable Broad band Photo detector of cation engineered Hybrid Halide Perovskite

In this chapter of thesis we have studied optoelectronic properties of halide perovskites. We fabricated a "paper electronics" based broad band (300 -900 nm) detector for the first time using perovskite halide. We also introduced mixed cation namely $MA_xFA_{1-x}PbI_3$ *and studied the photo response behaviour along with the unsubstituted or pure compounds of MAPI & FAPI. It has been observed that the cation engineering not only enhances the photo response but also makes stable & broadband detector as compared to the single cation detector. The as fabricated detector is thus flexible, broadband and workable at low optical illumination intensity as well as low bias making compatible with battery powered electronics. The detailed optoelectronic properties and photo detector characteristics has been discussed in this chapter. A comparison among other paper based detector by other materials also been provided to get an insight paper electronics based photo detectors using halide perovskites.*

6.1. Introduction:

In recent days there is a considerable interest to study the optoelectronic properties of hybrid halide perovskite in view point of both fundamental and applications aspects. Lots of efforts have been put in fabrication of photo detector (PD) and other optoelectronic devices such as LED using halide perovskites for their excellent optical properties like long diffusion length, high carrier mobility, band gap tunability, high absorption coefficient etc [1-2].

Since inception, many researchers are working on halide perovskites to study the photo response property by fabrication of solution processed PDs tuning different parameters like composition, morphological, dimensional and substitutional engineering with different materials etc [3-6]. Still there is a serious challenge to improve the stability of such kind of photo detector without compromising performances. Beside this, most of the halide based PDs are operated in high bias (~10V); high illumination intensity that acts as impediment of their sensitivity to detect low optical signals and compatibility with battery powered electronics [7-10].

Moreover, flexible detector combined with broadband Responsivity and relatively high photo sustainability is essential to meet the growing demands of high performance optoelectronic devices. There are reports available on different materials on recent advancement in the field of wearable photo detectors based on different substrates like polymer, paper & fibre. Among them paper is preferred due to low cost, mechanical flexibility. Like other semiconductor photo PDs, reports on hybrid halide perovskite based photo detector are mainly fabricated on substrates like SiO_2/Si, glass and FTO, ITO, LAO etc[7,11-12]. Till now no report is available on paper electronics based photo detector by hybrid halide perovskites to the best of our knowledge other than ours [13].

In chapter 2 we have shown that different morphologies can be obtained of a particular perovskite by tuning the substrates, which also been observed from our group in the field of binary oxides [14]. We have seen that paper based halide perovskites are superior for their uniform coverage and stability as discussed in chapter 2. In last three chapters (3,4,5) we have also seen that paper based ammonia gas sensors can be made using the family of lead halide perovskites with long term stability up to 6 months with good response. This motivated us to explore whether an optical detector with a moderate responsivity can be made on paper instead of substrates like glass, ITO etc.

One of the main motivations of this chapter is to study the stabilized photo response of perovskite halides due to cation engineering using paper electronics with enhanced broadband spectral response.

The mixed cation was chosen to combine the higher response of MAPI and stability of FAPI. In this chapter, we have fabricated paper based photo detectors using mixed cation $MA_{1-x}Fa_xPbI_3$ with optimized substitution of FA cation and compared the spectral response with pure (unsubstituted) single cation MAPI, FAPI over a broad range (300-900 nm). Interestingly, it has been observed that cation engineering enhances both the stability as well as Response over the whole region. The detector using mixed cation organic halide is also able to detect photon at low optical illumination intensity (0.1 μW/cm^2) and at a low bias of 5V. The sensor can reach a moderate peak responsivity of 0.27 A/Watt at 800nm. Tailoring of photo response due to different cation size, morphology, shape has also been discussed emphasizing on using low operating bias voltage, low optical power (~ few micro watt).This significantly boosts use of cost effective technology compatible with low power paper electronics as sensitive photo detector[13].

6.2. Basic Operational Principle behind Photo response:

The basic mechanism behind photo response of any material closely associated with the absorption of the electromagnetic wave in certain region and corresponding extra carrier generation in the material due to photon energy of the optical illumination. These extra carriers primarily enhance conductivity of the material under illumination and hence photo current increases. This is the core of any kind of photo detector [15].

Typical photo detectors are –

i) Photo Diode

ii) Photo Conductor

iii) Photo- Transistor.

In our case, we have studied the photo response property of the single and mixed cation hybrid halide perovskite using planner photo conductor type geometry.

6.3. Experimental Process and Related Parameters:

The details of experimental procedure have been discussed in the chapter 2. A customised chamber was made to perform the optoelectronic measurements (~ up to $10^{-3}mbar$) to prevent the samples from moisture, high transparent quartz glass was used to pass the light

through the chamber (shown in figure 2.23). Also, dry Nitrogen (N_2) gas was injected to protect the environment moisture free during the experiment. There is issue of stabilizing dark current and also photo response under atmospheric condition due to humidity prone nature of perovskite samples. In this section we discuss about the useful parameters that are used to evaluate the quantitative description of the photo detector characteristics.

The main experiments for photo response consist of measuring the following:

- Device current (I) as a function of bias (V) at a fixed wavelength (λ) by with different optical illumination intensities (J) by turning illumination ON and OFF known as $I-t$ curves.
- The $I-V$ curves in dark and under illumination varying illumination intensities (J)
- Spectral Response i.e photocurrent (PC) as a function of wavelengths in the spectral range 300-900 nm for a fixed bias. The PC is defined as $I_{pc} \equiv I_{light} - I_{dark}$ for a given bias, illumination intensity and wavelength.I_{light} is the device current under illumination and I_{dark} the device current in dark at same bias.

These measurements lead to evaluate useful parameters to define photo detector performances. The major important parameters which have used -

- Responsivity (R)
- Photo Conductive Gain(G)

Responsivity (R): It is defined as the photo current generated (i_p) per unit optical power impinging on the sample. It represents the electrical output to the optical input of a optoelectronic device. The formula for Responsivity is

($R = \frac{i_p}{P_{sample}}$) where, i_p is the photo current, P_{sample} is the power falling on the sample for a fixed intensity. The incident power was calculated using the relation $P_{sample} = P_{opt} \times A$ assuming the full power falling on surface of the material is getting absorbed (P_{opt} being optical power density & A is effective exposed area.

Photo-Conductive Gain (G): It is defined as the ratio of the photo-generated carriers per unit time (I_p) to the incident number photons of frequency (ν) in unit time $P_{sample}/h\nu$ for a fixed frequency. It is directly associated with two time scales which correlates intrinsic material parameter to the device parameters. In a two probe metal-semiconductor-metal (MSM) detector the Gain in related to the material parameter ($\tau_{lifetime}$) i.e. carrier lifetime/ recombination time to the device parameter ($\tau_{transit}$)so that

$G = \frac{N_{carrier}}{N_{photon}} = \frac{\tau_{lifetime}}{\tau_{transit}}$ ..... (6.1)

Transit time($\tau_{transit}$) is the time a taken by a carrier to reach an electrode in the MSM (metal-semiconductor –metal) device (separated by a distance, l) under a bias V. If μ is the mobility of the carrier and the carriers are to diffuse over a channel length l, the transit time is the carrier diffusion time

$\tau_{transit} = \frac{l^2}{\mu V}$.

Now,($\tau_{lifetime}$) is basically life time of a carrier before recombination. So,

$\tau_{lifetime} = \frac{d^2{}_{avg}}{D}$ where, d_{avg} is the average recombination length and D is the Diffusion coefficient for an electron/hole.

Now if we replace the time scales in the equation (6.1) the gain G becomes ratio of two length scales namely recombination length(d_{avg}) and channel length (l) such that $G = \frac{\mu V}{D}(\frac{d_{avg}}{l})^2$.

It essentially shows that there is gain factor if the $d_{avg} > l$ and one can get enhanced photo response if the recombination length is greater than channel length.

6.4. Optoelectronic Study of single cation and mixed cation hybrid halide perovskite using paper electronics:

6.4.1 Optoelectronic Property of single cation hybrid halide perovskite ($MAPbI_3$/MAPI, $FAPbI_3$/FAPI and $MA_xFA_{1-x}PbI_3$):

As we mentioned out in introduction section that, one of our motivation was to study the cation engineered photo response by halide perovskite grown in paper. In order to do that, we check the essentiality of mixed cation in terms of stability and enhancement of optical response. First we observe the single cation response namely for MAPI and FAPI and then correlate the likely effect of mixed cation.

We have explored the photo response of single cation MAPI and FAPI using a broad band optical source. The spectral dependence of photo response $I_{ph}(\lambda)$of both the single cation halide perovskites photo detectors has been investigated in the wavelength range 300-900 nm as shown in figure 6.1. The data was taken at a bias of 5 Volt.

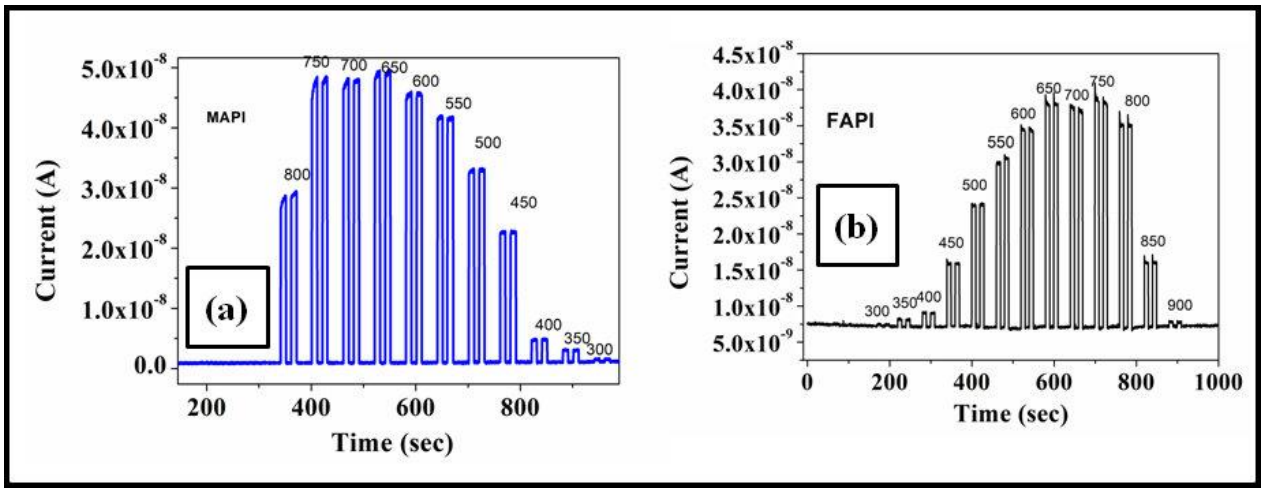

Figure 6.1: *Photo Response (I-t) curve of paper based photo detectors a) MAPI b) FAPI*

6.4.2 Enhancement of Photo Response and Stability by optimized mixed cation engineering:

Since FAPI is more stable relative to MAPI, our intension was to stabilize the photo response by incorporation of FAPI without compromising the superior response from MAPI. We have designed the photo detector by cation engineering with suitable doping of precursor MAI and FAI. We have optimized the substitution level of FA in MA site and grown the mixed cation based halide perovskite sample $MA_{1-x}FA_x\ PbI_3$ on paper. In figure 6.2(a) we have plotted, the photocurrent as a function of x at two illumination wavelengths in the substituted system $MA_{1-x}FA_x\ PbI_3$. The maximum response is seen at $x \approx 0.4$ showing that this is the optimum concentration. The photocurrent was measured at a bias 5V and with two different wavelengths 300nm & 650 nm respectively.

The stability of detectors was checked by measuring the photo response under continuous photo irradiation. It has been observed that performance of a MAPI photo detector under continuous illumination degrades faster than that of a FAPI or a mixed halide photo detector. Photocurrent of MAPI detector degrades ~60%/ hour whereas FAPI and mixed halide based detectors show approximately degradation of around ~20%/hour under continuous illumination at 650 nm with illumination intensity 120 $\mu W/cm^2$. The results indicate, FAPI provides more stable response compared to MAPI.

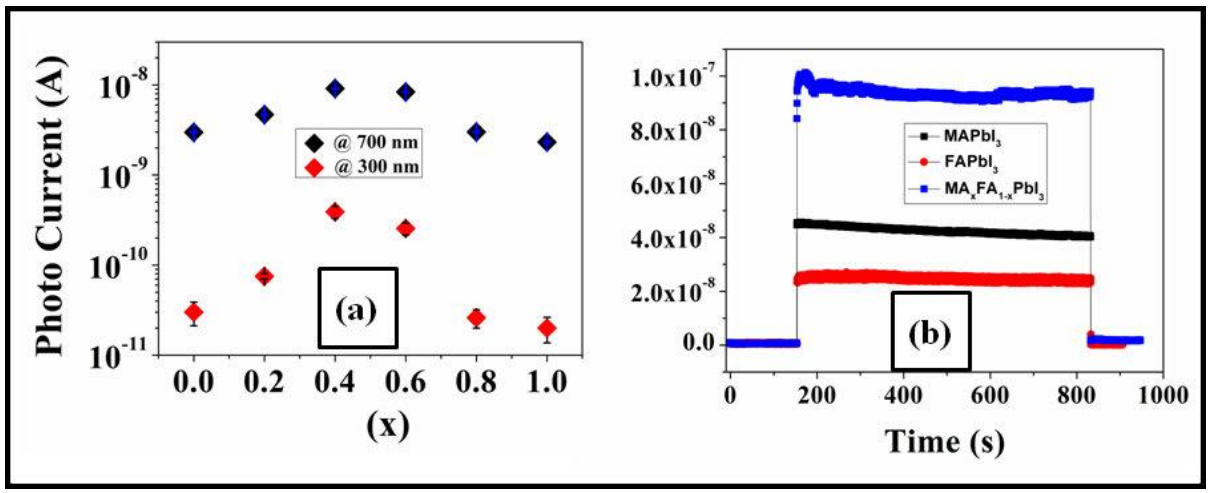

Figure 6.2: *(a) Photo current in the FA substituted as a function of x showing the optimal response at x=0.4. (b) Comparison of Photocurrent under continuous irradiation of 650 nm among three detectors*

We have observed that, mixed cation shows degradation of current ~21%/hour which proves that incorporation of FAPI improves stability under continuous photo stress with enhanced response, shown in figure 6.2(b). The data was taken at 650 nm keeping all parameters identical for all three detectors. The better insight of stable photo response can be rationalized from stabilization of crystal structural due to cation engineering as revealed from XRD data. The XRD of the mixed cation perovskite halide ($MA_{1-x}FA_xPbI_3$) films along with the end compounds MAPI & FAPI on paper are shown in figure 6.3. The X-ray diffraction indicates that substitution of FA on MA sites retain the lattice structure. Similar observation has been reported by Slimi.B.et.al [16]. Although FAPI is known to exhibit better thermal stability than MAPI, still there is a slow spontaneous degradation in normal ambience (although less as compared to MAPI) towards polymorphic non-perovskite (δ) phase (known as yellow δ phase) from its pristine black (α) phase that occurs unintentionally even at room temperature which inhibits the desired photo response. Hence this δ phase is undesirable. For mixed cation, this non-perovskite δ phase of FAPI disappears which indicates restoration of black (α) phase. Thus, mixed cation shows greater stability relative to the single cation. The major peaks corresponding to δ phase of FAPI are (010) at 11.8° and (021) at 26.3° disappear in mixed cation as shown from XRD given in figure 6.3. Absence of δ phase of FAPI in mixed cation stabilizes the structure relative to individual FAPI and shows better response and enhanced stability. The hump like peak ~ 22.7° present in all cases corresponds to paper substrate as we have discussed in chapter 2(section 2.3).

So, study of mixed cation photo response is worthwhile for its superior photo stability. It motivated us to study more detail characteristics of the mixed cation perovskite halide based paper photo detector. In following section we have discussed the photo detector characteristics of cation engineered perovskite halide.

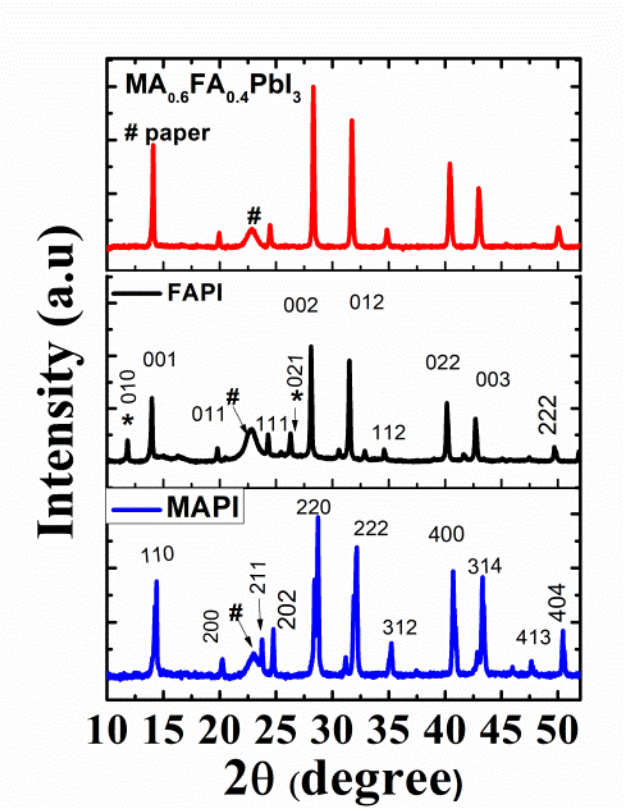

Figure 6.3. *X-Ray Diffraction of single cation & mixed cation ($MA_{0.6}FA_{0.4}PbI_3$) halide photo detectors grown on paper. In XRD data for FAPI* ******* *indicating peaks corresponding to the δ phase of FAPI. The peak marked as # at 22.7 ° present in all cases comes from the paper substrate*

6.5 Detail Study of Photo Detector Characteristics using mixed cation Hybrid halide Perovskite:

6.5.1 Broad Band Spectral Response of the Mixed Cation Photo Detector:

The spectral dependence of photo current $I_{Ph}(\lambda)$of the mixed cation halide perovskite photo detector has been investigated in the wavelength range 300-900 nm as shown in figure 6.4(a). The spectral response shows maximum response in the visible region although it has measurable response in the UV region as well as in the NIR region. The peak responsivity occur around 800 nm corresponding to the band gap of mixed cation photo detector due to

minimal favourable energy (band gap energy) leading to transition of electron from valence band to conduction band maximizes the photo carrier generation and hence photo response & responsivity. The spectral response has direct correlation with the absorbance curve shown in inset of figure 6.4(a) and it starts to rolls-off at around the fundamental absorption edge.

The spectral response (R) is one of the important figures of merit for a photo-detector which is defined as $R \equiv \frac{I_{Ph}}{P_{sample}}$, where $P_{sample} = P_{opt}A$ is the incident power absorbed by the material. We assume that full power falling on surface of the material is getting absorbed so that the total power $P_{sample} = P_{opt}A$ where, A is the effective geometric area of illumination; P_{opt} being the incident power density. Spectral response of R is shown in the figure 6.4(b). However, since the fill factor of the film is ~0.7 and is somewhat uncertain, the actual area over which the absorption occurs will be less than the effective geometric area making P_{sample} smaller. This thus leads to under estimation of the responsivity. This also makes the spectral response as a lower limit and actual R can actually be higher.

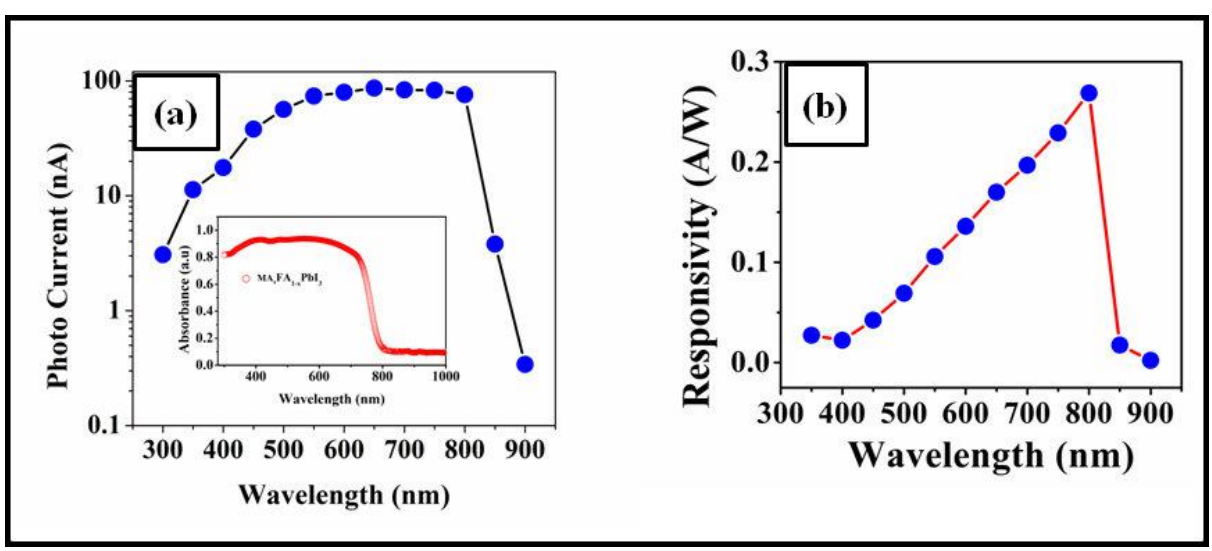

Figure 6.4: (*a) Spectral Response (photo current) of mixed halide paper based detector; Inset: shows the absorption spectra of the photo detector* (b) *Responsivity of the detector in that spectral range*

Specific Detectivity (D^*) is an important performance linked parameter of a photo-detector which gives an estimate of the minimum optical power that can be detected by a photo-detector. Taking account the main contribution from the shot noise, the specific detectivity is

defined as $D^* = \frac{R}{(2eJ_d)^{1/2}}$, where J_d is the dark current density and D^* is in a unit of $cmHz^{1/2}W^{-1}$.

The values of detectivity for three different wavelength regions (UV-Vis-NIR) at a bias of 5V for mixed cation organic perovskite paper photo detector have been tabulated in Table 6.1.

Detectivity *(D*)* (Jones)	Wavelength (nm)		
	350	650	800
	1.52×10^{11}	9.44×10^{11}	1.49×10^{12}

Table 6.1: *Detectivity of mixed cation photo detector at three different wavelength regions (UV-Vis-NIR)*

The dark current rms noise is$\leq 10pA$. With broad band responsivity $R \geq 0.1$ A/Watt the detector can detect optical power$\sim 100pW$. This is a high response for a paper based detector [13].

6.5.2 Dependency of Photo Current on illumination and Bias:

The photo current, defined as, $I_{ph} = I_{ill} - I_d$ at a fixed bias, of the device under test (DUT) as a function of illumination intensity was measured at a bias of 5 V. Data was taken at a wavelength λ=650nm at different incident power using a mechanical chopper. The data is shown in figure 6.5. The photo current increases with optical power density and have the dependence $I_{ph} \propto {P_{opt}}^{\beta}$. The exponent β depends on the process of electron-hole generation under illumination and on the distribution of trap states near the Fermi-level [17]. Due to sub linear dependency on optical power, Responsivity decreases as P_{opt} increases; for $1\mu W/cm^2$optical power density, Responsivity ~0.45A/W whereas for 120 $\mu W/cm^2$, intensity ~0.2A/W.

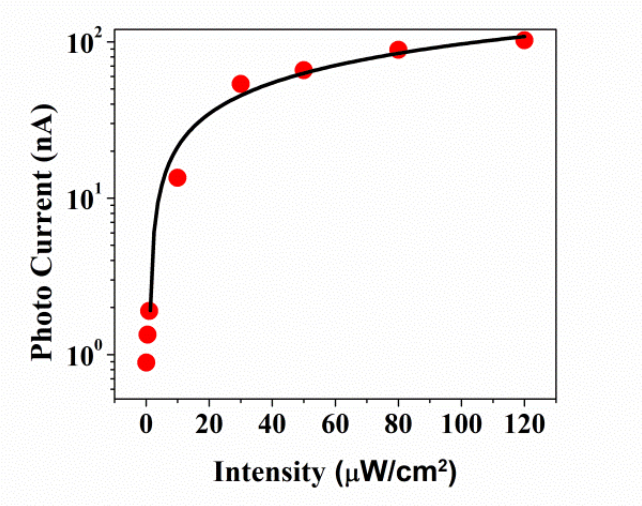

Figure 6.5: *Dependency of Photo Current on incident optical power density*

The optical gain of the device defined as $G \equiv \frac{I_{Ph}}{I_d} = \frac{I_{ill}-I_d}{I_d}$, I_{ill} and I_d are current under illumination and dark current respectively. In figure 6.6(a) we have shown the current in the device when the illumination is turned ON and OFF. In figure 6.6(b), the gain G as a function of the applied bias is shown for illumination at $\lambda = 650nm$ and illumination intensity 120 μW/cm^2. G has a strong dependence on bias and changes by 2 orders when the bias is changed from 1 V to 5V and then saturating at ~ 200 which is a sizeable gain for a device made on paper, where, the photoconductive material has a morphology consisting of microrods that may limit the carrier lifetime .

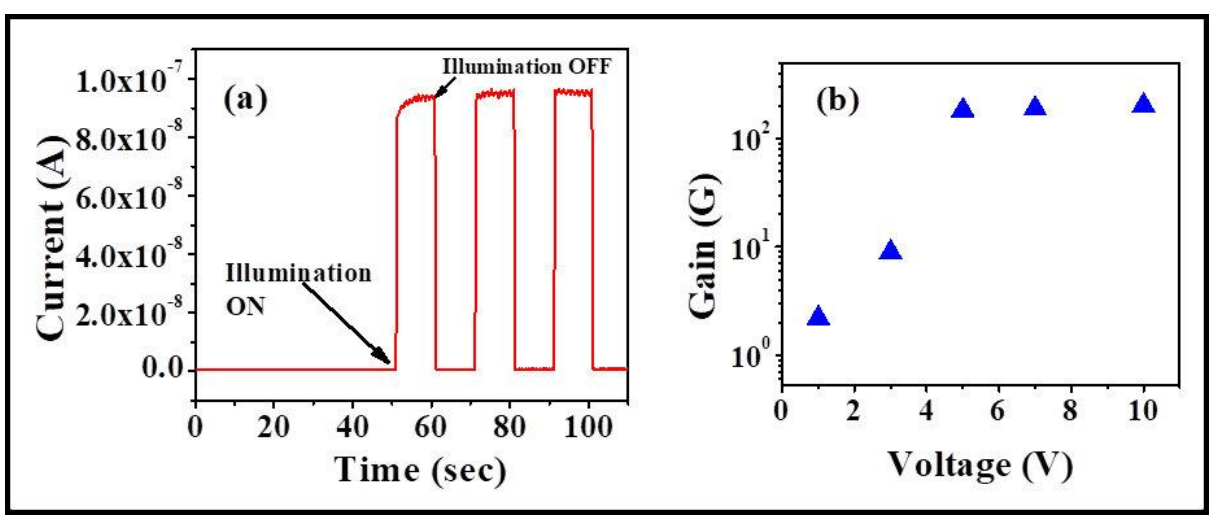

Figure 6.6: *(a) Photo Current for successive Illumination (ON/OFF) under 650 nm with illumination intensity of 120 μW/cm$^{2.}$ (b) The Optical Gain G as a function of bias voltage while other parameters remaining same.*

The variation of current gain G with respect to illumination intensity shows clearly three different regions as shown in figure 6.7. For low illumination intensityP_{opt}, ($P_{opt} \leq 10\mu W.cm^{-2}$) the gain increases following a power law ($G \propto {P_{opt}}^{\gamma}$) where $\gamma \approx 0.16$.Such a low value of γ has been seen in photo-response in photo-detectors based on ordered arrays of Nanowires [18]. For $100\ \mu W.cm^{-2} > P_{opt} > 10\ \mu W.cm^{-2}$increases G linearly with P_{opt}, showing saturation of trap states by the charge carriers generated by illumination. Eventually at higher illumination power G satuares to a high value of ≈ 200. It is important to point out that in the reported mixed cation perovskite halide photo-detector made on glass plate[7] ,

the lowest illumination power tested was >340 $\mu W.cm^{-2}$ which is nearly the same as the highest illumination intensity used by us. The detector reported here shows detect measurable gain even at illumination intensity as low as 1 $\mu W.cm^{-2}$

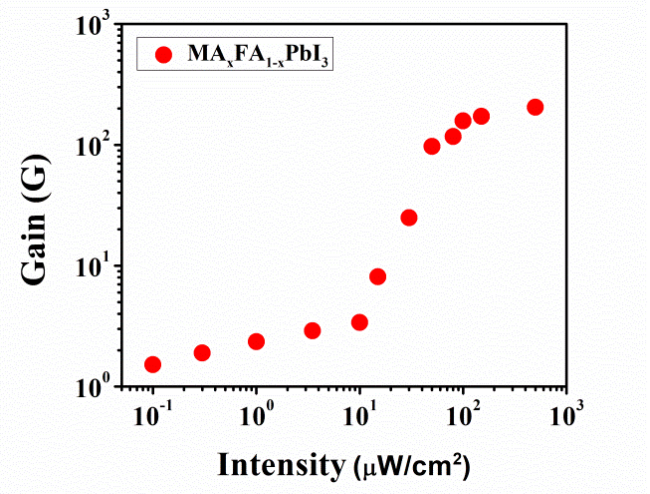

Figure 6. 7: *Optical Current Gain (G) as function of illumination intensity*

6.5.4 Long Term Stability & Mechanical Flexibility of the Paper Photo Detector:

Long term stability and sustainability under illumination are the major two key factors that limit the practical usage of perovskite halide based photo detectors [19]. The long term stability is also enhanced due to cation substitution in mixed halide lead perovskites. The stability for 1 month among all three detectors has been shown in figure 6.8(b) for a fixed wavelength 650nm with 5V bias and 120μW/cm^2 intensity. While photo current of MAPI based detector degrades 58% after 1 month, FAPI degrades 26 % in a month, whereas for the mixed cation degrades only ~ 5% in the same period. The disappearance of delta phase (as described in section 6.4) of FAPI gives more stability to the mixed cation that not only enhances the current but also improves the stability combing the high response of MAPI & stability of FAPI.

The long term stability is also tested by checking the response up to 1.5 month within an interval of 15 days. The data is shown in figure 6.8(a). The experiments were performed at 5V bias and 650 nm wavelength under illumination intensity $120\mu W/cm^2$ for every time. From figure 6.8(b) it can be seen that the photocurrent after 1 month changes by ~ 4% suggests high stability. Such stability under continuous photo irradiation and long term stability are quite important for sustainability of halide photo detectors.

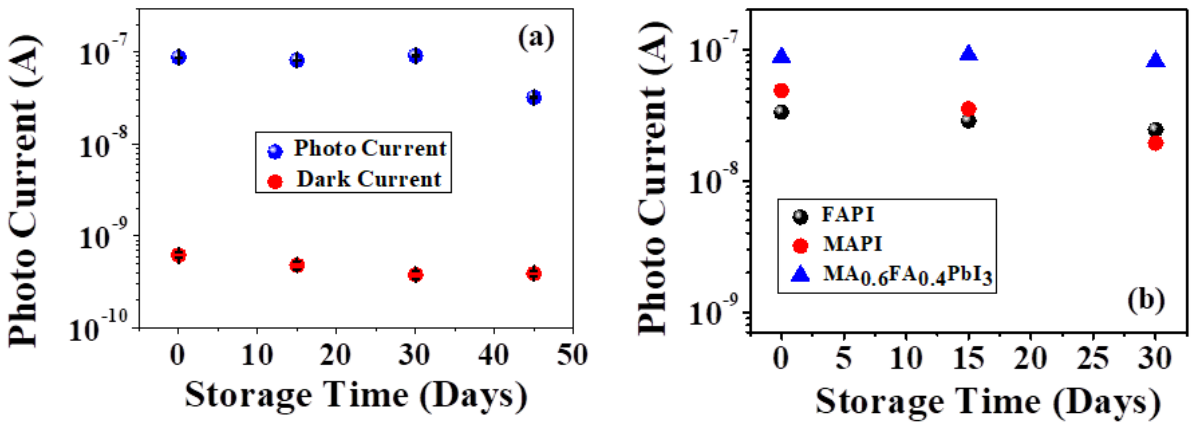

Figure 6. 8: *(a) Stability of the photo as well as the dark current in the Photo detector over a period of 45 days (error bars are smaller than symbols) (b) Comparison of stability of photo current among three detectors*

We have tested the photo response of the detector at bending condition as well with bending radius down to 3 of mm keeping same the measurement parameters (for 650 nm with 5V bias at 120μW/cm^2 intensity) similar to that used for testing in flat condition. The data has shown in figure 6.9. We have observed that the change in photo response < 5% in the bent condition suggesting good mechanical stability and flexibility of the paper detector.

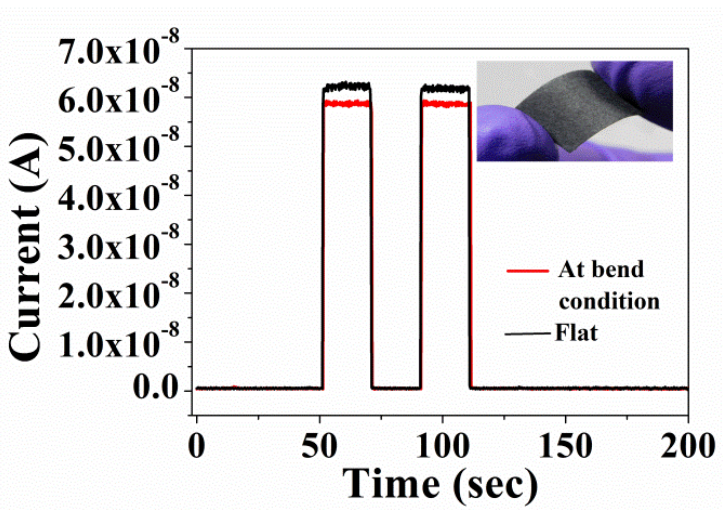

Figure 6.9: *Comparison of photo response of mixed cation photo detector at flat and bend condition (bending radius 3 mm). For both cases data were taken at a wavelength of 650 nm with 5V bias with intensity of 120μW/cm^2. Inset: The photograph of the flexible photo detector at bend condition.*

6.5.5 Transient Response of the Photo Detector:

Speed of a photo detector is an important parameter. We measured the transient response of mixed cation photo detector using short pulse of optical illumination controlling the chopper frequency. The data is shown in figure 6.10. From the graph the rising time is calculated as 65 ms which is quiet fast and recovery time is ~ 200ms. The time scale observed in the photo-response is limited by the band -width of digitization of the source- meter and is around 3 Hz. Likely; the intrinsic response is much faster. However this response in ms timescale from a paper based photo detector is quite appreciable.

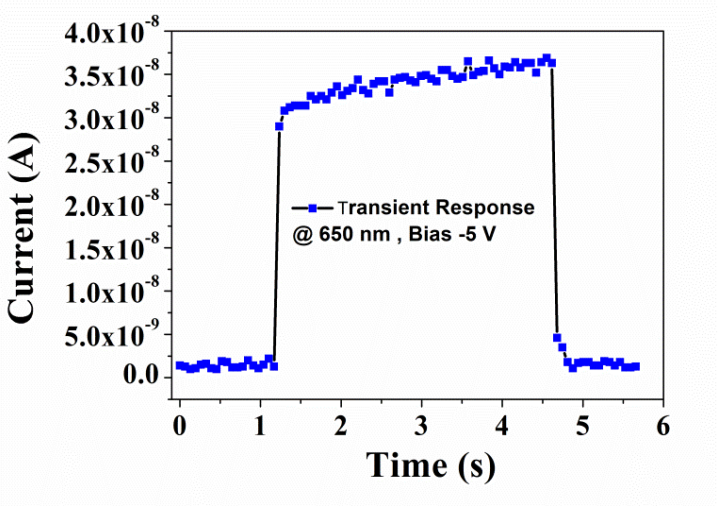

Figure 6.10: *Transient Response of the detector for determining response –recovery time*

6.6. Discussions:

6.6.1 Comparison of perovskite halide based Photo Detectors:

A comparison of optical response of a detector made from cation substituted $MA_{0.6}FA_{0.4}PbI_3$ has been made with those made from unsubstituted single cation halide perovskites MAPI and FAPI. MAPI has band gap ~1.6 eV (775nm) and FAPI has band gap of ~1.49 eV (832 nm) [20]. Absorbance data are shown in figure 6.11.MAPI and the mixed halide have very close absorbance and the absorption edge, while that for FAPI is red shifted to longer wavelengths.

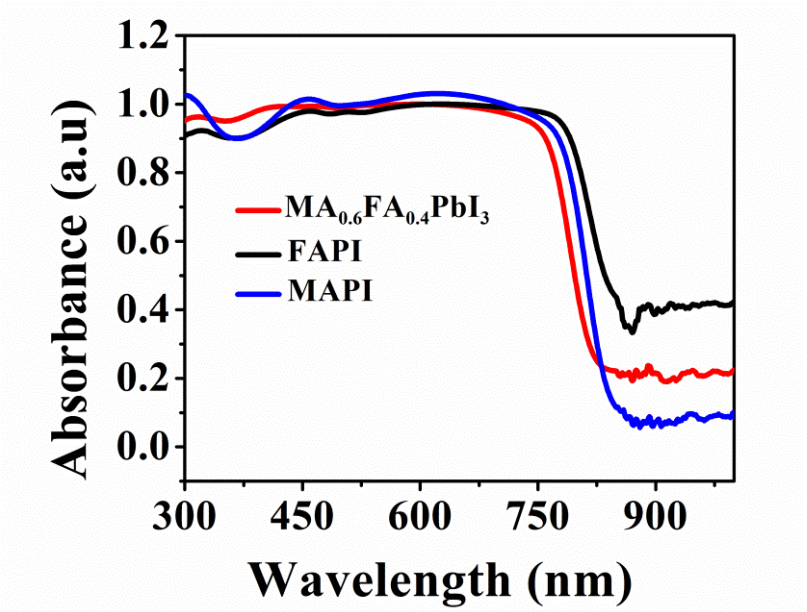

Figure 6.11: *Comparison of absorption spectra among three detectors*

Figure 6.12 shows comparison of the responsivity *R* in the three photo detectors taken in the illumination range 350-900nm. While at longer wavelengths they have comparable performance for wavelength < 800nm and in UV the mixed halide based detector has much superior performance. UV response of mixed cation is

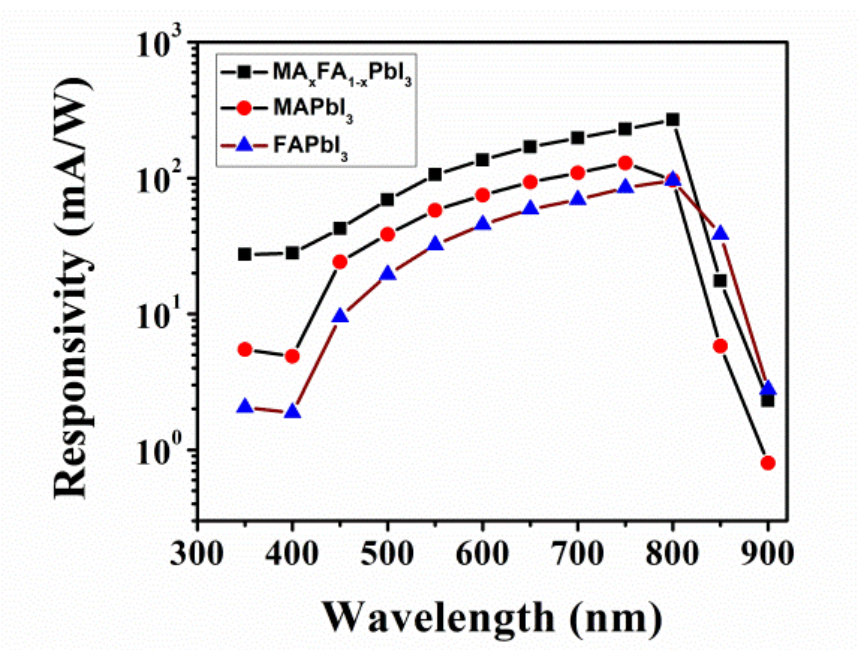

Figure 6.12: *Comparison of responsivity among single cations (MAPI & FAPI) and mixed cation based photo detectors over the spectral range 350 to 900 nm.*

enhanced by more than one order (~ 15 times) compared to that of FAPI and 5 times compared to that of MAPI.

6.6.2 Essentiality & Novelty on Paper based Perovskite Photo Detector:

There are reports on single cation and mixed cation photo response on halide perovskites. But enhancement of such paper electronics based broadband Responsivity from UV to NIR region using cation engineered hybrid perovskite material is not reported to the best of our knowledge. It can be seen that the paper based photo detector can reach substantial responsivity while retaining the advantages of a paper photo detector. Also report on optical response (R~ 270 mA/W) of halide perovskite from highly resistive paper substrate ($\rho \sim 10^8 \Omega - cm$) is important.

The lower responsivity of a photo detector made on paper substrate likely can be traced to its morphology of microrods with large number of internal boundaries that can reduce the carrier diffusion length compared to that in photo detector film grown on a substrate like glass that in the composition that is being investigated here. Here photo detector film grown on a substrate has fairly uniform thickness and morphology that enables longer range carrier diffusion before recombining.

The paper photo detector has another advantage that it can work with a low bias as low as 1V although the optimum bias is 5V, beyond which the responsivity as well as the photo gain saturates. At a bias of 5V the typical device dark current is $< 10^{-9}$ A. Since the photo current being $< 10^{-7}$ A, the dissipation and power requirement during detector operation is < $0.5\mu W$. Such a low power requirement makes the detector fully compatible with Li ion battery based electronics.

We have also compared performances of different paper based photo detectors reported in the literature along with the detector reported here. We have found that the mixed cation based lead halide photo detector reported here is quiet superior in terms of responsivity as compared to other similar detectors. In table 6.3 we have listed the photo response performance of different paper based photo detectors along with the photo response of the paper based mixed cation halide photo detector reported here. The performance of the photo detector based photo detector here can be seen to be much superior to the performances of other reported paper photo detectors [21-23].

Materials	Spectrum Covered (nm)	Responsivity (A/W)	Minimum operational optical intensity	References
WSe_2/PANI composite	Reported Only at 670	0.016 @ 670 nm	1 mW/cm^2	[21]
WSe_2 nanodots	390-880	0.018 @ 590 nm	1 mW/cm^2	[22]
TMDC Nanosheets ($MOSe_2$, $MOTe_2$)	450-650	1.69×10^{-6} @ 488 nm	< 80 μW/cm^2	[23]
$MA_{0.6}FA_{0.4}PbI_3$	300-900	0.27 @ 800 nm	0.05 μW/cm^2	This Work

Table 6.2: *Comparison of different photo detector properties among other paper based photo detector.*

6.7 Conclusions:

In summary we have demonstrated a paper based mixed cation hybrid halide broad band photo detector working from UV to NIR region, with peak responsivity reaching 0.27 A/W. The paper based optical detector exhibits enhanced response in UV region as compared to other perovskite based photo detectors. Cation engineering, in which MA is substituted by FA, makes not only the photo detector more stable than a single cation based photo detector but also enhances the response. The optimum response and stability is reached for the composition $MA_{0.6}FA_{0.4}$ PbI_3. The detector film can be fabricated by a simple one pot synthesis method. The detector is also operable at very low optical illumination ($< 1\mu W.cm^{-2}$) that makes it high sensitive photo-detector and needs low operative power. The detector with dark current rms noise is $\leq 10pA$ can detect optical power $\sim 100pW$ with a broad band responsivity $R \geq 0.1$ A/Watt. The detector shows good stability under continuous illumination and has a reasonable shelf life.

References:

6.1 Yixin Zhao and Kai Zhu, *Chem. Soc. Rev.*, 45, 655, 2016

6.2 Li Na Quan, Joohoon Kang, Cun-Zheng Ning, and Peidong Yang, Chem. Rev. 119, 9153−9169, 2019,

6.3 Zhou,J.; Huang,J. *Adv. Sci*. *5*, 1700256, 2018

6.4 Li,P.; Shivananju,B.N; Zhang,Y; Li,S; Bao,Q. *J. Phys. D: Appl. Phys. 50*, 094002, 2017

6.5 Hu,X; Zhang ,X.; Liang,L.; Bao,J; Li,S; Yang ,W.; Xie,Y. *Adv. Funct. Mater. 24*, 7373–7380, 2014,

6.6 Dou, L. ; Yang,Y.; You,J.; Hong,Z.; Chang,W.; Li,G.; Yang,Y. *Nat. Commun. 5*, 5404, 2014.

6.7 Li,S.; Tong,S.; Yang ,J.; Xia,H.; Zhang,C.; Zhang,C.; Shen,J.; Xiao,S.; He,J.; Gao,Y. *Organic Electronics*, *52*, 190, 2018

6.8 Liu.Y.; Sun,J.; Yang,Z.; Yang, D.; Ren, X.; Xu,H.; Yang,Z.; Liu,S. *Advance Optical Material 4*, 1829, 2016,

6.9 Wang,W.; Ma,Y.; Limin,Q. *Adv. Funct. Mater. 27*, 1603653, 2017

6.10. Xu.X; Chueh,C.; Jing,P.; Yang,Z.; Shi,X.; Zhao,T.;Lin,Y.L.;Jen,A. *Adv. Funct. Mater. 27*, 1701053, 2017

6.11 Yan,K.; Wei,Z.; Zhang,T.; Zheng,X.; Long,M.; Chen,Z.; Xie,W.; Zhang,T.; Zhao, Y.; Xu,J. *Adv. Funct. Mater. 26*, 8545–8554, 2016,

6.12 Lixia Ren, Min Wang, Shuanhu Wang, Zhan Zhang, and Kexin Jin; *J. Phys. Chem. C* , 122, 19, 10495–10500, 2018

6.13 Avisek Maity, A.K.Raychaudhuri,Barnali Ghosh ; Paper based stable broad band optical detector made from mixed cation Perovskite Halides; *Journal of Physical Chemistry C* ,125, 19, 10646–10652,2021

6.14 Ankita Ghatak, Samik Roy Moulik, Barnali Ghosh, *RSc Advances* , **6**, 31705-31716, 2016,

6.15 L. Dou, Y. Yang, J. You, Z. Hong, W.-H. Chang, G. Li, Y. Yang, *Nat. Commun. 5*, 5404, 2014,

6.16 Slimi.B.; Mollar,M.; Assaker,I.;Kriaa,I.; Chtorou,R.;Mari,B. *Energy Procedia 102*,87-95, 2016,

6.17. Rose,A. Concepts in Photoconductivity and Allied Problems. Krieger, New York, 1978.

6.18Basori,R.; Das,K.; Kumar,P.; Narayan, K. S.; Raychaudhuri, A. K. *Appl. Phys. Lett. 102*, 061111, 2013,

6.19 Li,Y.; Xu,X.; Wang,C.; Ecker,B.; Yang,J.; Huang,J.; Gao,Y*J. Phys. Chem. C*, *121*, 3904−3910, 2017.

6.20 Reinoso,M,A.; Otálora,C.; Gordillo,G.. *Materials, 12*, 1394, 2019

6.21 Kannichankandya,D.; Pataniyab, P.; Zankata,C.K.; Tannaranaa,M.; Pathaka,V.; Solankia,G.K.; Patela,K.D.. *Applied Surface Science, 524*,146589, 2020

6.22. Pataniya,P; Zankat,C.; Tannarana,M.; Sumesh, C. K.; Narayan,S.; Solanki, G. K.; Patel, K. D.; Pathak,V; Jha.P.. *ACS Appl. Nano Mater*. *2*, 2758−2766, 2019,

6.23 McManus,D.; Dal Santo,A.; Selvasundaram, P B.; Krupke,R.; LiBassi, A.; Casiraghi, C.. *Flex. Print. Electron.* 3034005, 2018,

Chapter 7

Direct detection of Gamma-ray photons down to nano curie activity at room temperature using highly radiation resistant Organic Perovskite Halide {$FAPbI_3$; FA= $CH(NH_2)_2$} highly oriented Crystal

In this chapter of thesis we have explored the radiation detection properties of halide perovskite. The as grown solution processed highly oriented bulk crystal of $FAPbI_3$ (FAPI) has been used to trace hard radiation like gamma (γ) ray. A relatively simple and direct detection technique has been adopted to trace gamma ray using electrical read-out. Also comprehensive study of detector parameters like mobility-life time product, shelf life, radiation sustainability etc has been studied in great detail. Also, a proof of concept of a flexible γ-ray detector for wearable, low cost radiation detector has been established using paper electronic based γ-ray detector by halide perovskites FAPI.

7.1 Introduction:

Realization of high performance, room temperature, cost effective, radiation detector has been a considerable interest for over many decades due to diverse application in scientific, industrial and medical research like homeland security, national defense and radiation therapy[1-2]. Radiation detectors not only trace the presence of radiation, whereas it carries about the information about the radiation energy, location or type. For instance, high precision measurement of spatial distribution of radiation intensity is very crucial for nuclear medical imaging whereas, national security demands information about the energy and identification of the type of radiation and isotopes. Specifically, among the radiations , detection of gamma rays is concerned with a wide range of energies varying from ~ 10 KeV (medical imagining, radiochemistry) to several TeV (for astrophysics)[1-2].

Perspective semiconductors could serve as a potential candidate for solid state gamma ray detection if it meets several desirable features simultaneously like high (mobility-lifetime) $\mu\tau$ product for efficient charge/carrier collection, high bulk resistivity and high average atomic number for capability of absorbing high energy photons[4]. Moreover, high crystalline material is preferred to maximize the $\mu\tau$ product due to reduced grain boundary scattering during charge transport. However, such kind of high Z value, high crystalline semiconducting materials are limited exhibiting simultaneously robust chemically and mechanically under radiation.

In previous chapters, we have discussed gas sensing and photodetection properties of lead based halide perovskites. In recent few years, there is boost in use of halide perovskite as hard radiation detector materials (like X-ray &γ-ray) apart from its well known applications in optoelectronics and energy/solar cell due to their long carrier diffusion length (hence large carrier recombination time), large bulk resistivity, and low cost solution growth of bulk crystal[5-7]. These outstanding features would also be extremely important ingredients for designing a radiation detector. This further motivates us to explore also the radiation detection property of perovskite halides. Most of the reports focus on detection of γ -ray photon only by conventional energy resolution technique which requires special arrangement of gamma spectrometry and nuclear instrumentation that makes them not much attractive as a tool for rapid detection of presence of γ -ray irrespective of the photon energy E_γ as well as isotopic signature even using halide perovskites [8-10]. It is also worthwhile to mention that though there are reports of use of perovskite halides as γ -ray detector, but there is a lack of

comprehensive complete study on features like repeatability, operational stability, detection window of radiation energy & activity and effect of sustained exposure to radiation on material properties. There are several areas like nuclear imaging, cancer therapy; security checking where needs radiation detector just as a quick tracer of presence of gamma ray [1]. So study of quick tracer of gamma ray and their detailed property as an efficient detector for real field use in a cost effective way using perovskite halide would be an important avenue of research.

In this chapter of thesis, we have taken a deviated approach for gamma ray detection not by energy resolution rather attempted as quick marker for detection of presence of gamma ray. We have shown solution growth technique at temperatures < 150^0C gives highly oriented crystals which we show can be used to make effective solid state γ -ray detectors with simple associated electronics where the detection is done by change in resistance of the crystal on exposure to radiation, very similar to a photoconductive optical detector. Unlike conventional semiconductor detectors where radiation is mainly characterized by energy resolution, where this detector primarily developed to trace the gamma ray (of known energy) by virtue of changing of its resistance in presence of gamma ray photons and varies accordingly energy of the gamma photon and activity. We choose $FAPbI_3$ for high effective Z value and good chemical stability as compared to other organic halide perovskites.

The detection process was found to be independent of E_γ which has been tested in the window 120 KeV to 1.1MeV. This technique could be extremely useful in radiation prone areas since this method acts as a quick marker of γ ray where fine energy resolution is not a primary concern. Our detector developed for use with $\gamma-$ray can detect activity from KCi source to mCi source with current noise detection limit of 50 nCi. It exhibits relatively good $\mu\tau$~$10^{-3}cm^2V^{-1}$ with diffusion length exceeding 100 μm. It shows high dark resistivity ($\sim 10^{10}\Omega - cm$) and a long shelf life of at-least 6 months. Importantly the material was found to be stable under sustained radiation with cumulative dose > 3.2KGy and it retains its structural properties without significant defect creation as established from optical properties which is completely new observation of effect of sustained gamma ray exposure to the halide perovskite material. Also a proof of concept has been established towards flexible, cost-effective solid state gamma ray detector using paper electronics based halide perovskite [11].

7.2. Basic of Radiation Detection Measurement & Primary Class of Radiation Detector Materials:

Any radiation detection system consists of mainly two primary aspects. These are broadly

I. Material
II. Instrumentation

The block diagram of a radiation detection measurement is as follows –

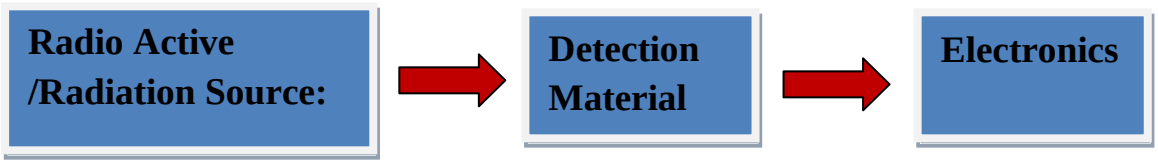

The primary classes of radiation detector materials are basically 1) semiconductor and 2) scintillators

- **Semiconductor:** In this type of detector material, electron-hole pair is produced that carries full information and applied through electric field between surface electrodes
- **Scintillators:** Based on optical signals, most efficiently and rapidly generates light and must be highly transparent in their optical radiation.[1,12]

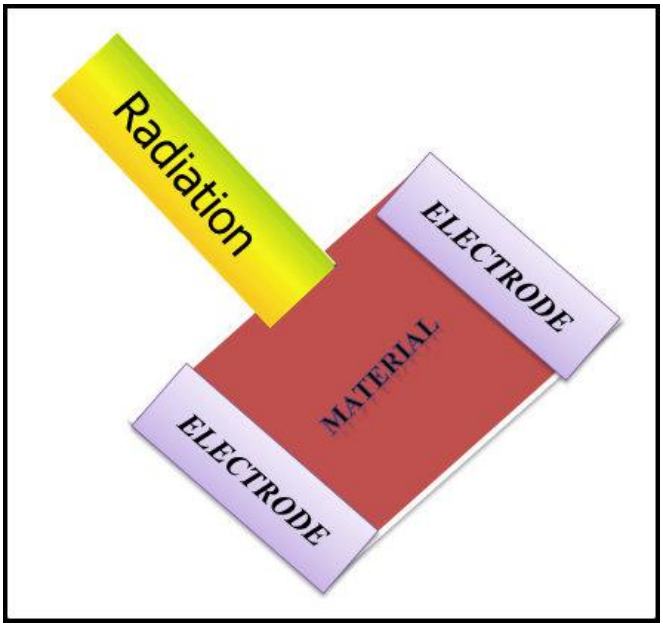

Figure 7.1 *A simple schematic of electrical read out based radiation detection*

7.2.1. Some radio-active terminologies used in this thesis:

It is useful to discuss and recapitulate few basic terminologies and their units for radiation detection. More often it is very important effect of radiation where it is being impinged. Generally it is expressed as dose and it is also feasible parameter how the dose being injected i.e dose rate. There are several kind of doses used in radiation science aspect.

Absorbed Dose: Basically defines the concentration of energy deposited in tissue as a result of an exposure to ionizing radiation. Absorbed dose describes the intensity of the energy deposited in any small amount of tissue located anywhere in the body. The unit of measurement for absorbed dose is the milligray (mGy) [13].

Equivalent Dose: is an amount that takes the damaging properties of different types of radiation into account.

The basic difference between absorbed dose in tissue and equivalent dose is-

1. Absorbed dose tells us the energy deposit in a small volume of tissue.
2. Equivalent dose addresses the impact that the type of radiation has on that tissue

Because all radiation used in diagnostic medicine has the same low-harm potential, the absorbed dose and the equivalent dose are numerically the same. Only the units are different.

For diagnostic radiation: The equivalent dose in milliSievert (mSv) = the absorbed dose in mGy

7.3. Experimental Procedure & Measurements:

7.3.1. Highly Oriented Crystal Growth by inverse solubility method:

Details descriptions of the synthesis of oriented crystal $FAPbI_3$ and characterization have been discussed in experimental section of chapter 2 (section 2.2). For sake of convenience we briefly discussed the synthesis process of highly oriented crystal. The bulk crystals of $FAPbI_3$ are prepared using solution growth process with standard inverse solubility mechanism. We used GBL as a solvent for its good solubility to the precursors (FAI and PbI_2) as well as remarkable solubility gradient with temperature. Typical crystal of dimension ~ 4mm x 4 mm with thickness ~ 2 mm. is used for our study.

7.3.2 Basic Characterization of as grown highly oriented crystal:

The as grown crystal was characterized by optical spectroscopy like PL & UV-Vis spectra.

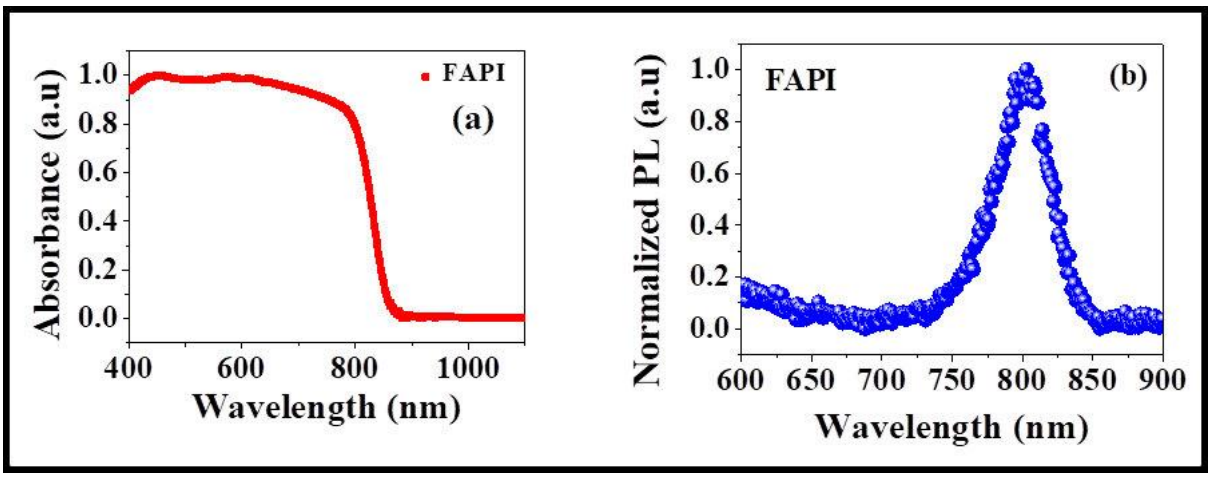

Figure 7.2: *UV-Visible and PL spectra of the γ –ray detector FAPI crystal.*

The PL spectra show that the band to band transition occurs at around 800 nm. Absence of other sub band-gap peaks signifies absence of significant defects that can trap carriers. The UV-Visible spectra were recorded in reflectance mode in solid sample attachment. Both PL and UV-Visible spectra are consistent with its band edge emission and absorption edge with corresponding band gap ~ 1.51eV and well agreed with reported values. Data are given in Figure7. 2.

The microstructure of the as grown crystal was characterized by using Atomic Force Microscopy (AFM). Figure 7.3 shows the surface morphology of the FAPI bulk oriented crystal over a scan area of 1.0μm × 1.0μm. The film surface is highly compact with root mean square roughness (rms) of ~ 2.7 nm.

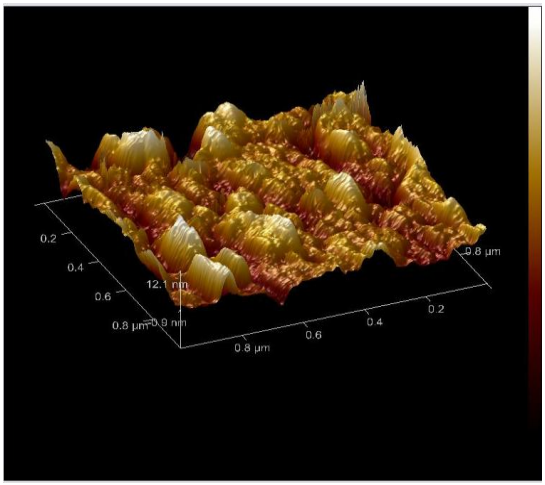

Figure 7.3: *AFM topography of the FAPI detector crystal with rms roughness of ~ 2.7 nm.*

7.3.2 Measurements:

The as grown bulk crystals were metalized in both faces by evaporation to make "vertical photoconductor" type detector. Cu was chosen to form ohmic contacts as we discussed in chapter 2. The schematic of the device geometry along with actual device is shown in Figure7.4. The material was tested with high active Co-60 gamma ray source with characteristics gamma energy of 1.1 MeV and activity ~ 1KCi as well as low energy gamma source Co-57 of 122KeV with 0.5 μCi activity. The facility (gamma source) was provided by UGC-DAE CSR Kolkata.

The main experiments for photo response consist of measuring the following:

- Device current (I) as a function of bias (V) at a fixed radiation source of known activity by turning radiation ON and OFF known as $I-t$ curves.
- The $I-V$ curves in dark and under radiation environment varying activity of the source

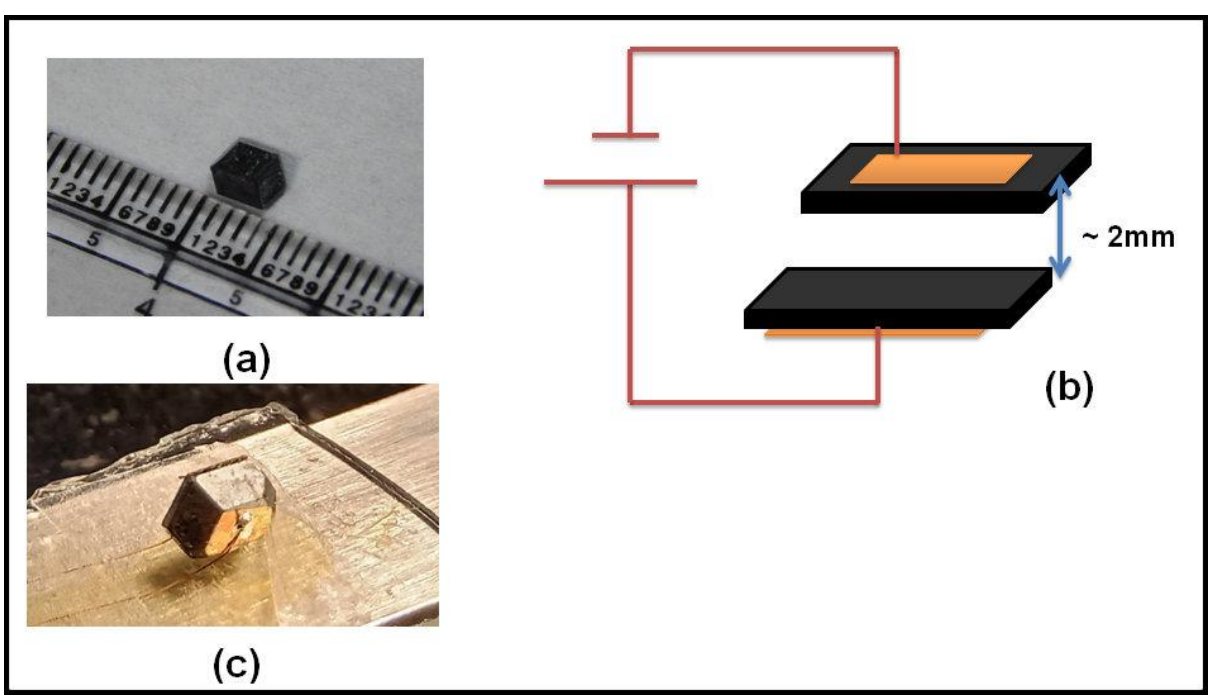

Figure7.4: *a) Actual photograph of the as grown highly oriented crystal $FAPbI_3$ detector b) Schematic of the device along with c) real photograph of the device*

The $I-V$ and $I-t$ measurements were done using a Source-Meter with a custom developed programme employing two probe configuration. All measurements for detection were carried out at room temperature.

7.4. Study of Gamma Ray Detection using $FAPbI_3$ oriented crystal by electrical read-out:

7.4.1 Current-Response by the Gamma Ray Detector:

The radiation detection property of the material towards γ-ray was studied by placing the sample in the γ chamber impinged on sample over a receiving area of ~ 4mm^2. The radial distance between source and sample (detector) distance was about 8 cm. The data are given in Figure 7.5 for a Co-60 source with 1KCi activity. The detector a response to γ- ray occurs with a response time $\leq$ 10 sec. The current increases more than one order under γ irradiation at bias 30V.The detector current increase with bias and eventually saturates for a bias > 50V.

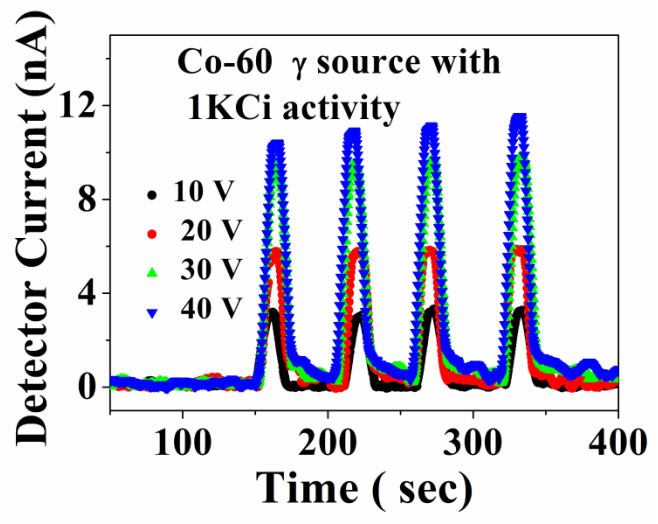

Figure7.5: *Current Response by FAPI γ ray detector (using Co-60 source).*

We define the detector response in terms of sensitivity analogous to other type of sensors (like e.g, a photo detector) as $\mathscr{R} = \frac{R_0 - R_\gamma}{R_0}$where R_γ is the resistance under γ-ray exposure. R_0 is the resistance of the unexposed detector. Since, in our case $R_\gamma < R_0$, $\mathscr{R}$ is positive.

7.4.2 Dependency of Response on bias & dose of the Gamma Ray Detector:

The enhancement of current hence response increases with increasing bias initially and gets saturated at higher bias as shown from the Figure 7.6(a).The safe limit of continuous applied operational bias was 50V corresponding to a field of 250 V/cm, although, the crystal can sustain up to a bias of 100 V (field ~ 500V/cm) for a shorter duration.

It is also noteworthy that the response increases with application of increasing bias initially and gets saturated under high bias as shown from the Figure 7.6(a) which is the

manifestation of higher mobility-lifetime (μτ) product at lower applied bias voltage (i.e μτ $\geq L^2/V$). We will discuss about mobility-lifetime (μτ) product in detail in later section. Similar effect of current saturation also been observed with increment of absorbed dose. In Figure 7.6(b) we have plotted the detector- current with absorbed dose (dose rate 0.44 Gy/sec). The detector current has a logarithmic dependence on the dose for 3 decades. The above two figures suggest the increment of response is restricted by both bias voltage and radiation exposure. Detection of such kind of high energy and high radio-active gamma ray could be very useful in medical industry for sterilization where Co-60 source is frequently used.

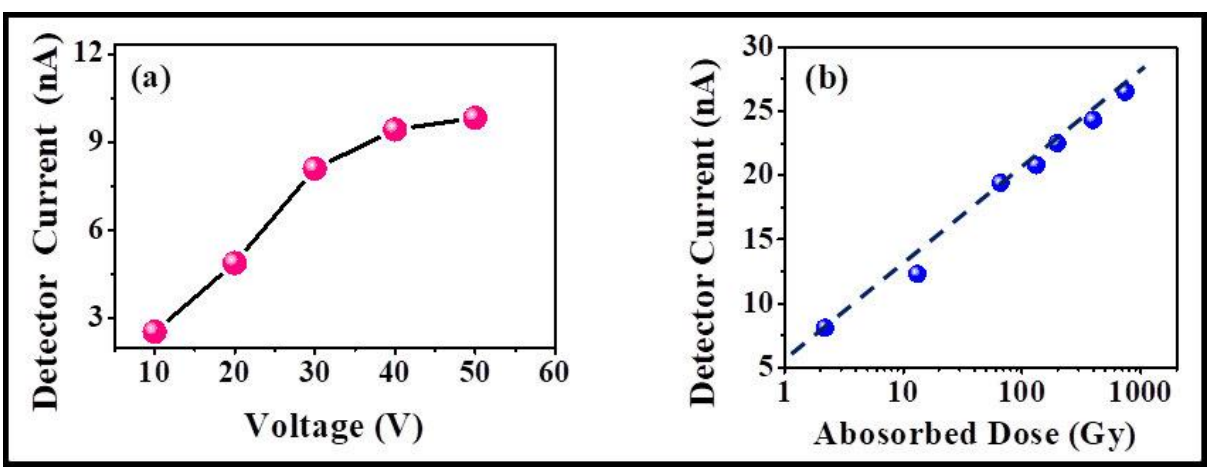

Figure 7.6: *a) Voltage dependent current response by the detector (20 seconds exposure time for each voltage) b) Detector Current as function of absorbed dose*

7.4.3 Detection Capability down to nano curie level:

Detection capability at micro-curie level (μCi) under low active radiation source points to good quality of detector with high sensitivity. We have also checked the detection capability of the $FAPbI_3$crystal detector to sub-micro Curie source using a portable Co-57 source with activity around 0.5μCi. The change in current is ~ 0.1nA of the detector under 0.5 μCi (source - detector distance was ~ 8cm) activity with γ photon of energy 122 KeV as shown in Figure 7.7. From the observed current change and noise level in the detector current (rms noise in current) we can get an estimation of noise limited detection capability. The rms noise in current is around 10pA.

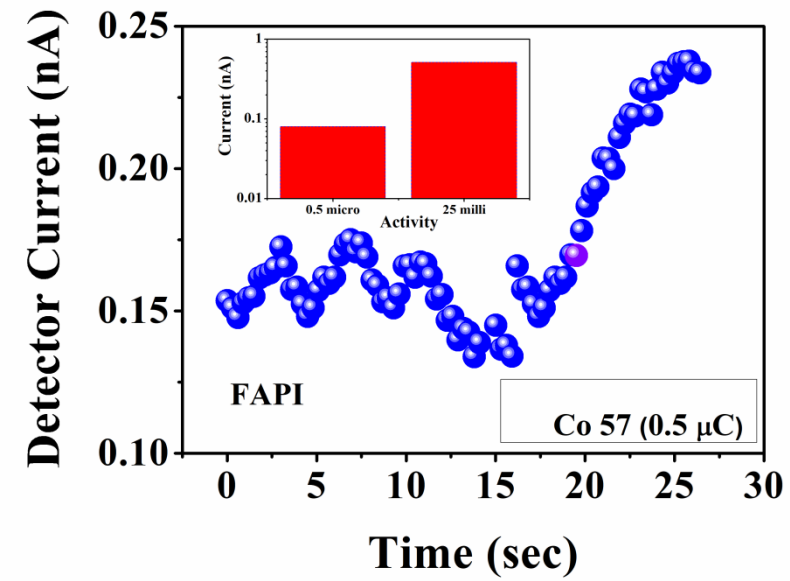

Figure 7.7: *Detection by FAPI highly oriented crystal γ ray detector at low radioactivity (μC)* level using Co-57 source; Inset: Detector-current for exposure to sources of Co-57 with different activity.

Thus the noise limited detectability comes around 50 nCi. Such low activity and low energy detection limit could be extremely useful for nuclear medicine and medical imaging where proper spatial tracing of the radioactive sources/isotopes is highly desirable. Thus the detector as developed, could act as low power portable γ-ray detector with relatively simple direct detection technique. Thus our detector could act as low power portable gamma ray detector with relatively simple direct detection technique.

Furthermore to get an estimation, how response depends on source activity, we measured the response of our detector under different activity of same energy gamma photon (Co-57). The graph is shown in inset of figure 7.7. It can be seen that there is good enhancement of response (more than one order) when we move from μCi to mCi activity. In Table 7.1 we have listed the sources used in our experiment with their activity and corresponding current response under them [11].

Sources	**Gamma Photon Energy (KeV)**	**Activity**	**Detector-Current (nA) at 30V bias**
Co-57	122	0.5 μCi	0.08
		25 mCi	0.51
Co-60	1100	~ 1KCi	8.1

Table 7.1: *Current response of the FAPI γ ray detector for different radio-active gamma sources with different activities for a fixed exposure time of 20 sec.*

7.4.4 Shelf Life of the Detector:

The stability and shelf life of any radiation detector under such high energetic photon flux extremely crucial because it reflects the detector's chemical and mechanical robustness without any physical damage. To check the shelf- life of the detector, we tested the sensitivity for a period of 6 month with tests after an interval of 2 months by keeping the sample preserved in vacuum- desiccators. The data is shown in figure 7.8. As shown in the graph, response decreases by about 5% of the initial sensitivity even after 6 months. This implies a reasonable shelf-life of the as grown crystal.

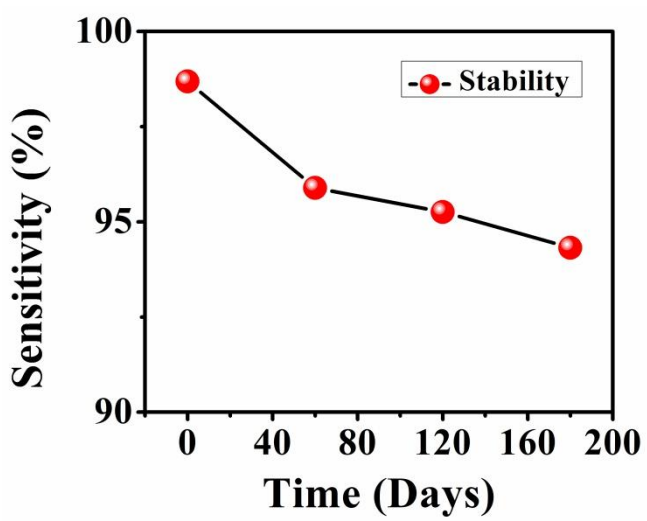

Figure 7.8: *Long term stability of the FAPI detector (shelf life up to 6 months).*

7.4.5 Transient Response & Repeatability of the detector:

For an efficient gamma ray detector, it is useful to trace its transient response towards radiation. To measure the response time, we have recorded long term response for 30 minutes under the bias of 30 V. However, maintaining response towards such high radiation suggests good chemical robustness/durability under radiation. We define response time as detector takes to reach 90% of the maximum final response output. We found response time ~ 2-3 sec which is pretty fast without using any pulse shaping instrument. The data is shown in Figure 7.9. We have also recorded the recovery time which is less than 10 sec (~ 7-8 sec) suggests fast recovery response behaviour.

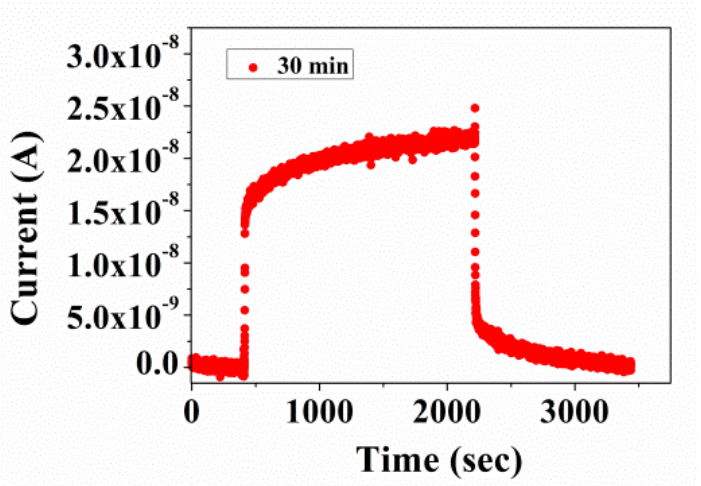

Figure 7.9: *Response –Recovery behaviour of the FAPI gamma ray detector*

Also, we have measured the repeatability of the detector which is very useful for practical use. We have measured six repeated cycles of the detector and found response stabilizes around 8% of a base value of current$1.12 \times 10^{-8}\ A$. The data is shown in Figure 7.10.

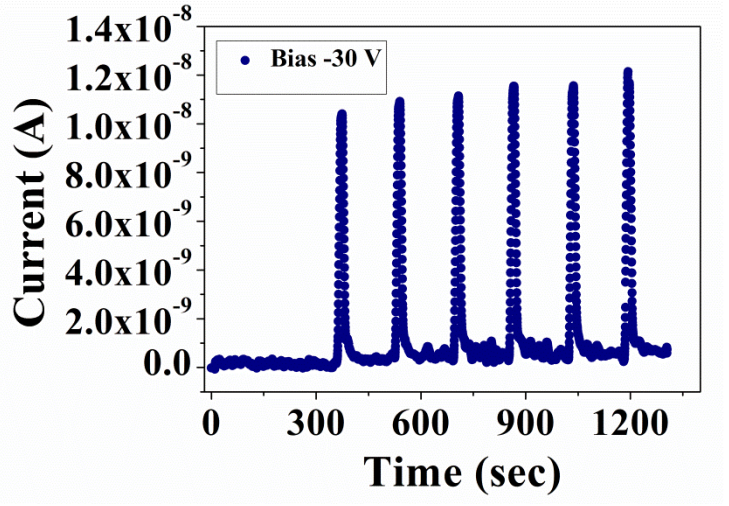

Figure 7.10 *Repeatability for 6 cycles of the FAPI detector*

7.5 Discussions:

7.5.1Analysis of electrical characteristics &charge transport parameters of the detector:

Efficient charge transport through the material signifies the quality of the detector. Mobility-lifetime product $(\mu\tau)$ is a fundamental figure of merit of any radiation detector which is a measure of the charge collection ability under a given bias and is limited by the carrier recombination time(τ). The applied bias V determines the transit time τ_t through the detector

given as $\tau_t = {d^2}/{\mu V}$ or $\mu\tau_t = {d^2}/{V}$, d being the separation of charge collecting electrodes.

The response is maximized when $\mu\tau \gg \mu\tau_t$ or $\frac{\tau}{\tau_t} \gg 1$.

The $\mu\tau$ product of the carrier were determined by radiation dependent current with different applied bias and value was extracted using Hecht Equation: $I(V) = I_0\{\frac{V\mu\tau(1-e^{\frac{-d^2}{V\mu\tau}})}{d^2}\}$, I_0 being the saturation current, d being the distance between electrodes. The data and the fit to the Hecht equation are shown in figure 7.11. The data shows that the detector current for bias variation is over nearly 3 decades. The fit to the equation as shown in the figure allowed us to obtain $\mu\tau$ as a fit parameter. From the we obtain $\mu\tau \approx 5.2 \times 10^{-3} cm^2V^{-1}$. The value of $\mu\tau$ the detector ($FAPbI_3$ crystal) turns out to be higher than that reported in commercially available detectors like TIBr and CdTe materials, where $\approx 10^{-4} - 10^{-5} cm^2V^{-1}$.[12] For the detector under consideration $d = 2mm$, even for a moderate bias of $V = 30$V, $\mu\tau_t = 1.33 \times 10^{-3}$ cm^2/V. Using the experimentally deduced value of $\mu\tau \approx 5.2 \times 10^{-3} cm^2V^{-1}$, we obtained $\frac{\tau}{\tau_t} \approx 4$. This is reasonable for a γ −ray detector. Using Einstein equation, $L_d = \sqrt{\frac{k_BT}{q}\mu\tau}$,(where K_B is the Boltzman Constant, T is the temperature (in Kelvin) and q is the electronic charge) the charge carrier diffusion length L_d was found to be ≈103 μm. This is comparable or better than that found in available benchmark detectors like CzTe [1].

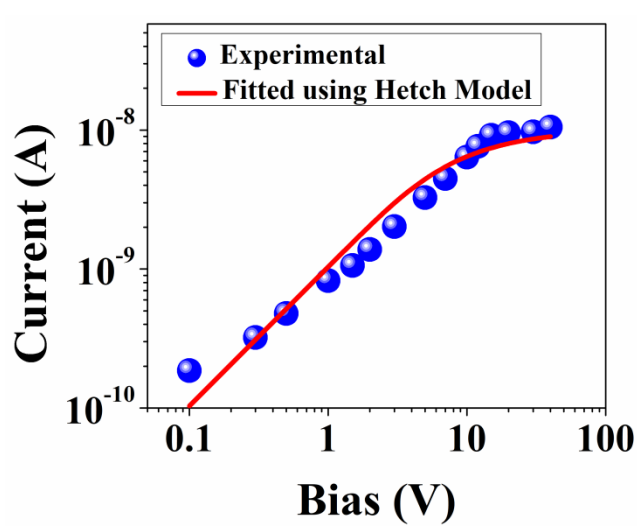

Figure 7.11: *The mobility-lifetime fitting according to Hecht Model*

The dark current–voltage$(I-V)$ characteristics and device geometry provides us the resistivity (ρ) of the detector ($3.3\times10^{9}\Omega-cm$). We have also checked the $(I-V)$ characteristics of the detector under gamma irradiated condition. The data is shown in fig 7.12. The detector crystal maintains similar ohmic nature during exposed condition as well as dark condition except increment of current ~ one order during exposure and slope of the $(I-V)$ curve changes.

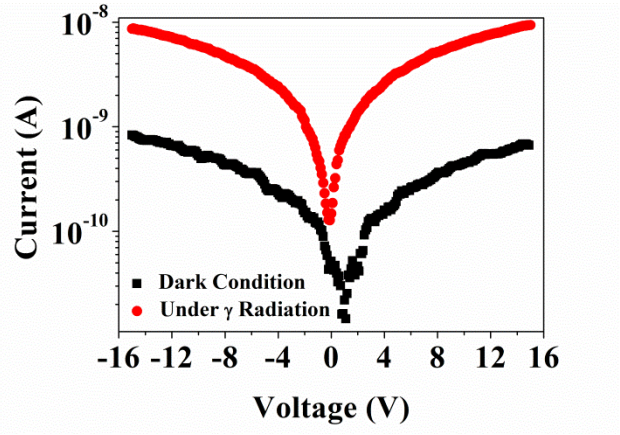

Figure 7.12: *Current-Voltage (I-V) characteristics in dark and under gamma radiation from Co-60 source (1KCi activity)*

Likely Mechanism: The primary mechanism of carrier generation in the detectors is suggested to be Compton scattering [14]. E_γ for the γ-ray used here is higher than the binding energy of the electrons in the atom. As a result the electrons can be considered free thus meeting the condition for Compton scattering. A Compton interaction can be considered to be an elastic collision between a photon and a loosely bound or unbound electron. In the process, the photon energy is reduced and the electron is set in motion. The collection electrodes capture these electrons.

7.5.2 Extension to Paper Electronics Based Radiation Detector:

To make a more cost effective and flexible radiation detector, we have explored the radiation detection property using a detector with FAPI grown on a paper other than oriented crystal of FAPI. We have grown the material in both side of the paper substrate and fabricated vertical geometry (similar to oriented crystal) by depositing Cu to make electrode on both side. It has been exposed to identical radiation condition and with the same applied bias (30 V). We have

found that the response is much slower that the oriented crystal as shown in figure 7.13. The slower response is linked to higher resistance of the paper sensor giving rise to a larger RC time constant. The main reason behind higher response in case of highly textured crystal is less scattering and absence of defects that makes the $\mu\tau$product larger. However the response from paper grown detector though small can be established as a proof of concept of a flexible γ-ray radiation detector for wearable, low cost detector that can be used with suitable device engineering for enhanced response.

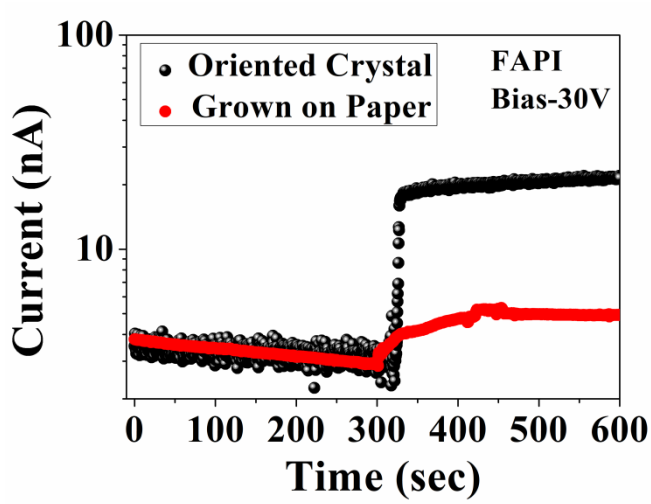

Figure 7.13: *Current response by FAPI paper based γ ray detector & comparison with the oriented crystal based detector (using Co-60 source).*

7.5.3 Stability of the FAPI crystal under sustained γ radiation:

Stability of a detector material under sustained radiation exposure is an important factor that decides feasibility of the material for use in detector. We checked the stability of performance of the FAPI crystal under prolonged exposure. We have checked the stability using structural, optical properties and detection performance as diagnostics tools. The effect of sustained radiation on perovskite crystal is completely new observation to the best of our knowledge.
We established the effect through several tools like spectroscopy & structural analysis. We placed the FAPI crystal based detector in gamma test chamber (given in figure 2.24) and exposed it for long time. After each exposure we have characterized the exposed samples by XRD, steady state photo luminescence (PL), time resolved photo luminescence (TRPL) and compared them with those observed for the pristine/as grown crystal.

7.5.3.1 Evidence from structural study

In figure 7.14, we have compared the XRD of the irradiated sample with that of the pristine sample. The sustained exposure was done for 2 hours in the gamma chamber containing Co-60 gamma source and the cumulative absorbed dose was 3.2KGy. No change /modification of crystal structure have been observed in X-ray diffraction data before or after radiation exposure as shown in figure. This indicates good structural stability of the FAPI crystal under radiation.

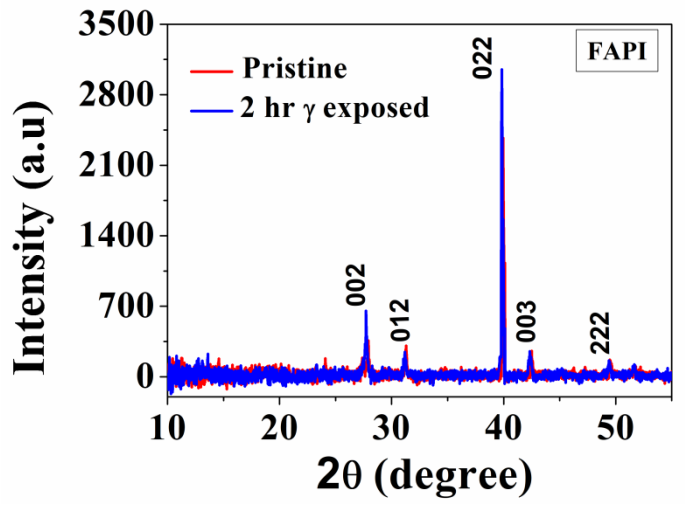

Figure 7.14: *XRD of the as grown oriented crystal. The flat face of the crystal is strongly textured along < 022> direction. The data are shown for a pristine crystal and the same crystal after sustained exposure to 1100 keV for a cumulative dose of 3.2KGy*

7.5.3.2 Evidence from spectroscopic study

To get insight further, we have performed the spectroscopic characterizations on exposed and pristine crystals. In figure 7.15 we have compared the PL of the 2 hr exposed FAPI crystal along with the pristine crystal before exposure. In the same graph we also show the *in- situ* steady state PL (taken under 25mCi Co-57 γ-ray source) to check any changes in optical properties during radiation. From figure 7.15, it can be seen that the main PL peak corresponding to band to band transition remains identical in all the cases. This suggests luminescence property also retained under radiation. Absence of any extra peaks during and after exposure indicates no defects has been created due to irradiation. Further we performed time resolved PL spectroscopy on both pristine and in situ irradiated sample to ascertain any change in the carrier lifetime during radiation. The data for both conditions is shown in figure 7.16.The carrier life time remains unaltered. This further proves that carrier life time also does not get affected by γ-ray exposure.

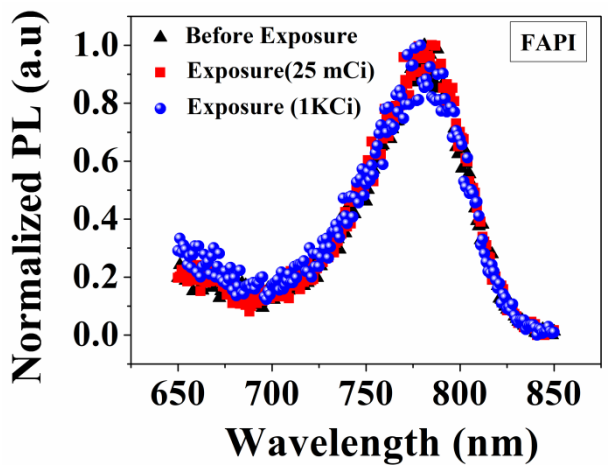

Figure 7.15: *Comparison of Steady State PL characteristics of the pristine, 2 hr exposed (Co-60 ~1KCi γ radiation) crystals along with in- situ (under Co-57 25 mCi radiation) exposure.*

Thus from above discussion, it can be concluded that our FAPI based γ detector shows excellent stability both structurally and optically under high γ energy radiation flux i.e exhibits good chemical/mechanical robustness under hard radiation. Such high radiation stability makes our detector potent where high energy γ-ray needs to be detected.

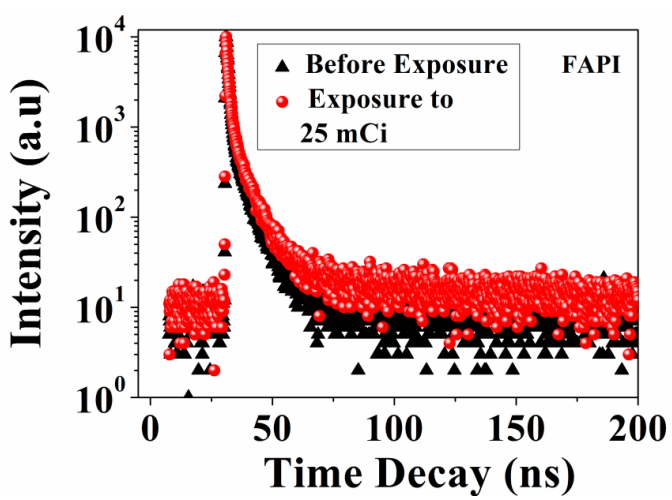

Figure 7.16: *Time Resolved PL of pristine & in situ exposed FAPI detector.*

7.5.4 Comparison with existing gamma ray detector:

The benchmark materials for radiation detector such as Si and Ge, few inorganic compounds, especially CdTe, TlBr show spectroscopic response with good charge transport efficiency. But there are issues of crystal growth and device operation associated with them. Similarly requirement of low temperature and high purity for operations blocks the possibility robust and ease use of HPGe as a solid state gamma ray detector though it posses fine resolution

(~.2%) to detect gamma ray[1]. Moreover, till date, there are very few materials that fulfill these requirements at room temperature. Only ultrapure CdTe and CdZnTe, generally grown by Czochralski method have been commercially viable to be operational at room temperature [1, 4]. But all these detectors are based on energy resolution based and main application of them in the area of determining and differentiating the energies of gamma ray. Moreover, the detection ability of low activity has not been explored /reported by them. However, in our case since the method is based on electric read out, it can be directly used as quick tracer of gamma ray. Moreover low detection ability would be extremely useful for protecting the tissues adjacent to the tissues to be burned by determining spatial position of cells. Thus it could be a viable tool in radiation therapy like gamma ray camera.

7.6 Conclusions:

In summary, we have demonstrated that a solution processed perovskite crystal FAPI can be used to make a simple γ-ray detector which operates at room temperature under normal ambience and uses resistance measurement as the detection technique much like that used in optical detectors. Detector demonstrated does not have the energy resolution but can be used as a quick tool to detect presence of γ-ray in wide energy range which is at least from 100-1000 KeV range. Operation for wider energy range could not be tested for absence of suitable calibrated source. The sensitivity of the detector is limited by the current noise and is estimated to be 50 nCi. The FAPI detector has reasonable $\mu\tau \approx 5.2 \times 10^{-3} cm^2 V^{-1}$. It also exhibits higher bulk resistivity (~$10^{10} \Omega - cm$), long carrier diffusion length ~ 100 μm under bias free condition and a high shelf life of at least 6 months. The FAPI crystal based detector shows excellent structural and mechanical robustness under high energy γ- ray with sufficient long exposure. The simple fabrication process of detector is expected to have potential applications in industries as well as in nuclear medicine, homeland security. This detection technique could be extremely useful in radiation prone areas since this method acts as a quick marker of gamma ray, where fine energy resolution is not a primary concern.

We also demonstrated that a simple paper based radiation detector using FAPI can be made although with less sensitivity as agreement with proof of concept to extend its future application using paper electronics.

References:

7.1 Milbrath, B.D.; Peurrung, A.J.; Bliss, M. and Weber, W.J. *J. Mater. Res.*, 23, 10, 2008

7.2 Laura Basiricò, Andrea Ciavatti, and Beatrice Fraboni, *Adv. Mater. Technol*. 6, 2000475, 2021

7.3 Oliver D. I. Moseley, Tiarnan A. S. Doherty, Richard Parmee, Miguel Anaya and Samuel D. Stranks, *J. Mater. Chem. C*, 9, 11588, 2021

7.4 Sellin, J. P.*Nuclear Instruments and Methods in Physics Research A*, 513 ,332–339, 2003,

7.5 Kakavelakis,George.et.al; *Adv. Sci.*, 2002098, 2020

7.6 Stepan Demchyshyn, Matteo Verdi, Laura Basiricò, Andrea Ciavatti, Bekele Hailegnaw, Daniela Cavalcoli, Markus Clark Scharber, Niyazi Serdar Sariciftci, Martin Kaltenbrunner, and Beatrice Fraboni, *Adv. Sci.* 7, 2002586,2020

7.7 Jingying Liu,.et.al; Adv. Mater. 31, 1901644, 2019

7.8 HaotongWei.et.al;, *Nature Materials*, 16, 826–833, 2017 DOI: 10.1038/NMAT4927

7.9 He, Yihui.et.al; *Nature Communication*,9,1609,2018, DOI: 10.1038/s41467-018-04073-3

7.10. Y.Serigi.et.al;,*Nature Photonics*,10**,**585-589, 2016

7.11 Avisek Maity,Chandni Das, A.K.Raychaudhuri, Abhijit Saha,Barnali Ghosh;; *Journal of Physics D: Applied Physics*, 54, 455104, 2021

7.12. Nuclear Physics, S N Ghosal, ISBN81-219-0413-7

7.13 https://www.ndsu.edu/fileadmin/policesafety/docs/rad_glossary.pdf

7.14 Lechner.A**;** 2017,*Proceedings of the CAS–CERN Accelerator School: Beam Injection, Extraction and Transfer*, https://doi.org/10.23730/CYRSP-2018-005.47

Chapter 8

Summary & Future Outlook

In this final chapter, we have summarized the major and important observations of the thesis work and also discussed the scope for further explorations. We have spent time to controlled growth of perovskite halides from nano/micro structured thin films to bulk highly oriented crystal tailoring shape, size, and morphology tuning different parameters. This thesis focuses selected section of important application potential and physical properties of perovskite halides by structural, morphological and ionic tuning. The important application potential of the material as detectors in different form , like gas ,photo and radiation detectors has been investigated in details, moreover the physical properties investigated include optoelectronic, structural and gas sensing and radiation detection properties of the perovskite halides, thin films, bulk crystals and micro/nanostructures. Attempt has also been carried out towards technology transfer of the prototypes made for gas sensing utilizing novel and new application potentials of these emerging classes of materials investigated.

The major observations and important outcomes of this thesis are summarized below:

8.1 Growth & Fabrication:

- One of the major achievements of this thesis in prospective of synthesis is to successfully grow these solution processed very good quality perovskite halide materials on flexible porous substrate like paper beyond conventional substrates like ITO, FTO, and Glass etc in which uniform surface coverage is a major challenge and we could obtain definite results. Introduction of paper as a substrate to grow these materials helps to achieve good coverage as well as enhancing chemical stability.
- We also observed that surface morphology can be tuned by substrates and substrate like paper give rise to specific surface morphology that modifies the physical properties. Growth of perovskite halide using paper substrate is a completely new and innovative achievement. We could tune also surface morphologies (like MAPI on paper shows nanorod like structure but MAPB on paper shows Microcube and FAPI shows fibrous structures) of different perovskite halides grown on paper that leads to tune the physical properties.
- The most of the measurements described in this thesis is paper electronics based. Usage of perovskite halides towards paper electronics based devices in completely new and first time reported by us. Paper grown materials are used to fabricate as devices which is new for perovskite halides. Also metallization on such paper substrates is an important challenge and making of paper electronic based device for different detectors is the novelty our research.

8.2 Investigation of Perovskite Halides as an active gas sensor material & understanding the sensing mechanism :

The major or central observation of this thesis encompasses with finding potential application of hybrid halide perovskites as active materials for gas sensor. The detail findings and study of the sensing properties by these emerging classes of materials have described through several chapters:

- In chapter 3, we, first time fabricated a simple flexible paper based ammonia sensor using active material methyl ammonium lead iodide ($CH_3NH_3PbI_3$) by a simple visual color change effect. The black colored MAPI paper sensor changes to yellow color in presence of ammonia (NH_3) gas. The sensor has very fast response (~12 sec for 10 ppm ammonia)

by a visual color change as well as selectivity towards ammonia gas and exhibits good stability. Investigation of color change has been established using a collection of techniques like XRD, EDX, UV-Visible absorption and Photo Luminescence and Conversion/decomposition of MAPI to PbI_2 on exposure to NH_3 has been proposed as the mechanism of color change. This proof of concept leads us 'Granted patent' as well as prototype development.

- In chapter 4, we have described electrical gas sensor using MAPI to go below visual limit by fabricating paper electronics based gas sensor. In this electrical sensor, the current increases by one order through the channel on exposure to only 10 ppm NH_3 gas. The calibrated sensitivity is ~55% for 1ppm of NH_3 gas in Nitrogen or Air. The current noise limited resolution estimated to be ~ 10 ppb. This work establishes perovskite halide as a new solid state gas sensing material that can reach sub ppm sensitivity using simple paper electronics. Use of paper and also solution method used to grow the active material makes the sensor cost effective and easy to manufacture. This type of disposable high sensitive paper sensor can be used for detection of NH_3 as a marker in exhaled breathes for non-invasive diagnosis. Being grown on the paper and since it supports unheated operation; it is very much compatible with low power paper electronics. This proof of concept was also been applied for patent.

- In chapter 5, we have extended our study of gas sensing property to other lead based altering cation and anion like $MAPBBr_3$ and $FAPbI_3$ both by visual and electrical detection method using paper electronics. We observed that response towards NH_3 gas is qualitatively independent of substitution/alteration of cation or anion; surface morphology, crystal structure, and electronic band gap although there are quantitative differences. Quantitative intercomparison of the halides with different anions and cations as gas sensor materials turns out that the sensitivity of MAPI based sensor is higher compared to those made from MAPB and FAPI. Thus the lead based perovskite halide family could provide a general platform for room temperature (unheated) solid state NH_3 gas sensor which is also compatible with flexible, wearable paper electronics.

- In the same chapter, we have also proposed a generalized sensing mechanism to understand the fascinating sensing behaviour by these emerging classes of materials. It

has been proposed that the sensitivity (as well as specific selectivity) of the lead based perovskite halide family to NH_3 gas arise from the fact that the material decomposes to the respective lead halides during interaction with NH_3 that give rise to the color change as well as reduction of resistance of the material. The proposed mechanism has been substantiated by molecular dynamics simulations based on preferential adsorption of NH_3 gas molecules .The simulation result turns out the highest adsorption energy for MAPI based sensor causing fast and rapid chemical reaction that enhances the speed of response which is consistent with the experimental observations. The main outcome of this observation is that, sensing mechanism by perovskite halide is completely different from conventional metal oxide semiconductors (MOS) gas sensing mechanism based on redox reaction mechanism.

8.3 Translational research based on novel application of perovskite halides:

In recent past, an appreciable interest is being noticed on translational research to transfer the technology from the new, novel invention of scientific observation in laboratory. One of the major achievements of this thesis is to translate our novel idea of tracing ammonia gas using perovskite halide (MAPI has been used for applying patent) towards technology transfer. In chapter 3 and chapter 4 we have addressed the development of prototypes to make the ammonia gas sensor (both visual & electrical) useful in Environment protection and health care sector. This unique idea by visual colorimetric effect for tracing the gas has been utilized to get a 'Granted patent' (for the visual gas sensor) and an applied patent (for the electrical gas sensor). Furthermore also lab based prototype in the form of wrist watch called "**Ammo Watch**" has been designed towards as a part of technology transfer. This kind of prototype might be useful for routine use in areas like food sector, healthcare sector for practical use in disposable manner. We have further developed a batch of sensor strips and also grown it in a relatively large paper (4-5 inch) to enhance the scalability.

8.4 Cation engineered stable broad band photo detector by mixed halide perovskite using paper electronics:

In chapter 6, we, first time observed that paper electronic based photo detector can be made using lead based perovskite family with a broad band spectral range (300-900nm) with excellent stability. We fabricated a cation engineered paper based photo detector (planner photo-conductor type geometry) using solution grown mixed cation perovskite ($FAPbI_3$ and $MAPbI_3$) halides with stable photo response and enhanced detectivity in UV region. A

detailed optoelectronic property study has been done of single cation (MAPI & FAPI) and mixed cation halide perovskites using paper electronics in the broadband spectral range 300 - 900 nm. We found optimized substitution in mixture of cation ($MA_{0.6}FA_{0.4}$) enhances the Responsivity (highest ~0.27A/W) as well as provides much more stable response than individual single cation (for FAPI 0.085A/W and MAPI 0.13A/W) halide response. Investigation of photo response of mixed halides grown on paper is completely new relative to the conventional conducting substrates used for photo detector fabrication. In such paper based device the photo current being $< 10^{-7}$ A, the dissipation and power requirement during detector operation is < $0.5\mu W$. Such a low power requirement makes the detector fully compatible with Li ion battery based electronics. Thus photo-conductive response observed using substrate like paper may pave the halide perovskite as compatible with new generation cost effective bio compatible flexible, disposable paper based broadband optical sensor.

8.5 Realization of new generation room temperature high radiation sustained gamma ray detector by solution processed Perovskite Halide :

In chapter 7, we extend our study to explore the radiation detection property by these materials. We investigated the radiation detection (γ Ray) using paper based highly oriented crystals as well as $FAPbI_3$ film grown on paper. The oriented crystal was chosen for achieving higher response as well as to trace low dose (μC) for low defect density, higher mobility etc. We demonstrated a different approach to directly trace the presence of gamma ray using perovskite halide using electrical read out. The $FAPbI_3$ based detector traces radiation by electrical red out and shows quick response (< 10 sec for ~ 1kC radioactivity) with high mobility-lifetime product (μτ) (~$10^{-3}\ cm^2V^{-1}$) as compared to conventional scintillators (HpGe~ $10^{-4}\ cm^2V^{-1}$) detectors. The radiation detection using $FAPbI_3$ halide is also capable to trace very low activity gamma ray and estimated activity down to 50nCi by noise limited detectibility. The FAPI crystal based detector shows excellent structural and mechanical robustness under high energy γ- ray with sufficiently long exposure. The simple and an easy to fabricate detector is expected to have potential applications in industries as well as in nuclear medicine, homeland security and this method could acts as a quick marker of gamma ray, where fine energy resolution is not a primary concern.

8.6 Scope for future work:

- In synthesis front, it would be interesting study to explore the growth of these kind of materials on other porous substrates and intercompare the physical properties tuned by the porosity of the substrates.
- It would be fascinating to extend this kind of paper substrate based synthesis technique to other lead free perovskite halides also. Since we have metalized such kind paper based substrate, it would be a rewarding to grow the materials by co-evaporation/physical vapour deposition method on this kind of substrates to control the thickness.
- From gas sensing point of view, it will be excellent to study the response of lead free perovskites also and to find any unification is possible for similar mechanism observed by lead based perovskite.
- Since, MAPI turns out to be the best candidates among lead based halides family with sub ppm detectivity towards NH_3 , it would extend the possibility of studying exhaled breathe analysis by this material for non invasive clinical applications where extremely low concentration of NH_3 needs to be detected. Furthermore, there is a scope to modulate the response towards gas by tuning/ engineering different parameters and to check the detection possibility for other hazards pollutants by these materials.
- We have studied the paper based photo detector by "A" site cation engineering for lead halide perovskites. It would be interesting to study incorporation of plasmonic Au to enhance in UV region as well as to study the photo gating effect. It would be also challenging and fascinating to study the Photo-Hall effect further to check if there is a change in carrier mobility due to concentration gradient caused by optical illumination.
- From radiation detection prospective, it would be an excellent attempt to explore the possibility of radiation detection other than gamma ray (like neutron) and develop flexible radiation detector towards medical devices like tomography.